

Investigating the growth of diamond onto zirconium for potential use in nuclear fuel rod cladding

Fiona Brannan

Supervisor: Professor Paul W. May

Second Assessor: Professor Mike N. R. Ashfold

March 2014



University of
BRISTOL

School of Chemistry

This thesis is submitted in partial fulfilment of the requirements for the
Honours degree of Bachelor of Science in Chemistry

Acknowledgements

There are several people who have influenced and assisted me throughout the course of this investigation that I wish to thank. Most notable is my primary supervisor and assessor Professor Paul May, for his day-to-day attention, guidance and supervision both in the lab and with analysis of the results; without him this project would not have been possible. Additionally, I would like to thank my secondary assessor Professor Mike Ashfold and Dr. Simon Hall for their ideas and input relating to various areas of my report and presentation.

My appreciations go to the staff at the mechanical workshop in the Chemistry Dept. at the University of Bristol for their assistance in the pre-carburisation of samples, and to Miss Sarah Halliwell for conducting SIMS analysis on my behalf, as well as talking me through the procedure, explaining the process and assisting in the analysis of results achieved from this.

Lastly, thank you to the Bristol Diamond Group as a whole for miscellaneous help around the laboratory, and for making this year an extremely enjoyable one.

Abstract

This thesis comprises of two distinct yet associated sections; a literature review of diamond, chemical vapour deposition (CVD) and zirconium and an experimental section based upon the findings of the review. In the first part, a literature review was conducted of the history and chemistry of diamond, chemical vapour deposition (CVD) and zirconium. Particular attention was paid to the reviewing of the use of zirconium in nuclear applications: it is the main component of the alloys used to make fuel cladding for solid fuel pellets in nuclear reactors, and despite being well suited in most aspects, recent events would suggest there is a problem that needs to be addressed. The oxidation of zirconium by water has been found to be responsible for the phenomenon of delayed hydride cracking (DHC), hydrogen embrittlement and the more serious and publicly known nuclear disaster at Fukushima, Japan in 2011. The mechanisms by which oxidation, carburisation and hydrogenation occur in and on zirconium metal have been studied as a precursor to the experimental section, as a means to understand the surface chemistry of the metal, and therefore predict the possible outcome of diamond growth by CVD on its surface.

The aim of the experimental section was to investigate a possible method of rectifying the problem witnessed at Fukushima. Attempts were made to grow diamond by CVD onto zirconium substrates to act as a protective barrier, thereby preventing the problematic oxidation of the metal from occurring.

Zirconium substrates were prepared for deposition by one of two methods: manual abrasion or pre-carburisation followed by electrospray. Samples prepared by the former were reacted at 25, 20 and 18A for 6, 12 and 18 hours respectively. Successful diamond growth was observed in all cases, however adhesion of diamond to substrate was only observed at 20 and 18A, when there was not a continuous film across the surface of the metal. The film of the highest quality was obtained at 18A, where there was an approximate coverage of 90% across the substrate, and a film thickness of ~200 nm. Diamond also grew successfully on both pre-carburised zirconium substrates, forming a continuous film however only adhered to one sample. This particular sample shattered upon handling, suggesting that carburisation of the metal had been perhaps too successful. Samples were analysed prior to and after depositions by Raman spectroscopy and secondary ion mass spectrometry (SIMS), and by optical microscopy and SEM after reaction.

Table of Contents

Acknowledgements	iii
Abstract	iv
1. Literature review and introduction	1
1.1 An Introduction to diamond; properties, history and uses	1
1.2 Chemical Vapour Deposition	4
1.2.1 Introduction and types of CVD	4
1.2.2. Mechanism of Diamond Growth by Chemical Vapour Deposition.....	7
1.3 Zirconium: properties, compounds and their uses	9
1.3.1 Physical and Chemical Characteristics of Zirconium Metal	9
1.3.2 Zirconium Dioxide; properties, uses and chemistry	13
1.3.3 Properties, uses and chemistry of zirconium carbide.....	16
1.3.4 Preparation, properties and chemistry of zirconium hydride.....	18
1.4 Nuclear Applications of Zirconium Alloys	20
1.4.1 Types of zirconium alloys, their chemistry and use.....	20
1.4.2 Oxidation of zirconium in nuclear reactors	22
1.4.3 Role of hydrogen; hydrogen embrittlement and delayed hydride cracking	23
1.5 The Fukushima disaster and need for change	25
1.6 Conclusion	27
2. Experimental Method and Techniques	28
2.1 Aim	28
2.2 Sample Preparation	28
2.2.1 Manual abrasion	28
2.2.2 Pre-Carburisation.....	28
2.2.3 Electrospray.....	29
2.3 The Reactor	31
2.3.1 Hot filament CVD reactor	31
2.4 Reaction times and conditions	33
2.4.1 Standard conditions	33
2.4.2 Variable conditions.....	33
2.5 Analysis	34
2.5.1 Optical Microscope	34
2.5.2 Secondary ion mass spectrometry.....	34
2.5.3 Raman spectroscopy.....	35
2.5.4 Scanning electron microscopy (SEM).....	36
3. Results and Discussion	37
3.1 Initial investigations	37
3.1.1 Reaction in the hot filament and microwave reactors	37
3.1.1.1 Secondary ion mass spectrometry.....	37
3.2 Reaction at low temperature	40
3.2.1 Deposition at 20A.....	40
3.2.1.1 SEM Imaging	40
3.2.3 Deposition for 12 hours.....	43
3.2.3.1 Optical microscope imagining.....	43
3.2.5 Deposition at 18A.....	44
3.2.5.1 Raman spectroscopy	44
3.2.5.2 SEM imaging.....	46
3.2.5.3 SIMS	47
3.3 Pre-carburisation	48
3.3.1 Raman spectroscopy	49
3.3.2 SEMs.....	49

4. Conclusion	52
5. Further Work.....	54
6. Appendix	56
6.1 SIMS Results.....	56
6.1.1 Untreated zirconium.....	56
6.1.2 Sample 1	57
6.1.3 Sample 7	58
6.2 SEMs	60
6.2.1 Deposition 4.....	60
6.1.2 Deposition 7.....	61
6.1.3 Deposition 6.....	62
6.3 Optical Microscope Images.....	63
6.3.1 Deposition 4.....	63
6.4 Raman Spectra	64
6.4.1 Raman spectrum of sample 5.....	64
6.4.2 Raman spectra of sample 7	64
6.4.3 Raman spectrum of sample 6.....	67
Bibliography	68

1. Literature review and introduction

1.1 An Introduction to diamond; properties, history and uses

Diamond is one of the several allotropes of carbon, and is widely known as one of the hardest substances in the world. It also possesses the highest Young's Modulus and thermal conductivity as well as the lowest compressibility of all known materials. Throughout history, it has been highly valued for its appearance and hardness, being used prominently as a gemstone but also in cutting tools and parts of machinery, possibly for thousands of years [1]. Some of the physical properties of diamond show just how hard and compressible (or not) it is, while the very high refractive index explains why well-cut diamonds are so visually appealing – white light entering the crystal is reflected several times inside it before being split into the various wavelengths (and hence colours) of visible light as it exits, giving diamond's distinctive glittering rainbow appearance.

Table 1. A selection of the properties of diamond [2]

Property	Value	Units
Hardness	1000	kg mm ⁻²
Tensile Strength	>1.2	GPa
Compressive Strength	>110	GPa
Density	3.52	g cm ⁻³
Thermal Expansion	1	µm.m ⁻¹ .K ⁻¹
Thermal Conductivity	20	W cm ⁻¹ K ⁻¹
Young's Modulus	1220	GPa
Refractive Index	2.419	Dimensionless
Optical Transmissivity	225	Dimensionless
Band Gap	5.45	eV
Resistivity	1016	Ω cm

Carbon can take several different structural forms, and can be cubic, hexagonal (like graphene or graphite) or amorphous (for example the seven types of diamond-like carbon). The structure of diamond is an entirely face-centred cubic lattice, where for each unit cell there are eight 'corner' atoms, six 'face' atoms and four additional atoms. Each carbon is tetrahedrally coordinated to four others, and all bonds are σ bonds, thus by default each carbon has sp^3 character. Despite being exceptionally stable to physical and chemical processes, diamond is not the most stable form of carbon; the lowest energy allotrope is graphite (comparison in figure 1). The difference is structural only, and is less than one eV [3], [4]. However, the activation energy required to convert diamond into graphite is extremely large, which explains the presence of naturally occurring diamonds, as once formed it takes millennia to convert into the slightly more stable graphite. This stability at above the lowest energy form mean that diamond is said to be metastable at room temperature. Because diamond is the densest of all the

allotropes of carbon, it makes sense that the only condition under which diamond is usually observed to be the most stable, and thus allow natural formation is in extremely high pressure and temperature (HPHT) environments, like those that occur in the lithospheric mantle [1], the sites of meteor strikes [5] and (possibly) the atmospheres of Saturn and Jupiter [6]. Clearly the latter is completely inaccessible, and the previous two are rare (and mining and processing are labour intensive), accounting for the expense of buying the gemstone.

The chemical reactivity of diamond is minimal, however there are some circumstances in which it will partake in certain reactions. Some liquid hydroxides and metals (iron, nickel and cobalt) have a corrosive effect, and above 870 K, diamond will react with gaseous H_2O and CO_2 . At more elevated temperatures, it will oxidise in an atmosphere of air or oxygen. It is also possible for diamond to react with some metals, either forming carbides or dissolving in the metal. In the case of zirconium, tungsten and tantalum a carbide is formed, [7] which may be beneficial in this experiment as a means to adhere the diamond coating to the zirconium substrate, provided the carbide layer does not penetrate too deeply into the metal.

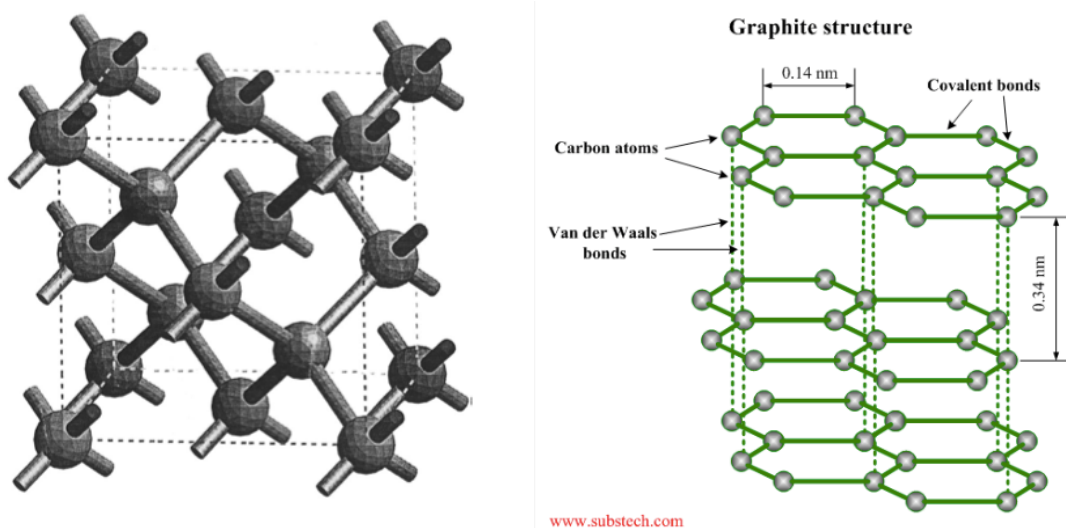


Figure 1. Comparison of the structural and visual differences of diamond (left) [7] and graphite (right) [8]

For centuries, diamond has been used as a hard coating for materials to enhance performance through preventing wear or improving cutting ability amongst other uses. With the highest thermal conductivity of all materials, diamond makes an extremely good heat spreader or heat sink. The exact value of the conductivity depends on the grain size and type; so controlled growth means that optimal conductivity can be achieved. It is also possible to combine the properties of diamond as a thermal conductor and electrical insulator to use in electronic applications [7]. More recently, that is in the past few decades, interest has grown in potential optical and electrochemical applications, and for this it was important to develop CVD synthesis, as the traditional HPHT method would not produce diamonds of the required shape or size.

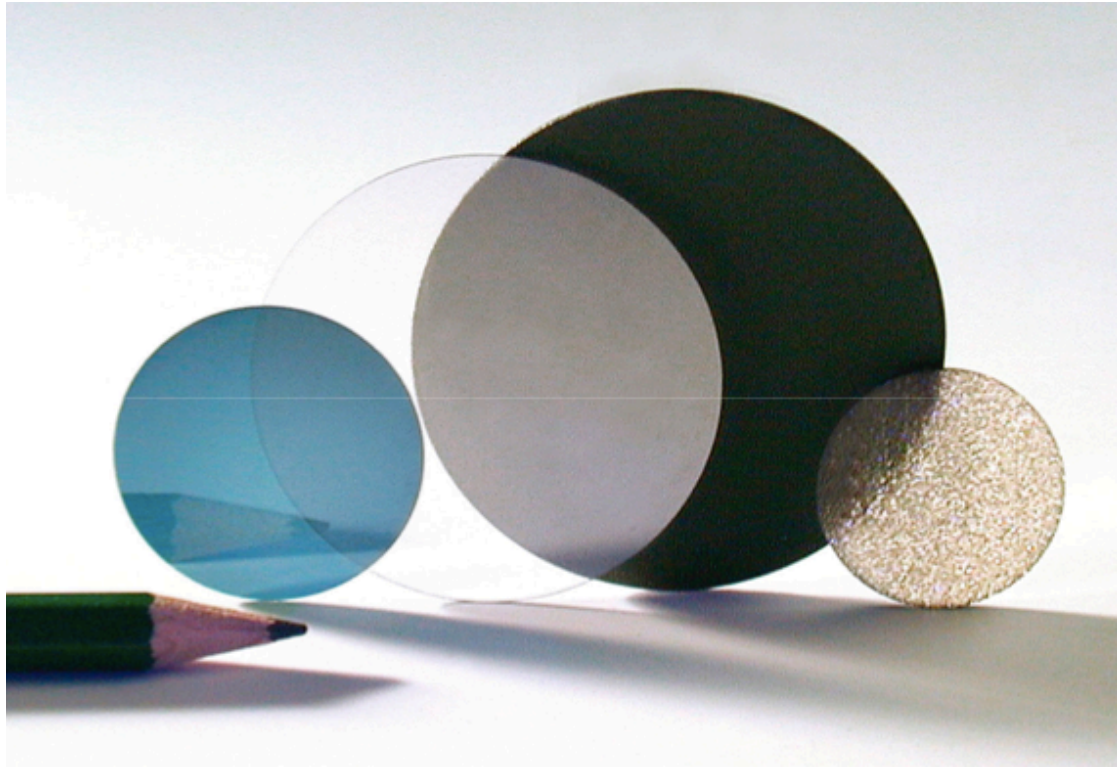


Figure 2. CVD diamond that has been prepared in different ways: (left to right) boron doped, optical grade, mechanical grade and unpolished [9]

This project aims to employ the physical hardness and resistance to corrosion of diamond. Current applications that use diamond in this capacity include the coating of drill bits, and in medicine it can be used in artificial heart valves and joint prostheses [10].

1.2 Chemical Vapour Deposition

1.2.1 Introduction and types of CVD

Chemical vapour deposition (CVD) is the creation of thin films of solid materials from the deposition of a precursor gas onto a substrate under high temperature and low pressure, typically in the region of around 20-40 Torr. It may be employed as a method of creating thin layers of many different materials, ranging from metals to non-metals and some particularly common examples are silicon (for semiconductors), gallium (light-emitting diodes) and aluminium or cadmium-based materials (other types of electrochemical devices) [7]. In addition to these, there are a host of other nitrides, oxides, silicides, borides and carbides that may be and are also prepared by CVD [11].

It was discovered in the 1950's that diamond could be created by this method, potentially providing a route for sourcing the material much cheaper and more efficiently than the traditional mining method. It seems counterintuitive to synthesise diamond at low pressure, given the extremes it takes to make it naturally, however there is a small area where with the right balance of temperature and pressure diamond is the more stable form of carbon (figure 2). Therefore, where a carbon-containing gas is activated near a substrate (see section: mechanism of CVD), the carbon deposition is diamond, rather than graphite as would occur under most circumstances.

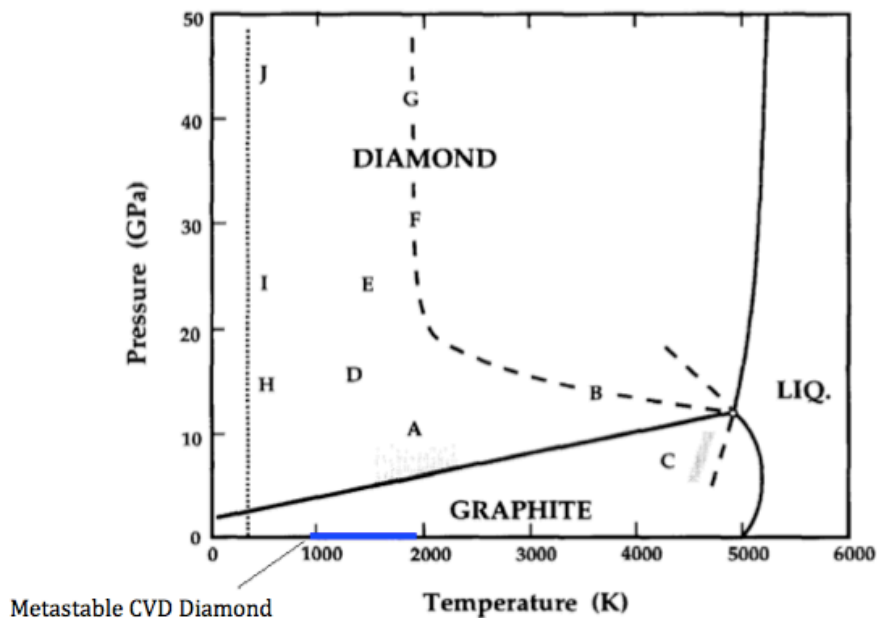


Figure 3. Pressure-temperature phase diagram to show the usual areas of graphite and diamond occurrence, and that of CVD diamond (area in blue) [12].

There are a variety of methods by which materials may be created by chemical vapour deposition, however they all work by the same basic principle: a gas phase reacts to diffuse onto a substrate depositing a solid film, and in order to do so the gas must first be activated to allow the necessary reactions to occur. Most reactors differ by the way the precursor gas is activated, as there are many ways to do this. Some of the most commonly used are described briefly below, however much more comprehensive reviews may be found in references [13] [2].

The first and oldest method is the hot filament CVD (HFCVD) reactor (figure 4), which has a filament made usually of tungsten or tantalum, heated up to 2000°C placed above a substrate heated from below to around 900°C, while the whole apparatus is kept at pressure of approximately 20 Torr. Gaseous CH₄ and H₂ are passed through the reaction chamber at a rate of 2 and 200 scm (cm³ min⁻¹) respectively, and carbon is deposited onto the substrate in a tetrahedral lattice arrangement. Diamond is formed layer by layer (for the mechanism, see section 1.2.2) at a rate of between 1-10 μm h⁻¹, depending on the reaction conditions [14]. The HFCVD method has several advantages such as the ease of use and low operating cost, however there are problems. As mentioned before, the filaments are sensitive to oxidation or reaction with several other gases, so this restricts the type of precursor gases that may be used. At high temperatures, the filaments will begin to degrade, which can lead to contamination of the film as atoms of tungsten or tantalum become incorporated into the diamond as it grows (rhenium is less susceptible to this so is a common replacement). It is possible to reduce this and obtain a purer sample by running the reaction at a lower temperature, for example at 1500°C [15], however this does reduce the growth rate so is not an ideal solution. This being said, contamination is not a particularly significant problem when the diamond being synthesised is to be used in applications that employ the mechanical properties of diamond, such as hard coatings. It is only when used in electronic devices that the purity has to be exceptionally high.

Alternative methods of activating the gas phase include: irradiation with microwaves (as in the microwave plasma CVD reactor) or combustion, either from an acetylene welding torch or plasma jet. In typical microwave plasma reactors, such as that designed by Applied Science and Technology, Inc. (ASTeX) the normal operating microwave power can be up to 1.5 kW and the pressure 40 Torr. The temperature of the plasma is kept at 2000°C and the substrate is heated separately to 800°C [7]. The main advantages of this type of reactor are the faster growth rates (of up to and in excess of 10 μm h⁻¹ [16]), the variety of gases that may be utilised and the cleaner atmosphere due to the absence of a metal filament. It is because of the latter reason that most diamond that is to be used in the electrochemical or electrical industry is made in a microwave CVD reactor, however this does generally cost more than the operation of most hot filament reactors, so in cases where the mechanical properties of diamond are to be employed (such as in this experiment), there may be no added benefit of using the more expensive option, accounting for why hot filament reactors are still the most popular.

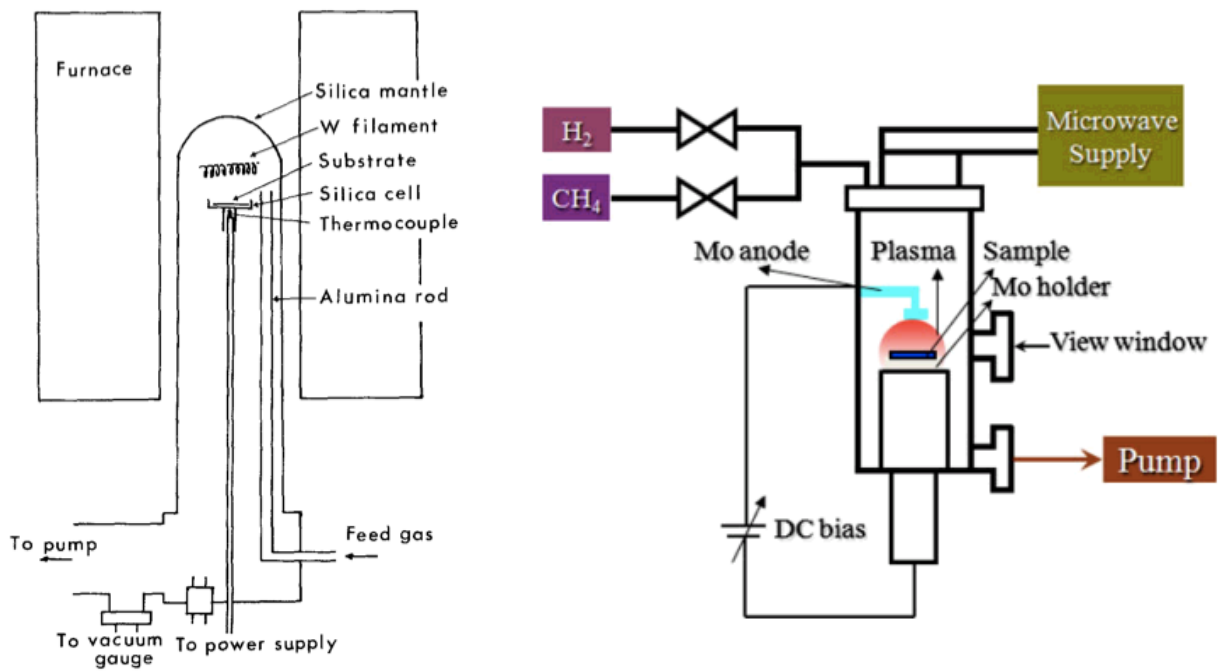


Figure 4a. Left; the hot filament reactor developed by the scientists at NIRIM (1982) [17]. Right; the setup of a typical microwave plasma enhanced CVD reactor [18]

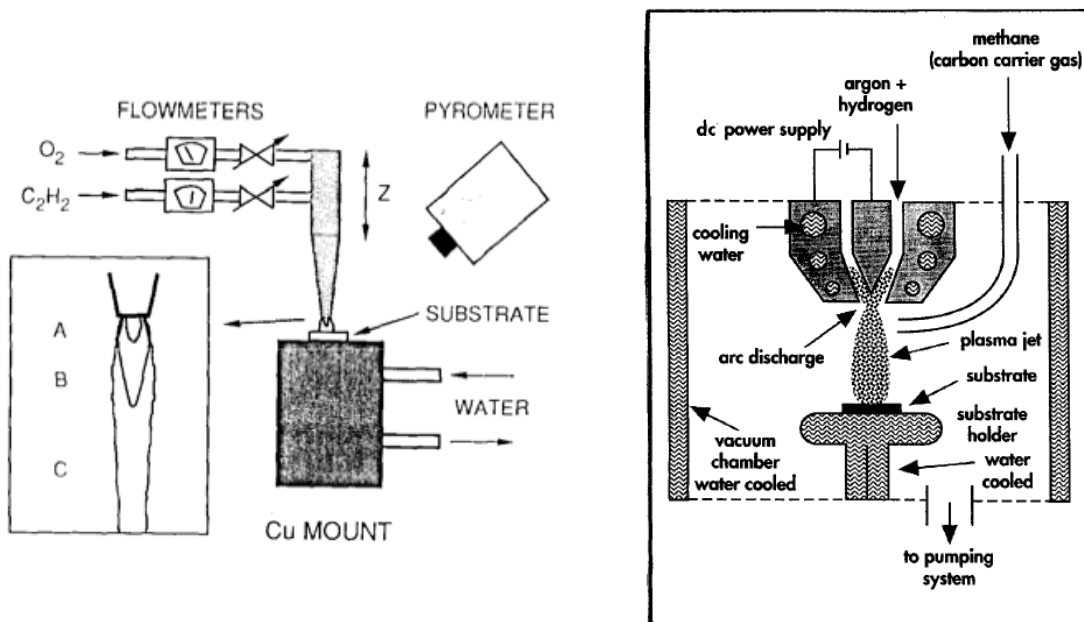
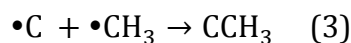


Figure 4b. Left: basic setup of the combustion method, the area of the flame enlarged to the left and marked 'B' is the acetylene feather [17]. Right: an example of the apparatus used for the plasma jet method [19].

1.2.2. Mechanism of Diamond Growth by Chemical Vapour Deposition

Although there are several ways by from to grow diamond via chemical vapour deposition, the same processes need to occur within each for this to happen, and so the mechanism is similar across most methods. For successful deposition of a solid substrate, a few main phases must happen: once the process gas is in the reaction chamber, a set of decomposition reactions must take place (1, 2); this is where molecules in the gas become activated. These active species are much more reactive than their molecular counterparts, and undergo homogeneous gas phase reactions as they diffuse towards the substrate, before adsorbing onto the solid surface via heterogeneous reactions with the surface (3, 4), producing the deposit. Any unreacted precursor gases or by-products are subsequently removed from the reaction chamber by the vacuum pump [20] [21] [16].



Scheme 1. Reactions involved in the formation of diamond by chemical vapour deposition

For the formation of diamond, the carbon for growth originates from the methane. However, it is imperative that if significant diamond evolution is to be observed a large excess of hydrogen is also necessary (ca. 99 %). The activated hydrogen has several roles at different stages of the deposition, including the abstraction of hydrogen from methane (reaction 2) to create the methyl radical [22].

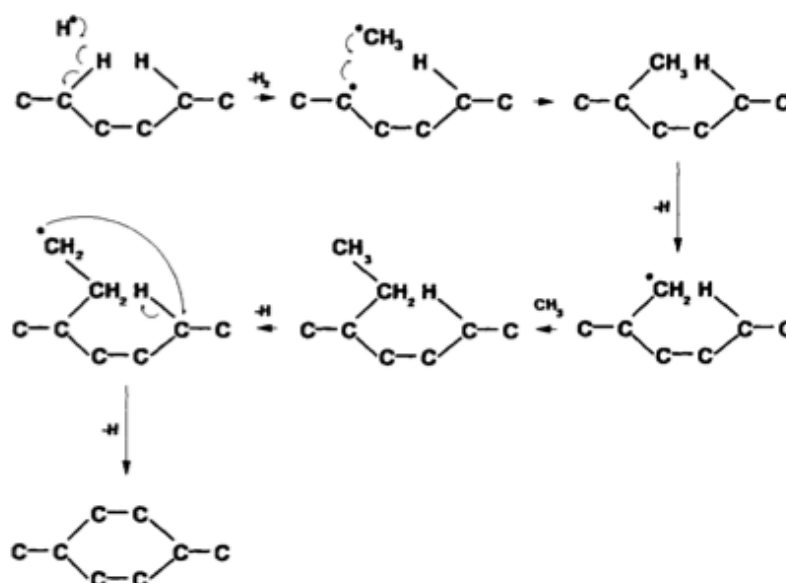


Figure 5. A possible mechanism of diamond growth [23]

At the surface of the substrate, the carbon radical species adsorb to it (reaction 3). The initial step is nucleation on the surface, where formation of a carbide between the substrate and carbon species provides a base for further growth (reaction 4). This occurs when diffusion along the surface of the substrate occurs, making an even film. The carbide is important as a means to bind the diamond and substrate together, as without it the diamond formed will usually break up or at the very least fall off the substrate. It is possible for diffusion of carbon into the substrate to arise, which is generally undesirable beyond a small amount as it can result in a large proportion reacting to form a carbide, with little to no diamond growth as a result.

1.3 Zirconium: properties, compounds and their uses

1.3.1 Physical and Chemical Characteristics of Zirconium Metal

Zirconium is a group four, second row transition metal that is fairly soft and ductile with a lustrous, pale grey appearance. Lying above hafnium and below titanium, it has many properties in common with these two other metals and in particular hafnium [24]. It is the fourth most abundant transition metal in the Earth's crust, although is not found as the pure metal; the two forms in which zirconium occurs naturally are baddelyite (ZrO_2) and zircon ($\text{Zr, HfSiO}_4 \cdot x\text{H}_2\text{O}$) [25]. Zircon, a mineral containing small amounts of hafnium in addition to zirconium is the primary source for obtaining zirconium metal and which occurs in parts of the USA, South Africa and Australia. There tends to be a presence of around 1-3% Hf [26] in the mineral (1-5% in the extracted zirconium metal) which usually remains after processing to obtain Zr metal, as its similar properties mean that under most circumstances it does not reduce performance of the metal in any way [27].

Commercial preparation and purification of zirconium metal can be achieved in two different ways. The first to be developed was the crystal bar or iodide process in the 1920s [28]. This method of refinement can only yield small quantities of zirconium, however what it does produce is of very high purity, so is still used under certain circumstances. Zirconium ore is heated to approximately 200°C in the presence of iodine until gaseous zirconium tetrachloride forms, leaving any impurities in the remaining solid left behind. Within the same reaction chamber, a filament made from tungsten is heated to 1300°C upon which the ZrCl_4 decomposes to leave a deposit of very pure Zr metal over the course of several hours or days [29].



Figure 6. Left; some samples of recently cut zirconium [30]. Right; zirconium that has been left open to the air for a year and as a result has developed a thick oxide layer and appears much duller [31].

The second, more commonly used processing technique is the Kroll process, which was invented by William Kroll soon after the crystal bar method was established in the 1930s [32]. Also known as the Magnesium Reduction process, the Kroll process is also

used to extract titanium from its ore, and for steel refinement to gain a superior grade of alloy by the removal of oxygen and nitrogen. In order to obtain zirconium, zircon is heated in a furnace or fluidised-bed reactor to 1000°C, before chlorine gas is introduced into the reaction mixture to afford the gaseous compound $ZrCl_4$, which is easily separated from the remaining solid to be condensed. A reduction by magnesium is then carried out to yield the pure metal [33] [34].

Despite being similar in several aspects, a very fundamental difference between Zr and Hf is that of the cross sectional neutron capture (neutron absorption). Zirconium has a very low value for this, and thus radiation in the form of neutron bombardment can pass through relatively unaffected. Conversely, hafnium has a cross sectional neutron capture value around 600 times that of zirconium, so even though Hf is only present in a few percent, it can significantly affect the performance of the metal in an environment where absorption of neutrons is undesirable [26]. Such an environment is that of within nuclear reactors, where zirconium-based alloys are used as cladding for nuclear fuel rods. In this situation, neutrons have to be able to pass almost unaffected through the metal, so it is imperative that hafnium is removed.

The separation of zirconium and hafnium is somewhat tricky, due to the number of properties that they share [35]. In addition to neutron capture, there are a few differences between the metal that can be exploited to ensure their successful separation. The density of zirconium is about half that of hafnium, and their melting points differ by a reasonable amount. One of the earliest methods of separation was to make use of the latter; the metal containing hafnium impurities would be heated until completely melted. After this point, the metal solution would be cooled and hafnium, with the lowest melting point, would condense first and sink to the bottom to be removed. After several cycles of this an acceptable purity of the zirconium could be achieved [29]. 'Acceptable' purity requires that the concentration of hafnium left within the metal is less than 100 ppm [24]. Some more commonly used, modern methods include solvent extraction [36] [37] [38], distillation of fused salts [39] [40] and ion exchange [41]. Solvent extraction can be carried out in a wide variety of solvents; one example is where $ZrCl_4/HfCl_4$ can be made into an aqueous solution then shaken with methyl isobutyl ketone. $ZrCl_4$ remains in the aqueous layer whilst $HfCl_4$ dissolves into the ketone; subsequently both layers can be separated and reduced into pure metal [42] [29]. In the tables below, the properties of particular interest with respect to separation or application within the nuclear industry are highlighted in bold.

Table 2: A selection of the physical and chemical properties of zirconium metal [43] [26]

Property	Value	Units
Atomic Weight	91.224	Atomic Mass Unit
Density	6.52	g cm⁻³
Melting Point	1855	°C
Boiling Point	4409	°C
Thermal Expansion	5.7	µm.m ⁻¹ .K ⁻¹
Electronegativity	1.33	Pauling Scale
Magnetic Properties	Paramagnetic	Units
Electrical Resistivity	421	nΩ.m
Thermal Conductivity	22.6	W.m ⁻¹ .K ⁻¹
Cross Sectional Neutron Capture	0.19	Barn
Young's Modulus	88	GPa
Mohs Hardness	5	Dimensionless

Table 3. Properties of hafnium metal [26]

Property	Value	Units
Atomic Weight	178.49	Atomic Mass Unit
Density	13.3	g cm⁻³
Melting Point	2233	Celsius
Boiling Point	4603	Celsius
Thermal Expansion	5.9	µm.m ⁻¹ .K ⁻¹
Electronegativity	1.33	Pauling Scale
Magnetic Properties	Paramagnetic	Units
Electrical Resistivity	331	nΩ.m
Thermal Conductivity	23	W.m ⁻¹ .K ⁻¹
Cross Sectional Neutron Capture	106	Barn
Young's Modulus	78	GPa
Mohs Hardness	5.5	No Units

Most applications of zirconium are based upon its limited reactivity under normal operating conditions; aside from its high melting and boiling points, zirconium is also very resistant to chemical attack or corrosion from most acids and alkalis, though this resistivity cannot be attributed directly to the metal. Almost instantaneously after processing, the surface of zirconium will react with any oxygen present in the surrounding atmosphere to form a passivation layer between 2-5 nm thick [44] of ZrO₂, an extremely stable dioxide that will not decompose except under very harsh conditions. It is because of this protective surface oxide that the metal is so resistant to heat and corrosion, allowing for its use in nuclear power as well as harsh chemical environments. Zirconium is not particularly sensitive to most acids or alkalis but will be corroded if it comes into contact with hydrogen fluoride, hot sulphuric or hot hydrochloric acid [43]. Additionally, the metal has a reasonably large solubility for light atoms (oxygen or smaller) [45].

In addition to the oxide, zirconium also forms strong hydrides and carbides, though it is far harder to make these initially. The former is created when, in the absence of oxygen, zirconium metal reacts with hydrogen gas and will occur slowly at room temperature, although if being made in quantity will usually be done closer to 500 or 600°C [46]. If a layer of oxide is present, it will not be displaced by hydrogen in favour of creating the hydride, however heating to over 500°C under vacuum causes the oxygen to diffuse away from the surface into the bulk zirconium allowing the hydride to be formed [47]. In order to achieve successful diamond growth, the formation of a zirconium carbide interface between the two materials is particularly important to ensure the adhesion of the diamond film to the substrate. High temperatures of several hundred to several thousand degrees are essential for the synthesis of ZrC, which is usually carried out by sintering or carbothermic reduction [48] [49]. Temperatures in the hot filament reactor to be used vary from approximately 2000°C at the filament to 900°C at the substrate, consequently there should be enough thermal energy available to activate a reaction between carbon in the process gas and the surface of the zirconium.

Of additional interest in this experiment is the coefficient of thermal expansion. If diamond is to grow on a zirconium substrate, it is desirable that the extent to which each expands under heating is as close as possible. Diamond expands very little when heated (just $1 \mu\text{m m}^{-1} \text{K}^{-1}$), and at 5.7 times larger, the expansion coefficient of zirconium is considerably more, which may pose a risk of the diamond film delaminating from the substrate. However, successful CVD growth is frequently observed on molybdenum substrates, which has a thermal expansion coefficient of $4.8 \mu\text{m m}^{-1} \text{K}^{-1}$ [26], which suggests that the diamond is able to sustain a certain amount of stress provided a strong enough carbide interface is formed. As there is not a particularly large difference between the coefficients of Mo and Zr it is hoped this will not be a concern.

There are several types of zirconium that are commercially available, from the pure metal to several different alloys or varying composition. What is termed 'commercial zirconium' is zirconium that has been processed to yield the metal without the removal of hafnium. 'Reactor grade' zirconium is that which has had very nearly all of the hafnium removed, and is usually then alloyed with a number of other metals before being used within nuclear reactors. Other types such as 'sponge zirconium', which is porous [50] and 'flashbulb-grade zirconium', which is high in oxygen [51], are also available, though less sought after. The high resistance to corrosion and low cross section for neutron capture have led to the primary use of zirconium (albeit in alloy form) being as cladding for fuel rods in water-cooled nuclear reactors and nuclear powered submarines. Depending on the size of the reactor, there may be over 150 km of zircaloy tubing present [26], so it is no surprise that over 90% of zirconium production is solely for the nuclear industry. The main use of non-reactor grade, unalloyed zirconium is in the chemical industry as part of plant construction where other elements are susceptible to corrosion, whilst other uses include as a getter in vacuum tubes, due to its ability to absorb oxygen and as an alloying agent in steel to provide extra strength. There is no known biological role for zirconium and it is non-toxic, which allows it to be used also in the medical profession as surgical tools. When

combined with niobium, the alloy becomes superconducting at low temperatures so also finds applications as superconducting magnets [25]

1.3.2 Zirconium Dioxide; properties, uses and chemistry

As mentioned previously, zirconium dioxide is the very dense, inert compound that forms readily on the surface of zirconium metal upon exposure to water or air. The most common oxide of Zr is the dioxide, due to the preferred oxidation state of +4. Also known as zirconia (not to be confused with zircon, which is the natural mineral), and the naturally occurring but rare mineral baddeleyite. In areas where silica is present, baddeleyite converts into zircon (Zr, Hf)SiO₄ • xH₂O (where Hf is present in the stated 1-3%), and the fact that silica is so common accounts for its scarcity [52].

Table 4. A selection of the properties of zirconium dioxide (cubic polymorph) [27] [26]

Property	Value	Units
Molecular Formula	ZrO ₂	N/A
Molar Mass	123.218	g mol ⁻¹
Density	5.68	g cm ⁻³
Melting Point	2715	°C
Boiling Point	4300	°C
Thermal Expansion	10.5	µm.m ⁻¹ .K ⁻¹
Thermal Conductivity	1.7	W.m ⁻¹ .K ⁻¹
Fracture Toughness	12	Mpa.m ^{1/2}
Young's Modulus	205	GPa
Mohs Hardness	8	Dimensionless
Solubility	Soluble in only HF and hot H ₂ SO ₄	N/A
Refractive Index	2.13	Dimensionless

Zirconia is a white, crystalline solid with a monoclinic prismatic crystal structure at temperatures below 1170°C [53]. Industrial production is achieved by the calcination of zirconium ores, as the thermal stability is so high that when zircon is heated in a furnace to around 1000°C, ZrO₂ is the sole remaining zirconium compound [27]. There are in fact three crystalline forms of ZrO₂, that form dependent on temperature, and two further orthorhombic forms that occur under high pressure [54], [55].



Figure 7. Shown on the left is the mineral form of ZrO_2 ; baddeleyite [56], right is a cut crystal of colourless cubic zirconia [57]

At room temperature and up to approximately $1000^{\circ}C$ zirconia has a monoclinic arrangement, however when heated to above this the structure transitions to a tetragonal arrangement. A further phase transition occurs above $2370^{\circ}C$ to a cubic structure; also known as the popular imitation diamond cubic zirconia [58]. This is a very stable, cubic crystalline form of zirconia that is made by the skull crucible method. This is a technique developed to overcome the problem that there is no commercially available material that can withstand the temperatures required to produce the cubic form. It involves heating of the powdered zirconia starting material by RF induction whilst cooling the outside so that solid zirconia forms a vessel for the molten compound inside. Cubic zirconia is naturally clear and colourless, though certain dopants (such as cerium or chromium) may be added to the starting material to achieve a coloured product [59]. In most commercial applications the crystal structure is likely to be either tetragonal or cubic, as the pure monoclinic polymorph is not as stable, having a tendency to shatter upon cooling.

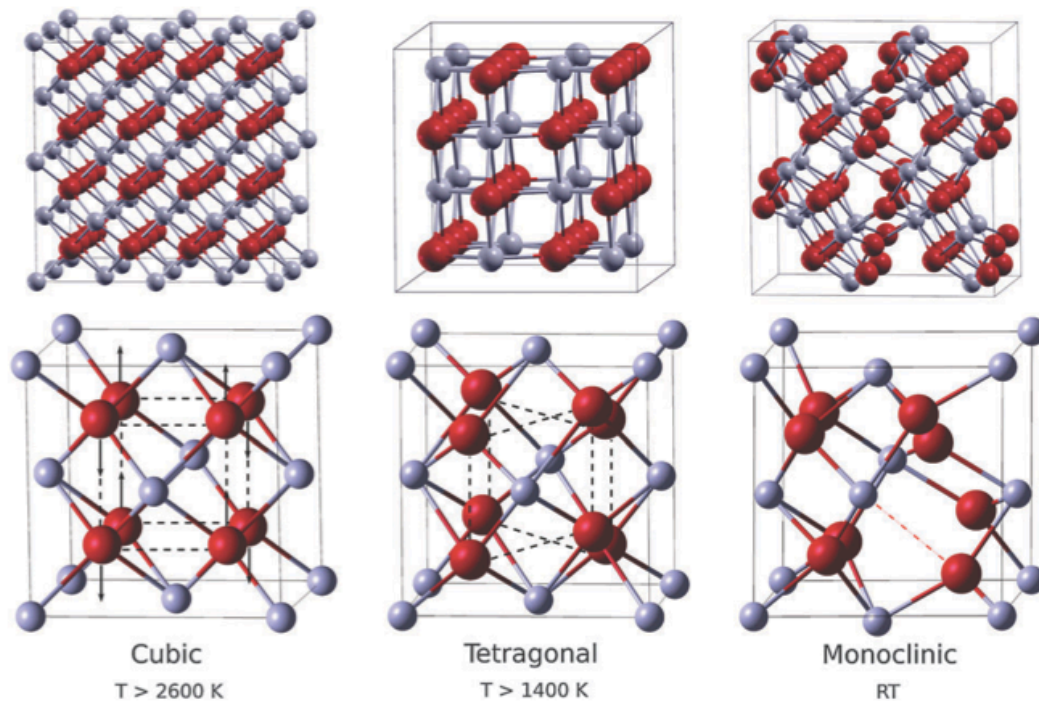


Figure 8. The three lattice structures that may be adopted by ZrO_2 and the temperatures at which they do so. The bottom line shows the unit cell whilst the top signifies the larger crystal structure. The red spheres represent zirconium and the grey ones oxygen [60].

The inherent stability of zirconia, especially that of the tetragonal and cubic forms means that its chemistry is fairly limited. Most commercial applications employ this inertness, however there are circumstances under which reactions can and will occur. Like zirconium metal, ZrO_2 is stable to attack from most acids and alkalis, but is susceptible to fluoride-containing reagents such as hydrogen fluoride or hot sulphuric acid. When heated to approximately 1000°C in the presence of a halogen (Cl, Br, I) the corresponding zirconium tetrahalide is formed; this is in fact the first step of the industrial Kroll Process (equation 5). If heated to over 2000°C in the presence of graphite, it is possible to yield the ceramic compound zirconium carbide.



There are several commercial applications that zirconia is commonly used for in industry. The high melting point, hardness and chemical inertness mean that zirconia-based ceramics such as yttria-stabilised zirconia are commonly used for enamels, abrasives [27] and in some biological applications such as dental veneers, due to the fact that it is also biologically inert [52]. Less well-known uses include as a replacement for silicon dioxide in certain electronics [61] [62] [63], as a catalyst [64] [65] or in high-temperature solid oxide fuel cells [66]. Zirconia has an ability to conduct oxygen, which allows for its use as an oxygen sensor in car exhausts or as a means to measure its partial pressure in the breathing gas in diving tanks [67].



Figure 9. Some applications of zirconia ceramics [68]

The properties of ZrO_2 may present a possible challenge in the experiments to be carried out as part of this study. In order for diamond to adhere properly to the zirconium substrate, the layer of oxide on the surface needs to be displaced in favour of forming the carbide interface between metal and diamond. ZrO_2 is the easiest zirconium compound to synthesise by far, and unless the reactor can replicate the extreme temperatures essential for this, the initial nucleation may not happen as efficiently as it should, if it does at all. The most likely scenario if the oxide remains during the reaction process, is that the carbon radicals will nucleate and grow on the substrate, but fail to adhere to it. Temperatures in the hot filament reactor that is to be used for the bulk of the experiments planned can reach up to 2000°C in the filament and 900°C by the substrate, so it is quite possible that the oxide will be burnt off in situ. Additionally, there are methods of pre-treatment that may address the issue. It is best to pre-seed or prepare the sample before reaction to aid nucleation and increase the quality of the film grown. A common way to do this is to manually abrade the surface of the substrate with diamond dust, which is likely to remove at least some of the oxide.

1.3.3 Properties, uses and chemistry of zirconium carbide

As mentioned previously, zirconium can and does form a carbide under certain conditions. This is extremely important, as diamond can grow by CVD on many different substrates, but if it is to adhere to said substrate a carbon-metal interface must form: in other words, a carbide.

Zirconium carbide is a very hard, black ceramic capable of withstanding extremely high temperatures and with many properties similar to titanium carbide [69]. It has a cubic NaCl-type structure [70] and the strong covalent bonds it possesses give rise to its high melting and boiling points, while the presence of some metallic bonding accounts for some thermal and electrical conductivity similar to that of zirconium metal [71].

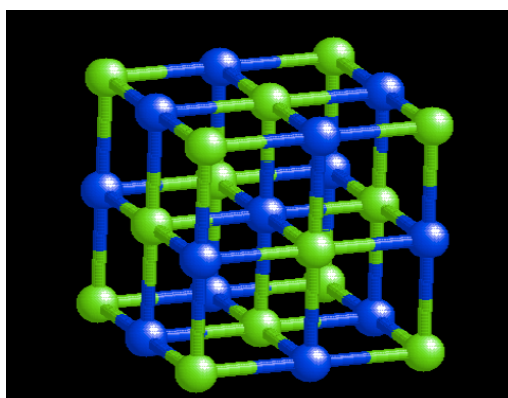


Figure 10. Left: the crystal structure of zirconium carbide [72]. Right: commercially available ZrC powder [73].

Table 5. Some properties of zirconium carbide [26] [74] [63] [75]

Property	Value	Units
Molecular Formula	ZrC	N/A
Molar Mass	103.235	g mol ⁻¹
Density	6.73	g cm ⁻³
Melting Point	3532	°C
Boiling Point	5100	°C
Thermal Expansion	6.6	µm.m ⁻¹ .K ⁻¹
Thermal Conductivity	20.5	W.m ⁻¹ .K ⁻¹
Fracture Toughness	3 to 4	Mpa.m ^{1/2}
Young's Modulus	400	GPa
Mohs Hardness	9	Dimensionless
Solubility	Soluble in only HF and hot H ₂ SO ₄	N/A

The preparation of ZrC in industry usually needs very extreme conditions; the most common commercial method of producing ZrC is sintering or the carbothermic reduction of zirconia (reaction 6) [76]. Sintering is carried out at temperatures between 1950 and 2300°C, under pressures of at least 40 MPa [77], whilst carbothermic reduction is a process that involves heating ZrO₂ in a graphite furnace to temperatures in excess of 2000°C [49]. It is possible to reduce the temperatures required for this synthesis to around 1000°C by using different techniques such as solution-based processing of nano-sized ZrC particles, but presently this is only done on a small scale, and is not an industrial process [78] [79].



An alternative method that has been studied for some time is that of using chemical vapour deposition to make a thin coating of zirconium carbide on a substrate (often

graphite, but other potential applications are being researched). As with CVD of diamond, gaseous precursors are required and the standard compounds used in this synthesis are methane and zirconium tetrachloride in a hydrogen/ argon atmosphere, and the temperature of reaction is kept at 1350°C [80]. ZrC made by CVD is of particular interest as it is being investigated as a possible replacement for silicon carbide (SiC) as a coating for fuel particles in certain types of nuclear reactor [81]. Zirconium carbide is superior to the currently used SiC in several ways, most notably its very low neutron capture cross section (similar to that of zirconium) and resistance to heat and radiation [82] [83]. Another potential application of CVD ZrC is as a protective coating on carbon-carbon composites, as it is so resistant to heat that it could be used to protect spacecraft as they leave and enter the Earth's atmosphere [84].

There are many additional proposed uses for the ceramic ZrC, however despite the extensive research that has been carried out over the last 40-50 years [85] [86] its use in industry is limited, most likely because the current means of synthesis are not quite up to the standard required. Development of the methods currently used is continuous and improving, for example new precursors are being investigated for CVD – tetraeneopentyl zirconium, $Zr[CH_2C(CH_3)_4]$ will allow carbide growth on a substrate at temperatures as low as 400°C. However, despite this advancement, the growth rates achieved under temperatures this low are only around 100 nm h⁻¹, and the stoichiometric control is poor; anything from ZrC to ZrC₅ has been observed on the product [87]. Current applications that are in use today include coatings on cutting tool and high performance kitchen knives, though their performance is often not up to the same standard as metal tools, so perhaps are not quite ready for commercial use.

The difficulty of forming ZrC may present a problem in the experimental part of this study. Most processing methods require zirconia to be in powder form to maximise surface area and reduce the temperature needed for reaction. Therefore, it may prove challenging to make the zirconium carbide interface that is crucial in order for the diamond layer to adhere to the metal substrate. It is possible that this will happen in the reactor; the temperature reached by the filament in the reactor to be used can reach 2000°C, which should be adequate for carbide formation, however whether it will react with the bulk metal remains to be seen.

1.3.4 Preparation, properties and chemistry of zirconium hydride

The name zirconium hydride can mean one of two things: the compound Zr(II)H₂, or the ZrH_x alloy where x can be a one of several values between 1 and 4. There is very little information available on the compound Zr(II)H₂ and few uses; most are in research [88]. Appearance is usually as dark grey, metallic powders and in terms of electronic and magnetic properties similar to zirconium metal. Once formed, zirconium hydride (ZrH₂) is stable to air and water at room temperature, though will convert to ZrO₂ if left open to the air. At temperatures of 250-300°C the compound will ignite spontaneously: one of its few uses employs this property by using it as a component of pyrotechnics [89]. Some other applications quoted include as part of the synthesis of some zirconium ceramics, investigating the oxidation of metal hydrides and creating certain ceramic composites via the metal alloy [90] [91].

The alloy has much more interesting chemistry and several more uses. Zirconium hydrides are the result of reacting zirconium metal with hydrogen gas, either at room temperature or, for faster synthesis in commercial processes at elevated temperatures of around 500-600°C [92]. Formation of the hydride is slow; even though it will form unassisted at room temperature, even when conducted at 600°C the reaction can still take up to several days to complete. The alloy is formed when hydrogen atoms diffuse into spaces in the zirconium lattice and as their presence in vacancies or between atoms prevents the metal atoms moving around very easily, the alloy is harder than the pure metal. There is more than one structural form of zirconium; at room temperature, the most stable is hexagonal close packed (HCP) α -zirconium, which can dissolve up to 5 or 6 atom % hydrogen. When heated to above 800°C or so the structure becomes body centred cubic BCC (β -zirconium), which has more space between atoms in the lattice, allowing more hydrogen to dissolve, ca. 20 atom % hydrogen [47]. The percentage of hydrogen that can be present in the alloy increases with temperature up to approximately 1400°C, when figures of over 60 atom % hydrogen can be reached (equivalent to ZrH_2) [93]. Density varies from 5.56 to 6.52 depending on the proportion of hydrogen dissolved into the lattice: there is no increase in volume as hydrogen is incorporated, so density increases with hydrogen addition [94].

This hydriding of zirconium has significant impact on the use of zirconium within the nuclear industry, and significant research has been conducted based on this, which is discussed in more detail in section 1.4.3.

In the CVD reactor, if the hydride is formed it is likely that at the temperature of the reactor, the BCC structure will be made. However, it is unlikely that there will be significant hydride formation as despite the excess of hydrogen gas in the atmosphere, the rate of reaction is slow enough that to get it to form to any appreciable degree, the usual process takes several days at around 800-900 K, and probably longer than the CVD experiments will run for [46]. Additionally, if conditions are able removal of the surface oxide, the carbide is likely to be formed in favour of the hydride, though it is quite probable that a small amount of hydrogen could dissolve into the substrate.

1.4 Nuclear Applications of Zirconium Alloys

1.4.1 Types of zirconium alloys, their chemistry and use

The properties of zirconium, and in particular its high resistance to corrosion and very low neutron absorption make it the ideal candidate for certain applications within the nuclear industry. Most uses are structural, and it has been used as fuel cladding and other structural components since the 1950s, however was initially only found in nuclear submarines belonging to the US Navy; it was deemed to expensive for use in commercial nuclear reactors. However, within a decade or so zirconium was commonplace in nuclear power stations: it had been decided that the material properties provided enough benefits to outweigh the higher cost when compared to the steel that was used previously. More specifically, zirconium is present in the fuel cladding (containment tubing) of UO_2 fuel in water-cooled reactors.

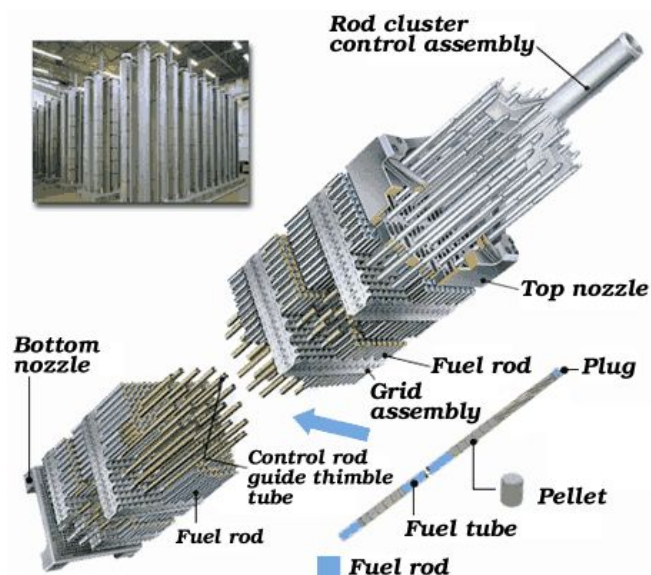


Figure 11. Left: a diagram depicting how fuel rods are assembled in a nuclear reactor: top left shows several assemblies: central is a close up of one assembly, containing up to ~250 fuel rods. Bottom right shows one fuel rod and a representation of a UO_2 fuel pellet [95].



Figure 12. Small sections of fuel rod cladding that demonstrate the diameter of the tubing. In an assay in a reactor, these tubes would be 4 meters long. [96]

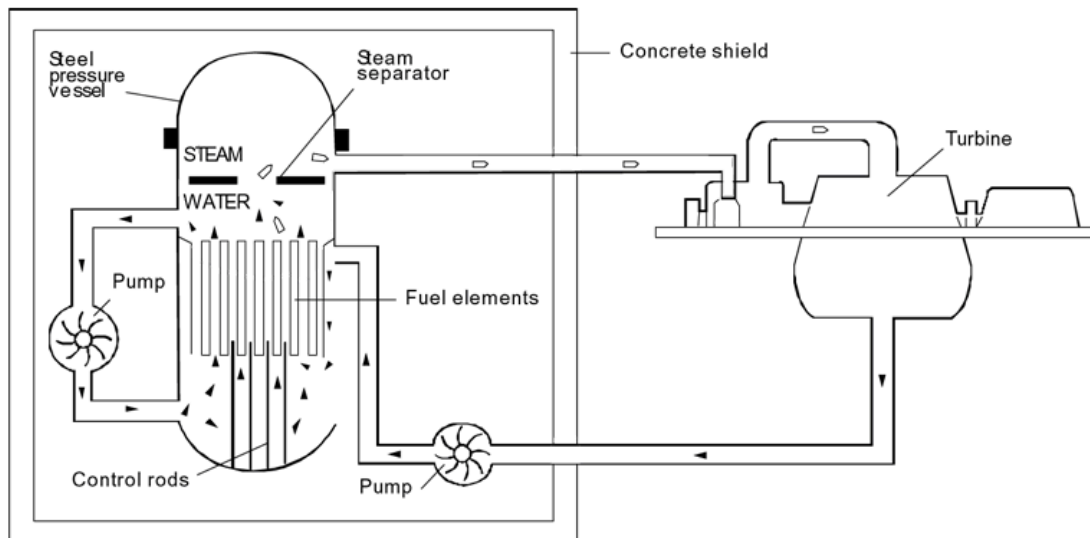


Figure 13. Diagram of a boiling water reactor (BWR) [97]. This type of reactor uses light water (rather than heavy or deuterated water, D_2O). During operation nuclear fission is occurring inside the fuel elements, which are clad in zirconium alloy. The heat produced by this causes the water (represented by black triangles) to turn into steam (white markers), which drives a turbine before condensing and returning to the reactor core [98].

There are several other types of nuclear reactor besides the BWR above, such as the pressurised water reactor (PWR), which also uses light water. Also in use are the heavy water reactors: the CANadian Deuterium Uranium (CANDU) and RBMK (stands for – in Russian: *Reaktor Bolshoy Moshchnosti Kanalnyy*, which is translated as ‘high-power channel-type reactor’). In the PWR and CANDU, water or heavy water is used as a moderator and coolant, and thus the chemistry with the zirconium cladding is similar to that within the BWR depicted above. Graphite is the main moderator in the RBMK, however the fuel rods clad in zirconium are still situated in water. Consequently, any chemistry discussed henceforth that concerns the moderator-cladding interaction would be applicable to any of these reactor designs.

In nuclear reactors, zirconium is not used as the pure metal, but instead made into one of several alloys before use in reactors; mainly to further increase its hardness and resistance to corrosion. The most common alloys used in water-cooled reactors in the UK come under the trade name Zircaloy, which refers to either of the alloys Zircaloy-2 or Zircaloy-4. Additionally, there are several other alloys used in the USA, Russia, and Japan, the composition of which is summarised below. Of note is that the hafnium content in nuclear grade zirconium is legally required to be below 0.01%, and that the remaining amount not shown in the table is comprised of zirconium (96-98%).

Table 6. Some of the commercially available zirconium alloys and their compositions [99] [100] [101]

Name of Alloy	Amount of Alloying Metal					
	Sn	Nb	Fe	Ni	Cr	O
Zircaloy-2	1.5	-	0.015	0.05	0.1	0.12
Zircaloy-4	1.5	-	0.21	-	0.09	0.12
ZIRLO	1	1	0.1	-	-	0.12
Zr-2.5 Nb	-	2.5	<0.15	-	-	0.12
Zr Sponge	-	-	0.04	-	-	0.075

Table 7. Physical properties of Zircaloy-4 [99] [102] [101]

Property	Value	Units
Density	6.55	g cm^{-3}
Melting Point	1850	$^{\circ}\text{C}$
Coefficient of Thermal Expansion	6	$\mu\text{m.m}^{-1}.\text{K}^{-1}$
Thermal Conductivity	21.5	$\text{W.m}^{-1}.\text{K}^{-1}$
Cross Sectional Neutron Capture	0.22	barn
Young's Modulus	99.3	GPa
Mohs Hardness	3.2	Dimensionless

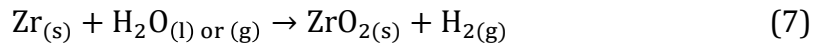
The Zircalloys -2 and -4 are composed of very similar amounts of alloying metals, apart from one small but noticeable difference. It was discovered in the late 1950s that nickel facilitated hydrogen pickup in zirconium [103]. As a result, the nickel-free Zircaloy-4 was developed, which absorbs less than half as much hydrogen as its predecessor [104] [105]. Although Zircaloy-4 has been present in reactors since the 1960s [106], the Ni containing Zircaloy-2 is still used today (in BWRs and the CANDU), which suggests that although hydrogen pickup is a problem, it is not so bad that it needs to be removed from all types of reactor [107].

Hydrogen pickup, or the dissolution of hydrogen into zirconium is one of the few, but significant drawbacks of using Zr alloys in nuclear reactors and can occur when the oxidation of zirconium liberates hydrogen. The corrosion mechanisms for both oxidation and hydriding have been studied extensively in order to discover the mechanisms of each, as together they are at present the main limiting factor in the lifetime of zircaloy cladding tubes.

1.4.2 Oxidation of zirconium in nuclear reactors

The air-formed oxide of a few nanometres that is always present on zirconium acts as a protective barrier against many things. However, in water-cooled nuclear reactors, the temperatures result in oxygen from water or steam corroding the zirconium component of the alloy in use via oxidation, in a process that liberates hydrogen (reaction 7) [108]. Initially, oxygen diffuses a short way into the top layer of the metal

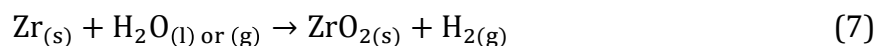
until the solubility limit is reached. After this, ZrO₂ begins to form and a layer gradually builds up, limited by the rate at which oxygen can diffuse through the oxide [109] until it reaches a depth of approximately 2 μm [44].



This process is termed ‘pre-transition’ and the oxide formed here is the tetragonal phase. According to data, the most stable oxide phase at room temperature and pressure is the monoclinic; however compressive stress between the metal and metal oxide incurred by the expansion on transitioning from one to the other is enough to make the tetragonal polymorph predominate [110]. Upon exceeding the pre-transition and entering the post-transition phase, the oxide layer reaches a thickness whereupon the compressive stress exerted is not sufficient to form the tetragonal phase, and the monoclinic structure results. This is much weaker and will crack or flake even at room temperature. Eventually there are enough cracks and fissure in the oxide layer to cause separation from the underlying metal, and the corrosion process starts over [111] [112]. Consequently, the metal is gradually worn down over time and will eventually need replacing.

1.4.3 Role of hydrogen; hydrogen embrittlement and delayed hydride cracking

Another, perhaps more serious effect of the oxidation of zirconium alloys is the hydrogen that is liberated during the process (reaction 7). Atomic hydrogen generated by the dissociation of water due to irradiation or molecular hydrogen from the oxidation reaction [106] (reactions 7 and 8/9) diffuses through the oxide layer via anion vacancies along grain boundaries and dislocations to reach the metal [113]. As with oxygen, a certain amount of hydrogen can dissolve into the zirconium, forming an interstitial solid solution.



Scheme 2. Methods by which hydrogen may be generated before absorption into zirconium alloy cladding; the oxidation (7) provides most free hydrogen. However, decomposition of water caused by irradiation (8) results in hydrogen cations, which pick up electrons and remain as atomic H (9) as they enter anion vacancies in the ZrO₂. Alternatively, the H atoms recombine to form atomic H₂ (10) and diffuse through the oxide layer as a molecule.

The quantity of hydrogen that can be dissolved depends on factors such as temperature, pressure and concentration of oxygen: zirconium is much more soluble to hydrogen at high temperatures. For example, 50% solubility above 500°C compared to 1% at 300°C and lower [114]. Evidence also shows that oxygen can affect the solubility

of hydrogen in several ways; up to 600°C, increasing oxygen concentration within the metal decreases the absorption of hydrogen [115]. However, between the temperatures of 600 and 750°C, oxygen concentration and hydrogen uptake/ solubility become proportional [116]. Additionally, absorption is easier and quicker before the transition period of oxide formation [117]. Certain alloys are less susceptible to hydrogen uptake than others; the realisation that nickel contributed to H₂ absorption led to the development of Zircaloy-4, a nickel-free version of Zircaloy-2. The hydrogen absorption in Zircaloy-2 is up to 50%, yet only around 20% in Zircaloy-4 [105] [104].

Up to this point, hydrogen is fully dissolved within the alloy in a solid solution; therefore the structure of the metal remains unchanged. Further absorption beyond that of the terminal solid solubility point results in precipitation in the form of zirconium hydride, and it is here that problems arise [118]. ZrH₂ is brittle, and its presence within the alloy causes a corresponding reduction in ductility and an increase in brittleness: something that can cause micro-cracks or fissures to occur. Because the solubility of hydrogen is relatively high at elevated temperatures (such as the operating temperature of a nuclear reactor) [119], precipitation usually tends to occur in large excess when the reactor is cooled down in order to load new fuel [120]. As the temperature is brought down, hydrogen that is dissolved in the metal precipitates into the zirconium hydride, making the cladding more prone to cracking or shattering in places, rendering it useless: this is termed 'hydrogen embrittlement' and is the source of the much studied delayed hydride cracking (DHC) [121]. This DHC, along with corrosion by oxidation, is the limiting factor in the lifetime of Zircaloy fuel cladding; hence a means to reduce or prevent this is very much sought after, though presently there seems to have been little advancement since the introduction of Zircaloy-4 in the 1960s.

1.5 The Fukushima disaster and need for change

The oxidation and hydriding process discussed in the previous section, though troublesome with respect to cooling down to reload the reactor core and lifetime of the cladding, rarely pose a real threat to health or safety during normal operating conditions: mainly because mechanical failure (if it is going to occur) is likely to happen when the reactor has already shut down. Yet a very serious issue can arise when operating conditions become abnormal, such as in the case of a nuclear accident or meltdown.

A nuclear meltdown describes a major accident that results in severe damage or melting of the radioactive core of a reactor. This occurs due to overheating, which is permitted to take place due to a failure of the cooling system or coolant: for example a loss or reduction in efficiency. If this occurs the fission reaction is not controlled and will increase to the point where it cannot be controlled and a vast amount of heat is generated, enough to melt the fuel itself [122]. Melted fuel will then breach the zirconium cladding and contaminate the surrounding water, as well as turning it to steam. The extreme temperatures are now enough to increase the exothermic oxidation reaction between zirconium and steam to such an extent that hydrogen cannot be absorbed into the cladding nor dissolved into water [123]. The hot, highly pressurised hydrogen gas in the reactor chamber is now prone to, and will explode when mixed with the outside atmosphere or correct combination of oxygen; exactly what occurred in the Fukushima Daiichi explosion of 2011.

On the 11th of March 2011, an earthquake struck the East coast of Japan. No damage was initially caused to any of the nuclear power reactors situated along this coast, and all were automatically shut down. However, the 15 m tsunami wave that hit within the next hour broke over the sea wall of just 12 m, and flooded three BWR units (out of fourteen in total between various powers stations) of the Fukushima Daiichi power station. This resulted in the disabling of the main power supply, as well as twelve out of thirteen backup generators. As a result, and despite the earlier shutdown, there was still enough residual heat present to incur complete or partial melting of all three reactor cores. A day later, almost to the hour a hydrogen explosion occurred in unit one. Temperatures had reached 2800°C, and the fuel had completely melted. The explosion was caused when the accumulation of hydrogen gas under high pressure, produced largely from the oxidation of zirconium by the water that should have been acting as the coolant, was able to mix with some air from the outside atmosphere and ignited spontaneously.

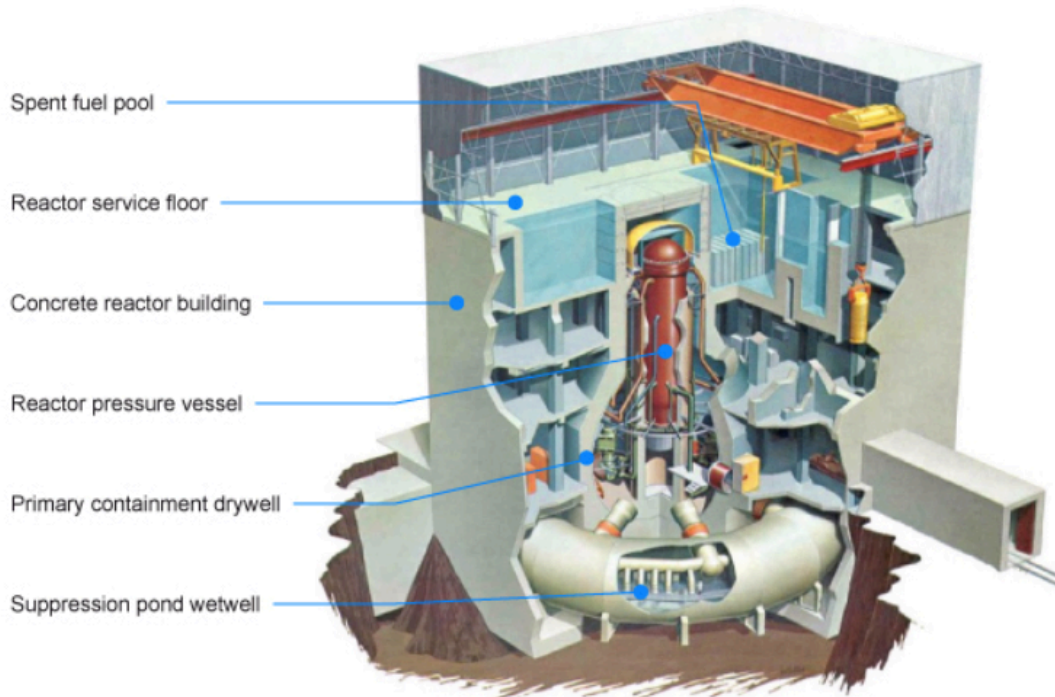


Figure 14. Diagram of the BWR used in the Fukushima power station. By the time the explosion occurred, all matter – melted fuel, fuel cladding and water had collected at the bottom of the reactor pressure vessel [124].

The remaining two reactor cores that had suffered from meltdown did not explode, as the venting of pressure from within the reactor vessels was successful. There was, however an explosion in unit four of the station, believed to occur due to hydrogen build up in unit three that reached it through shared vents [124].

This nuclear disaster was allocated a value of seven on the International Nuclear and Radiological Event Scale (INES) – this categorises a ‘major accident’ including release of a large amount of radioactive material, resulting in possible severe health and environmental effects. There have only ever been two disasters allocated to this category; the other was the infamous Chernobyl meltdown in 1986. Though Chernobyl was infinitely more devastating and directly resulted in the loss of many lives (there have been no deaths directly attributed to the Fukushima accident [125]), however the very fact that a disaster of this scale has occurred due to components present within the reactor warrants investigation. Despite the earthquake and tsunami, the outcome of investigations has been that the disaster was due to human error, and thus could have been avoided [126].

1.6 Conclusion

This literature report has reviewed many of the aspects associated with the chemistry of zirconium, its compounds and the role it accommodates in the nuclear industry. Despite possessing unique advantages, the oxidation and hydrogenation in addition to as well as the nuclear disaster at the Fukushima power plant in 2011 demonstrates that its use is not without fault. A possible remedy for all of these challenges accompanying its use would be to devise a coating for the cladding: one that is hard, resistant to heat, corrosion and radiation, as well as being resistant to temperature and transparent to neutrons. Diamond possesses all these properties and more, furthermore the development of processes such as chemical vapour deposition provide a means to deposit a secure, thin and protective coating upon the fuel cladding. If such a procedure were to be successful, the corrosion processes and accompanying hydrogen production could be greatly reduced, if not completely eliminated; thus vastly improving the safety and lessening the likelihood of another explosion, should a nuclear accident or meltdown occur.

2. Experimental Method and Techniques

2.1 Aim

Prompted by the nuclear disaster at Fukushima described previously, this investigation was conducted with the intention of discovering whether or not it was possible to coat zirconium metal (in place of zircaloy) in diamond. If this were possible, the notion was that the diamond layer would provide a barrier between fuel cladding and water within the core of a nuclear reactor, thereby preventing the oxidation reaction responsible for the explosion at Fukushima and DHC.

Chemical vapour deposition was used to grow thin films of diamond upon zirconium substrates. Most experiments were conducted using hot filament CVD, though one deposition was carried out in a microwave CVD reactor. Different pre-deposition processing techniques and temperatures were utilised to achieve different reaction conditions, in a bid to discover the most effective way to obtain diamond-coated zirconium.

2.2 Sample Preparation

2.2.1 Manual abrasion

The metal used in this investigation was zirconium of 99.2% purity, which was bought in a sheet 0.2 mm thick, and cut to 1 cm² samples in the laboratory. These samples were used for all experiments: the conditions were varied either by adjusting the reaction temperature and time, or differing the method by which samples were pre-treated.

The majority of zirconium samples were prepared for reaction via manual abrasion: a method by which nucleation sites are created from the scratches left by diamond particles. Diamond powder (1-3 μm diameter) was placed between two samples and abraded by rubbing the two together manually for a minimum of 1 minute. The samples were then cleaned thoroughly with methanol to remove the excess diamond powder. This was a very fast and convenient method of preparing samples, however the nature of this technique is fairly destructive to the surface of the substrate. Subsequently, certain samples that required a more subtle approach to creating nucleation sites were prepared by electrospray (section 2.1.3).

2.2.2 Pre-Carburisation

An attempt was made to pre-carburise the surface of some of the zirconium samples prior to reaction in the HF reactor. In order to achieve this, a sample was mounted upon a stone block whilst the flame of an oxyacetylene torch was passed across it until the metal glowed red-hot. The oxyacetylene flame was adjusted so that there was a high ratio of acetylene to oxygen in the gas mixture, and the tip of the yellow coloured flame, representing the hottest area that was rich in carbon, which was passed over the sample.

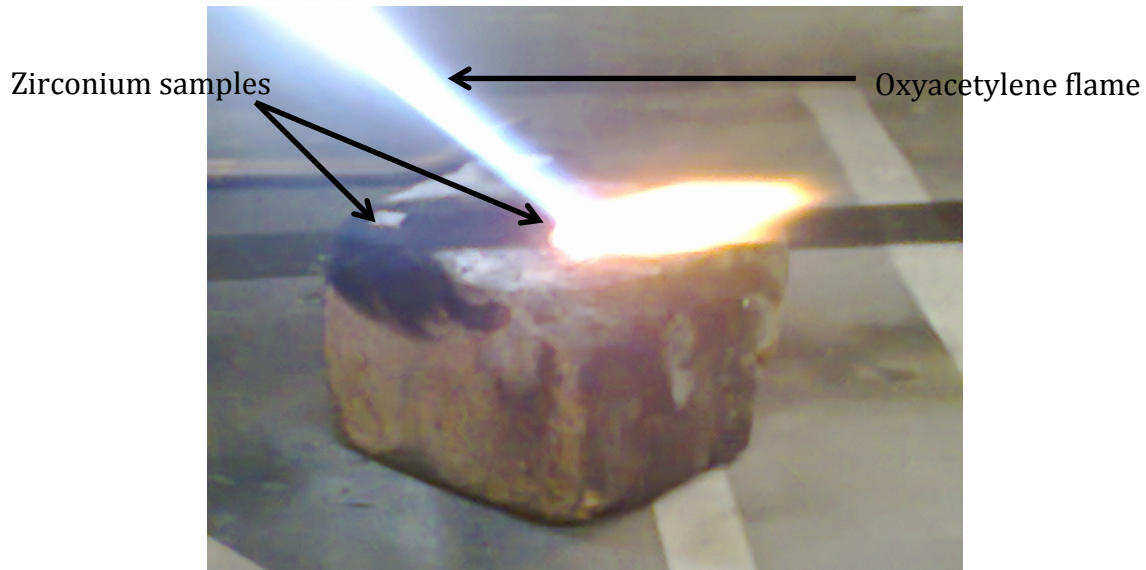


Figure 15. Picture showing how the oxyacetylene torch was used in an attempt to pre-carburise the surface of the zirconium. The tip of the yellow carbon flame (compared to the blue oxygen flame) is aimed at the zirconium sample, the square outline of which is just visible adjacent to the annotation arrow.

Several attempts were made to attain the desired result, as there was a limited degree of control over the composition of the flame. A total of four samples were retained: the remainder either melted or were rendered unusable before the correct gas ratio in the flame was achieved.

2.2.3 Electro spray

To avoid removal or disruption of any carbide or zirconium-carbon interface present on the samples that had been heated with the oxyacetylene torch, diamond nucleation was not assisted by manual abrasion. In place of this, diamond was seeded onto the substrate via electro spray. 1 ml of a suspension of nanodiamond in methanol was put into a syringe at the side of the electro spray chamber. The zirconium samples that had been pre-carburised were mounted onto the substrate holder inside the chamber, and the motor was turned on to a low speed to spin the samples, but not dislodge them. A voltage of 32 kV was applied to the tip of the syringe holding the suspension, to ionise the spray and allow it to be drawn across the chamber to the grounded substrate. By doing so a thin, uniform coating of nanodiamond was sprayed onto each sample in preparation for reaction in the CVD chamber.

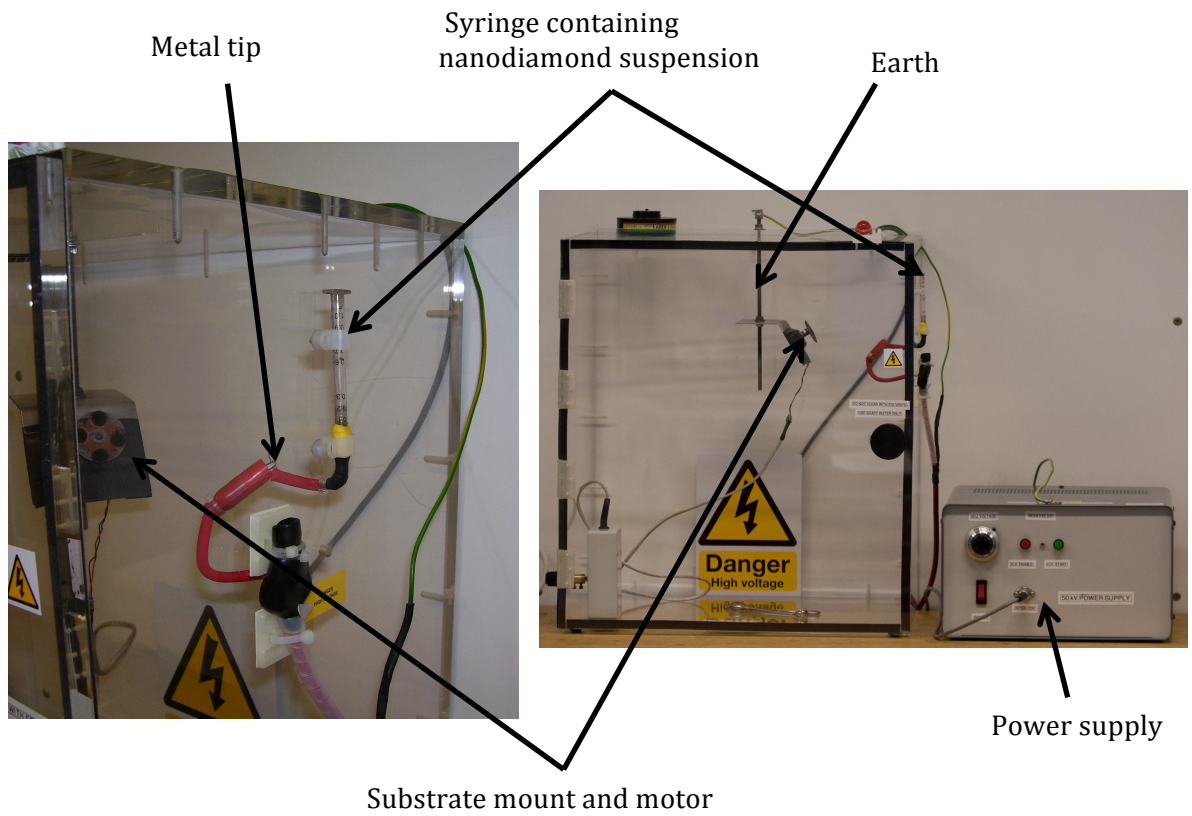


Figure 16. Diagram of the electro spray apparatus used to seed certain zirconium samples [127] [128]

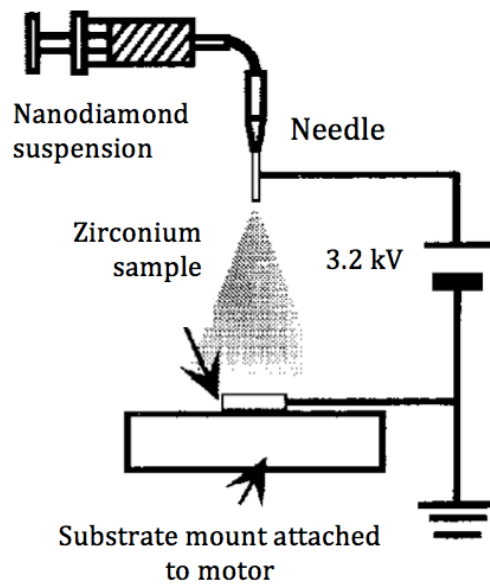


Figure 17. Diagram representing the electro spray process, adapted from [129]

2.3 The Reactor

2.3.1 Hot filament CVD reactor

The reactor used for all but one experiment in this project was a hot filament chemical vapour deposition (HFCVD) reactor, belonging to the University of Bristol (pictured below, figure 18). The reactor contains a substrate mount large enough to hold up to two 1 cm² samples at a time, situated a few millimetres below three rhenium filaments (figure 19).

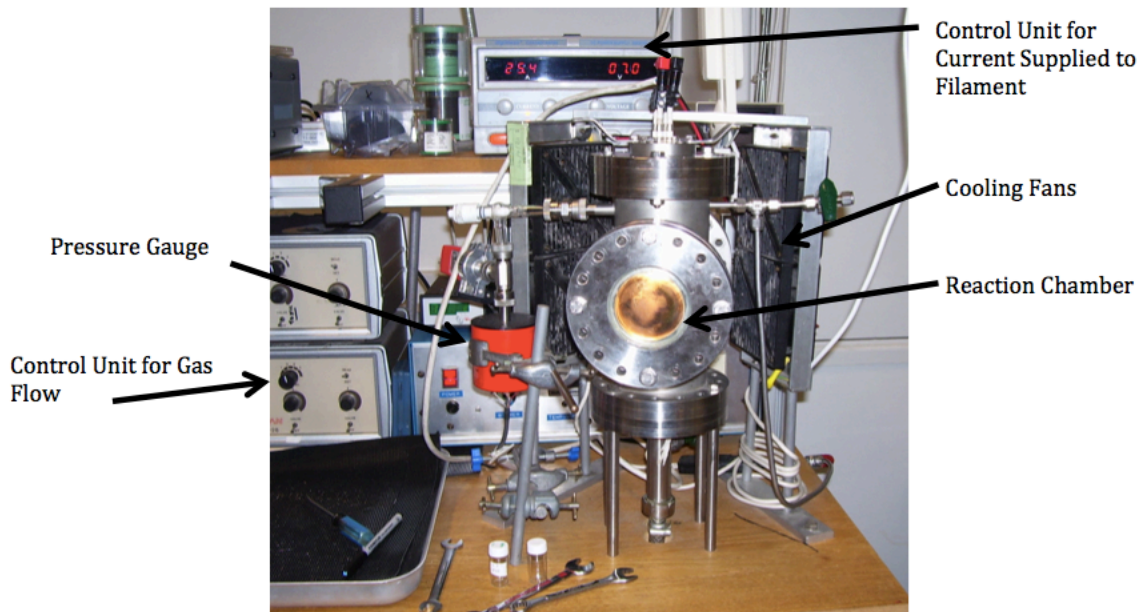


Figure 18. The hot filament CVD reactor used for experiments, adapted from [130]

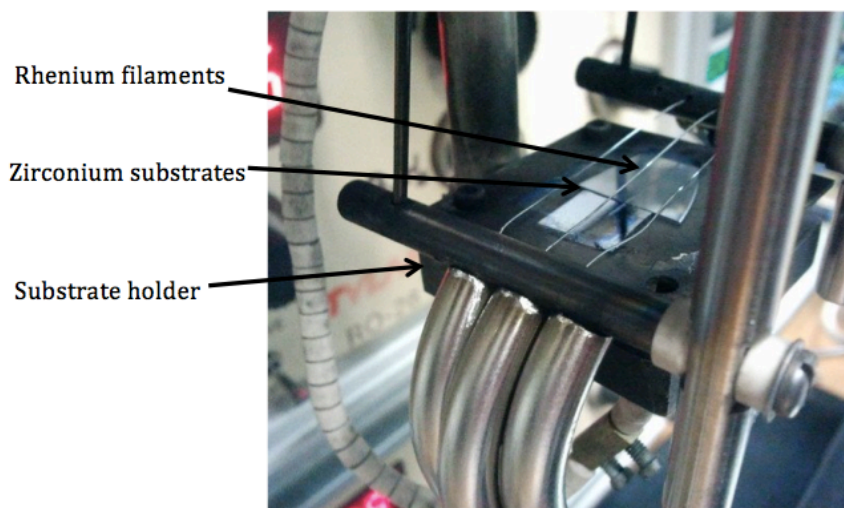


Figure 19. The substrate holder and filaments used inside the reactor, adapted from [131]

The reaction chamber of the reactor is kept permanently under vacuum when not in use to avoid corrosion of the filament in air. Therefore, before reaction, the vacuum was released to allow air into the chamber. Once at atmospheric pressure the substrate holder was removed and a pre-treated zirconium sample placed centrally beneath the filaments. The substrate holder was replaced in the reaction chamber, which was sealed and brought back under vacuum to remove atmospheric gases. After vacuum was established (20 mTorr) the substrate heater and cooling fans were turned on and left to come up to temperature, before the process gases of CH₄ and H₂ were introduced and the filament turned on. The zirconium substrate was then left in the reactor for the time required for a particular experiment.

After the reaction had run for the allotted time, the filament, substrate heater and process gases were turned off and the system allowed to cool. Once at room temperature the vacuum was released and the system allowed to reach atmospheric pressure. The substrate holder was then removed and the sample removed for analysis, before being replaced in the chamber and brought back under vacuum.

In one occasion where the HFCVD reactor was not used, an experiment was carried out in an ASTeX-type microwave plasma CVD (MPCVD) reactor. The reactor had a power of 1.5 kW, which produced microwave radiation of 2.45 GHz that was used to ionise the process gases of hydrogen and methane (a more detailed description is given in reference [132]). A zirconium sample, prepared by manual abrasion was placed into the centre of the substrate holder and left for 6 hours to grow a diamond film on its surface.

2.4 Reaction times and conditions

2.4.1 Standard conditions

Certain conditions remained constant between all experiments carried out in this investigation, which are stated in the table below. These parameters tend to be used in most depositions in the hot filament reactor, and although varying them would undoubtedly affect the diamond growth on the substrate, it is likely that deposition would not be influenced in a way that might affect the outcome in a particularly positive way.

Table 8. Standard conditions maintained during all experiments

Condition/ Units	Magnitude
Pressure (during reaction)/ Torr	25
Flow rate of H ₂ / sccm	200
Flow rate of CH ₄ / sccm	2
Current supplied to substrate heater/ A	4

2.4.2 Variable conditions

The parameters varied in this experiment in order to obtain different results were: temperature, time and pre-treatment technique. A description of the exact conditions is displayed in the table below.

Table 9. Conditions and reaction time in each experiment conducted; unless otherwise stated the experiment was carried out in the HFCVD reactor

Experiment/ sample No.	Current to filament/ A	Temperature/ °C	Time/ hours	Special Conditions
1	25	900	6	None
2	N/A	~900	6	Experiment conducted in MWCVD reactor
3	20	700	6	Substrate placed so that only half was situated beneath the filaments
4	20	700	12	Substrate fully under filaments, experiment conducted over two consecutive days
5	18	600	12	Experiment conducted over two days
6	22	800	6	Pre-carburised substrates used: two samples put into reactor
7	18	600	6	Substrate from experiment 4 replaced into reactor for a further 6 hours

2.5 Analysis

A variety of analytical techniques were used to discern the result of each experiment, the type used dependant on the trial carried out and what could be determined visually.

2.5.1 Optical Microscope

Following a minimum reaction time of 6 hours, each sample had a sufficient growth of diamond to be studied beneath a Zeiss Axiolab optical microscope at 5, 10, and 100× magnification. Where acquired, the computer program ScopePhoto 3.0 captured images which provided qualitative information on the size, uniformity and coverage of diamond over the substrate, providing an indication of whether or not further analysis would be beneficial.

2.5.2 Secondary ion mass spectrometry

In order to determine the exact composition of the samples used, secondary ion mass spectrometry (SIMS) was carried out on three samples:

- i. Untreated zirconium prior to reaction
- ii. Sample after reaction 1 was carried out
- iii. Sample after reactor 7 was carried out

The instrument used was a TOF-SIMS VG Ionex IX23LS belonging to the Interface Analysis Centre in the University of Bristol Physics Department. The sample was loaded onto the substrate holder and brought under vacuum. A beam of gallium ions was focussed on the substrate, which caused the surface of the sample to sputter (eject atoms or ions), before etching deeper into the metal. The secondary ions released were analysed by time-of-flight mass spectrometry, and the signal directly plotted. A program called SRIM was used to estimate the etch rate through the sample, which allowed the conversion of time into distance, and a depth profile of the sample to be compiled.

Separate scans were done to detect both positive and negative secondary ions that were emitted from the sample. The majority of ions detected were positive, as would be expected from a metallic substance. However, scanning for negative ions was used to obtain a clearer signal from the non-metallic compounds present, as this technique is less sensitive to secondary ions emitted from zirconium and hafnium, and could therefore attain a clearer signal for oxygen, ZrO_x and carbon.

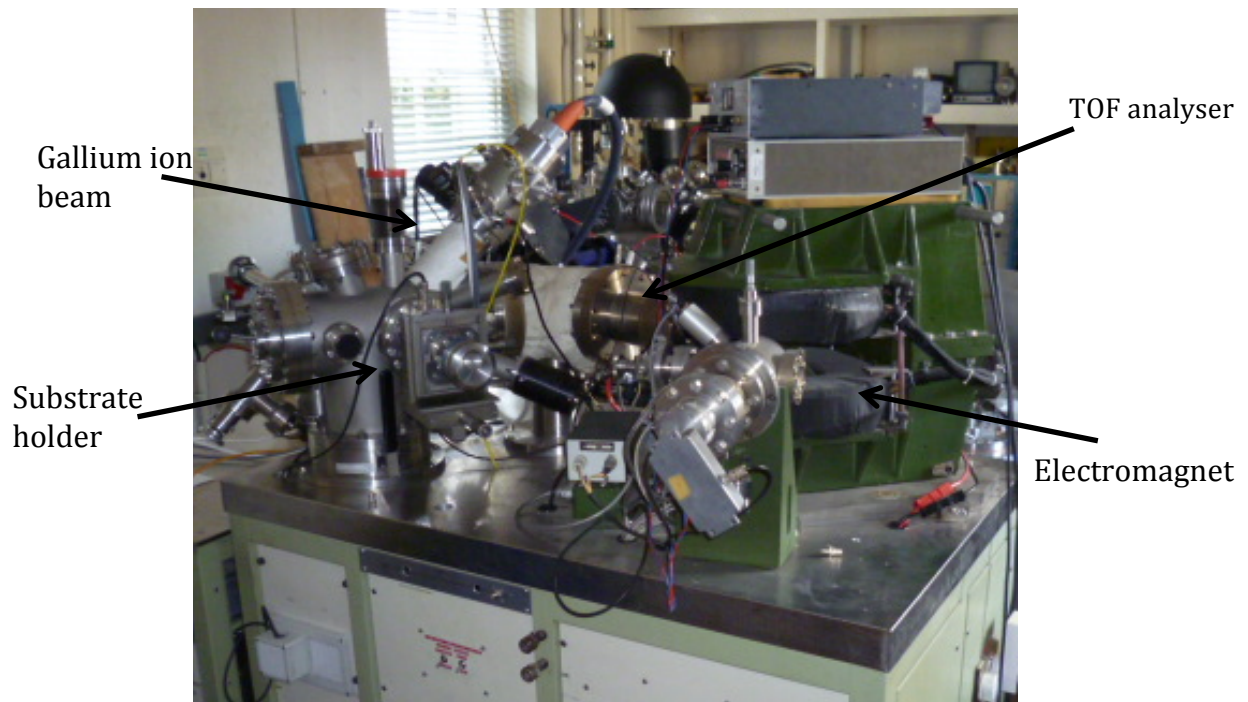


Figure 20. The TOF-SIMS instrument used in this investigation [133]

2.5.3 Raman spectroscopy

Raman spectroscopy was used to determine if diamond growth was successful, and whether other forms of carbon were present. Diamond exhibits a very distinctive, sharp peak at 1332 cm^{-1} , which provides a simple way to confirm the presence of diamond. Additionally, there are two graphite bands that will appear close by at 1582 and 1350 cm^{-1} that represent disordered and graphitic carbon, respectively [134].

This technique is fast, requires no preparation of the sample and is non-destructive. However the information gained from spectra is merely qualitative, and does not provide an indication of the grain size, extent of coverage or quality of diamond. Therefore, to achieve this level of further detail, SEM and SIMS were also conducted.

In this investigation, the model of spectrometer used was the Renishaw 2000. A green laser with a wavelength of 514 nm was used, connected to a CCD detector.

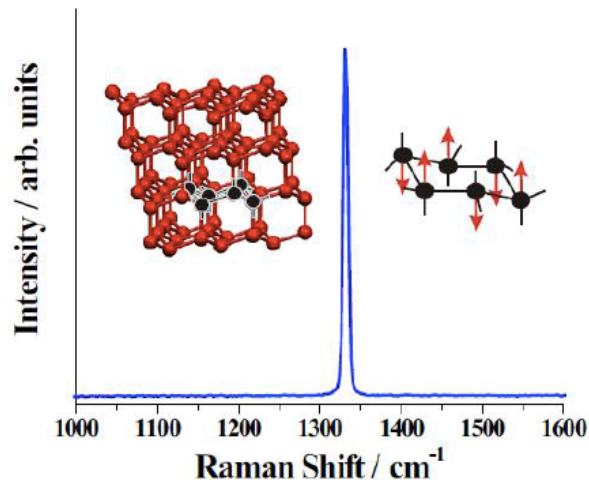


Figure 21. An example of the diamond peak on a spectrum achieved via Raman spectroscopy. The models represent the vibration in the diamond structure that this peak arises from [135]

2.5.4 Scanning electron microscopy (SEM)

High-resolution SEM images of diamond growth on samples were obtained by the use of a JEOL 5600V electron microscope. The sample to be analysed was mounted onto the substrate holder in the microscope chamber and brought under vacuum. An electron beam at 20 kV was focussed onto the sample, causing emission of secondary electrons from the surface. These electrons were captured and detected to produce images of between 270 and 19,000 \times magnification, which is high enough to determine the grain size of crystals, extent of coverage and in some cases the thickness of the diamond layer.

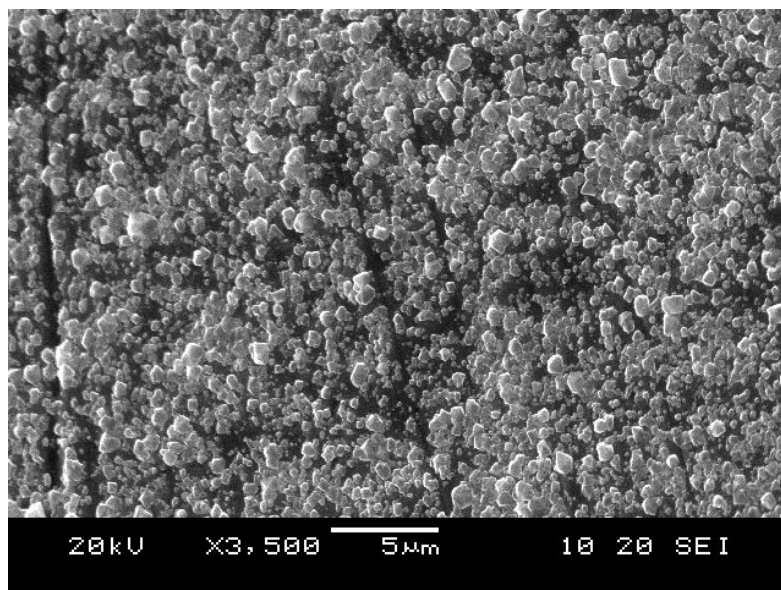


Figure 22. A typical SEM image taken in this experiment

3. Results and Discussion

3.1 Initial investigations

3.1.1 Reaction in the hot filament and microwave reactors

In order to gauge an idea of whether or not diamond would grow on a zirconium substrate, preliminary experiments were conducted in the hot filament (HF) and microwave (MW) reactors. Nucleation sites for diamond growth were created by manual abrasion (section 2.1.1), and one sample placed into the centre of the substrate holder in each reactor as described in section 2.3, table 9.

It was predicted previously that diamond should nucleate and grow on the zirconium substrate reasonably well. However, the passivation layer created by the strong oxide may prevent proper adhesion of the diamond to the surface of the metal, simply forming a freestanding film rather than the coating desired. As expected, after 6 h growth a diamond layer visible to the naked eye was formed upon both substrates. However, upon removal from the reactors it was found that the diamond had cracked and was not at all adhered to the metal. Possible explanations for this are that the thermal mismatch between zirconium and diamond is too large; the coefficient of thermal expansion for diamond is $1 \mu\text{m K}^{-1}$, while the values for zirconium and zirconium carbide are several times larger at 5.7 and $6.6 \mu\text{m K}^{-1}$, respectively. After a deposition at approximately 900°C , the compressive stress exerted on the diamond film upon cooling due to the zirconium decreasing in size over $5\times$ more would be enough to cause a break up and delamination of the diamond layer.

The alternative reasoning for the failure of successful growth is that the diamond never properly adhered to the surface, instead simply growing upon it as a thin sheet. This would occur if the ZrO_2 on the substrate surface was not changed or displaced, thus preventing a carbon-zirconium interface from forming at all. Conversely, if the oxide is displaced during the deposition time, it may be that zirconium does not form a sufficient carbide or Zr-C interface.

3.1.1.1 Secondary ion mass spectrometry

Although the failure of diamond to adhere to the substrate was not entirely unexpected, it remained problematic. It had been hypothesised that the delamination of the diamond from the metal was due to the strong passivation layer of oxide on the zirconium surface, but further evidence was needed to confirm this. To corroborate the findings with the prediction and discover other changes that may have occurred on the metal during deposition, SIMS analysis was undertaken to compare untreated, unreacted zirconium with the outcome of experiment 1 (6 h at 25A in the HF reactor).

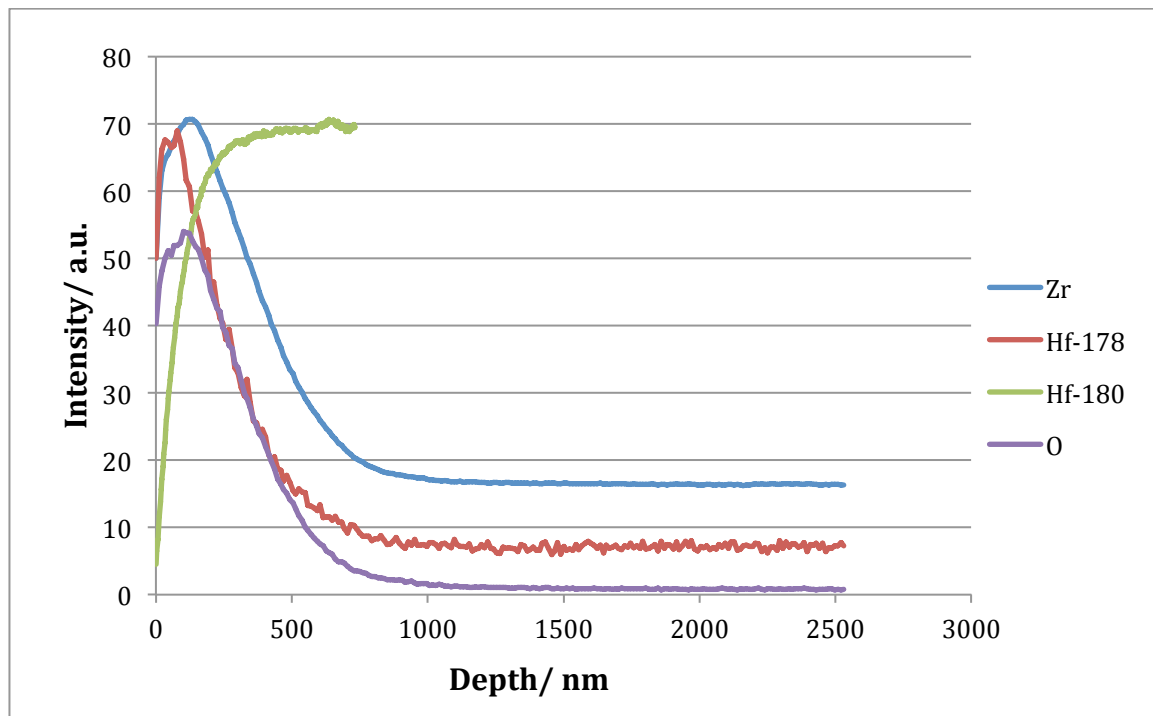


Figure 23. Graph showing the result of SIMS depth profiling carried out on an untreated zirconium sample. The signals represent the intensity of any positive secondary ions detected: the sharp increase or peak at the start signifies where the ions for an element are first identified, and the highest section of the peak corresponds to the depth of a particular element before the signal trails off. The depth profile was achieved by using the etch rate of zirconium metal as estimated by the computer program SRIM (0.29 nm/s) and the etch time.

The oxygen signal, shown in purple can be interpreted to give an oxygen-zirconium layer of ZrO_x of approximately 150 nm, but could possibly be more. This value does conflict with literature values considerably (2-4 nm), however this could be due to the sputtering process; as the ion beam progresses through the sample, oxygen could still be present around the edges of the hole, and subsequently secondary oxygen ions could still be detected in the mass spectrometer, leading to a signal for oxygen lasting longer than the depth of the zirconium/oxygen interface.

Hafnium-178 and zirconium follow a similar trend, as was expected in commercial grade zirconium which has a small percentage of hafnium present throughout the metal. Hafnium-180 does not follow the same trend, which could be due to the sensitivity of Hf ions to the detector. However, the readings concerning hafnium are not of particular interest in this study as the level present in the metal is very low, and should not affect diamond growth.

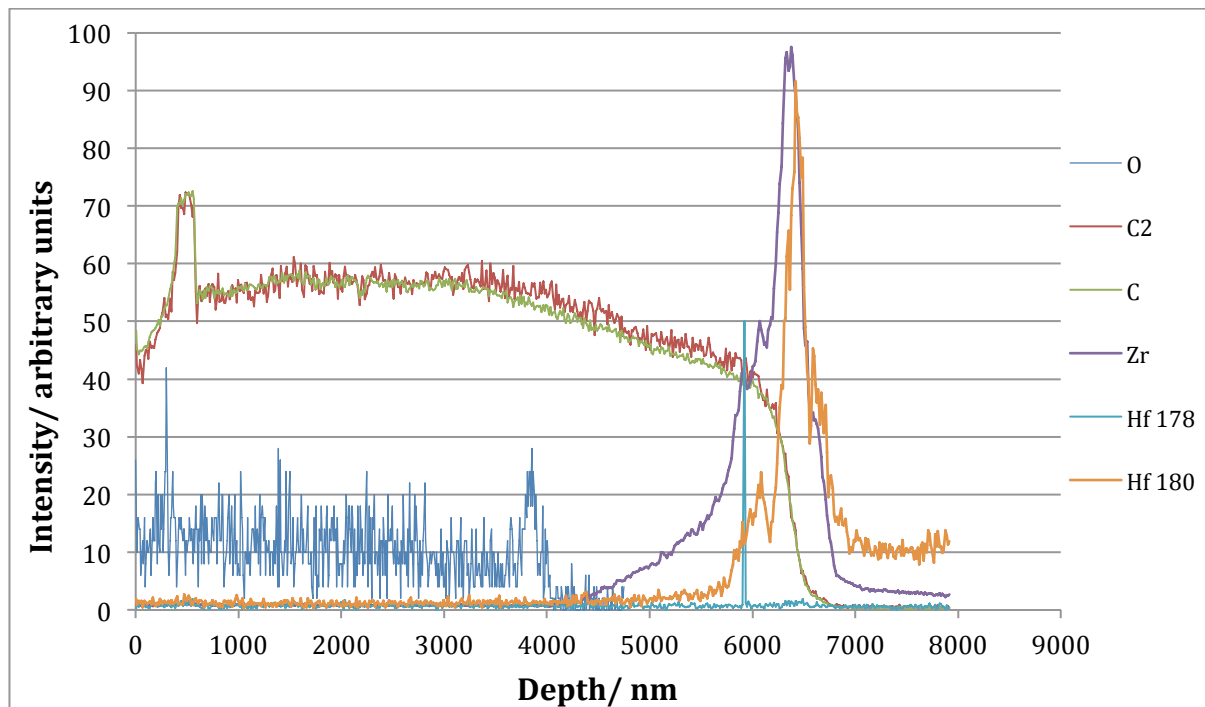


Figure 24. Results of the SIMS analysis (scanning for positive ions) on the sample used in reaction 1, post reaction in the HF reactor for 6 hours at 25 A. The high carbon signal for the first 4000 nm represents the diamond layer, before an interface of zirconium and carbon. Following the interface or carbide section, the increasing zirconium and hafnium signals represent the metal substrate. The etch rate was estimated to be approximately 0.6 nm/s, which corresponds to a carbon or diamond layer of 2.4 μm and a zirconium carbide interface of approximately 0.9 μm .

There is a variable oxygen signal present for the entirety of the diamond layer, though does appear to disappear once the zirconium carbide section is reached. This suggests that the oxide layer is burnt off or displaced during the deposition process, which was unexpected, yet should be favourable with respect to diamond growth. The relatively large coefficient of thermal expansion of ZrO_2 ($10.5 \mu\text{m K}^{-1}$) with respect to diamond may provide an explanation for the apparent disappearance of the oxide layer. The monoclinic oxide structure stable at room temperature is also the most brittle, and the difference in expansion between metal and oxide may have assisted in its displacement.

The loss of the oxide layer did suggest that the delamination of diamond from zirconium being due to the strength and stability of ZrO_2 was incorrect. However, it provided a suggestion of which routes to explore further; the two possible issues raised by the preliminary experiments were the large difference in expansion with temperature, and the possible difficulty in forming a suitable zirconium carbide interface between the two materials.

3.2 Reaction at low temperature

Of the two possible challenges associated with CVD of diamond on zirconium, the temperature was the simplest to manipulate, therefore this was investigated before attempting to alter the surface chemistry of the zirconium sample prior to deposition. It was theorised that the diamond film could be nucleating and growing on the zirconium, but only forming a thin or weak carbide interface. If this were indeed the case, the stress exerted on the film upon cooling would likely be sufficient to cause the delamination observed previously. By reducing the temperature during the deposition, the difference in expansion between diamond and zirconium could be reduced; hopefully enough that the resultant film would be able to withstand the strain upon cooling and remain adhered to the substrate.

3.2.1 Deposition at 20A

In an attempt to lessen the extent of thermal mismatch between diamond and zirconium during reaction, but still allow preferential growth of diamond over graphite the current supplied to the filament was decreased from 25 to 20 A, and all other growth conditions kept constant (tables 8 & 9). With this current, the temperature at the growing diamond surface during deposition was approximately 700°C. At this temperature of some 200°C lower than the previous reactions the zirconium should expand by 1 mm less than before and possibly avoid exerting too much stress on the diamond layer.

Post-reaction, due to the lower growth rate observed at lower temperature, there was no coating of diamond easily visible to the naked eye, though there was a slight discolouration and matte-effect visible on the end of the sample that had been situated directly beneath the filament. Additionally, the same end of the metal appeared to curl up slightly, implying that it was under some stress and that diamond had probably grown in a small amount. Some diamond growth was observed under the optical microscope, however was too small to be properly analysed by this.

3.2.1.1 SEM Imaging

To discern the extent of diamond growth and grain size on this sample, it was imaged by scanning electron microscopy at magnifications of 950, 2,500, 3,500, 9,000, 14,000 and 19,000. It was observed that diamond had grown on and adhered to the surface, as well as seeding across the whole substrate, however a completely continuous coating was not formed at any point. The maximum grain size was found to be approximately 1 µm and maximum coverage of roughly 80%, located at the end of the sample that was situated closest to the filament during the deposition. The smallest grains observed in an appreciable amount were around 20 nm, situated towards the opposite end of the sample to the larger ones, and diamond coverage by this point was <10%

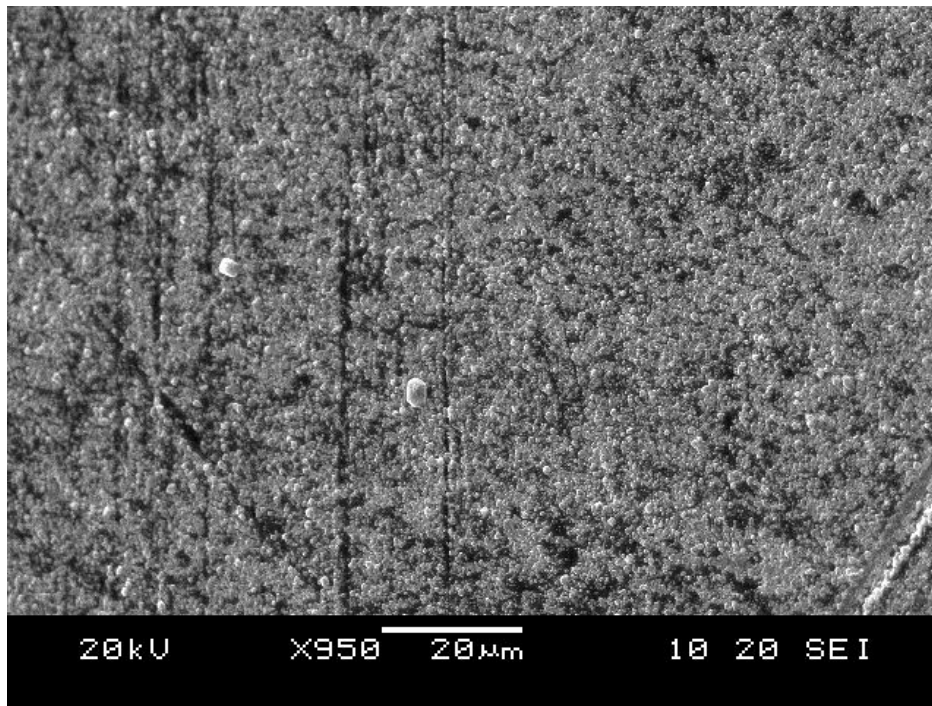


Figure 25. SEM image of the area on the sample which had the highest coverage of diamond. The average grain size cannot be determined at this point; apart from the anomalous grains visible at approximately $4 \times 5 \mu\text{m}$. However, it can be seen that though the diamond growth is not quite continuous, it would appear to cover between 80-90% of the metal and also to have adhered, unlike the films in the previous experiments.

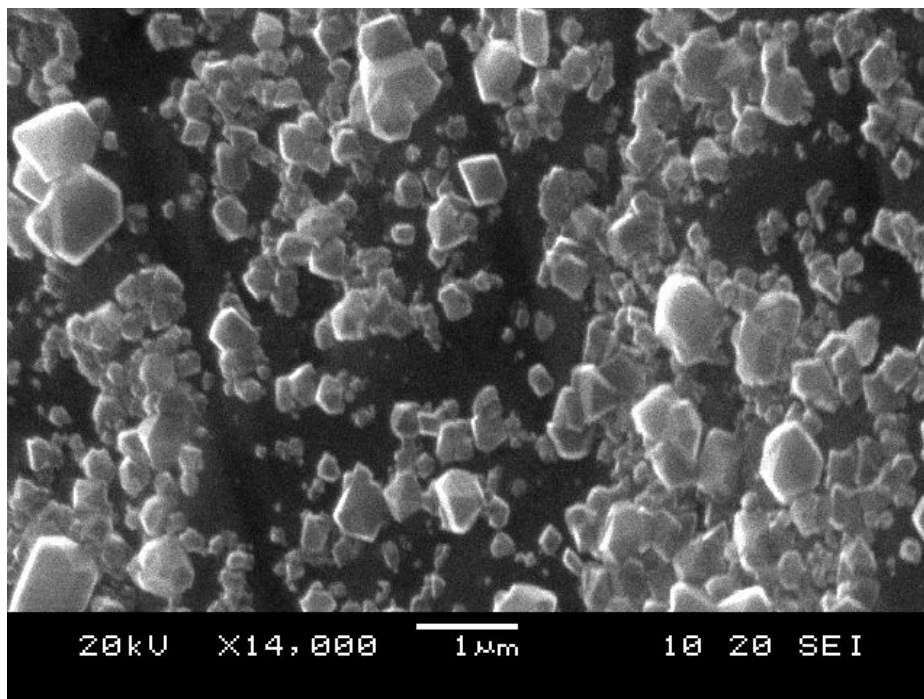


Figure 26. Image of the same area observed in figure 25 at a higher magnification, which allows the average grain size to be determined. The largest reach up to $1 \mu\text{m}$ in size, which accounts for about 30% of the total observed in this section. The

remainder are approximately $0.5 \mu\text{m}$. At this higher resolution, the extent of total coverage is appears closer to 80 than 90%.

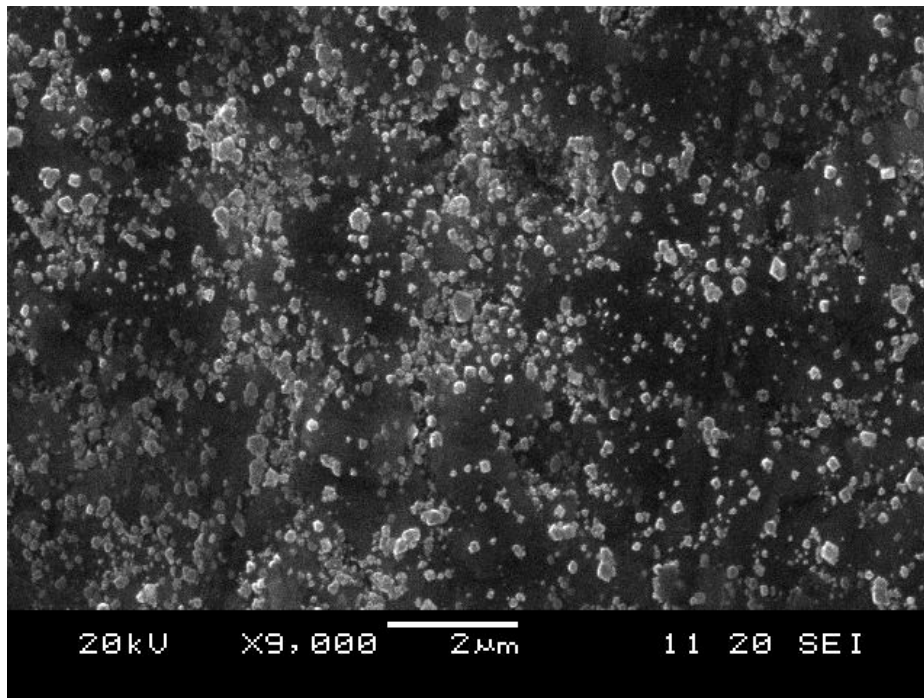


Figure 27. An image taken $\frac{3}{4}$ of the way down the substrate, away from the end situated beneath the filaments during deposition. Both the average grain size and coverage of diamond across the sample are visibly reduced when compared with the previous figures (25 & 26), which is not surprising as the increased distance from the filament means that there would have been a lower concentration of activated gas precursors to form diamond. Grain size varies from <0.1 to $0.5 \mu\text{m}$, with the average appearing to lie around halfway between the extremes at approximately $0.3 \mu\text{m}$. At this distance away from the filament, the level of diamond cover has decreased to around 10%.

As the sample was imaged further towards the less-covered end, the diamond grain size and proportion of cover across the substrate decreased further. All other micrographs taken of this sample are included in the appendix. This experiment had a much greater degree of success than the preliminary investigations, and suggested that the zirconium substrate was better suited to low deposition temperatures. However, with reduced temperature comes a slower growth rate, as is observed by the lack of a continuous film, leading to the next experiment, which was conducted over a longer period of time.

3.2.3 Deposition for 12 hours

The results of the previous experiment conducted at low temperature were promising, yet the reduced growth rate prevented the growth of a continuous diamond film. Hence, experiment 4 was conducted under almost identical conditions; the only change being the deposition time, which was doubled to a total of 12 hours. As expected, a continuous diamond film was formed but unfortunately delaminated in a similar fashion to the preliminary experiments as the temperature in the reaction chamber cooled after the deposition.

3.2.3.1 Optical microscope imaging

The diamond grown in this reaction was thick enough to be easily visible to the naked eye, and an analysis was conducted using the optical microscope to obtain clearer images of the fractures in the sample.

Examination under the optical microscope exhibited several areas where the film appeared to have cracked as if due to a compressive force, which would be in keeping with the theory of thermal mismatch between materials.

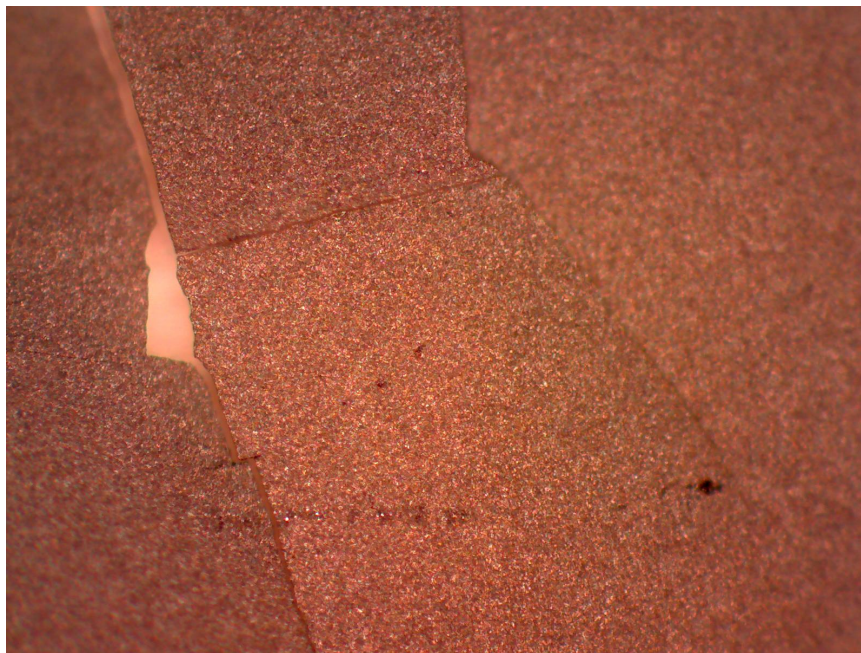


Figure 28. An image captured of cracks in the diamond film at 10× magnification. The areas out of focus demonstrate where the sample has cracked into plates and become uneven. The film is of a reasonable thickness and quality, and despite the cracks, has also remained in large pieces. This would suggest that deposition at low temperature is preferential, and that it may be fully successful if diamond growth can be observed at temperatures lower than that used in this particular experiment.

3.2.5 Deposition at 18A

After the promising results observed at a low deposition temperature achieved using 20 A of current, this line of investigation was extended by further decreasing the temperature to approximately 600°C (equivalent to a current of 18 A supplied to the filaments, experiment 7 in table 9). This very low temperature meant that the deposition rate was very low, so was carried out for 18 hours, over 3 deposition runs. On removal of the sample from the reactor, the only change visible by the naked eye after reaction was a slight discolouration of the surface; a more matte appearance compared to the reflective metal. Unlike some of the previous samples, the zirconium used in this experiment had not bent or curled up and instead remained as flat as it was prior to reaction. This implied that there was not the degree of stress being exerted on the metal; hopefully due to the decrease in expansion differences at this temperature.

3.2.5.1 Raman spectroscopy

Analysis by Raman spectroscopy after 12 hours of deposition confirmed the presence of diamond, but also some graphite, implying that the lower limit of the temperature successful diamond growth could be observed was being reached. Nonetheless, diamond was deposited, so the sample was returned to the reactor for an additional 6 hours under the same conditions.

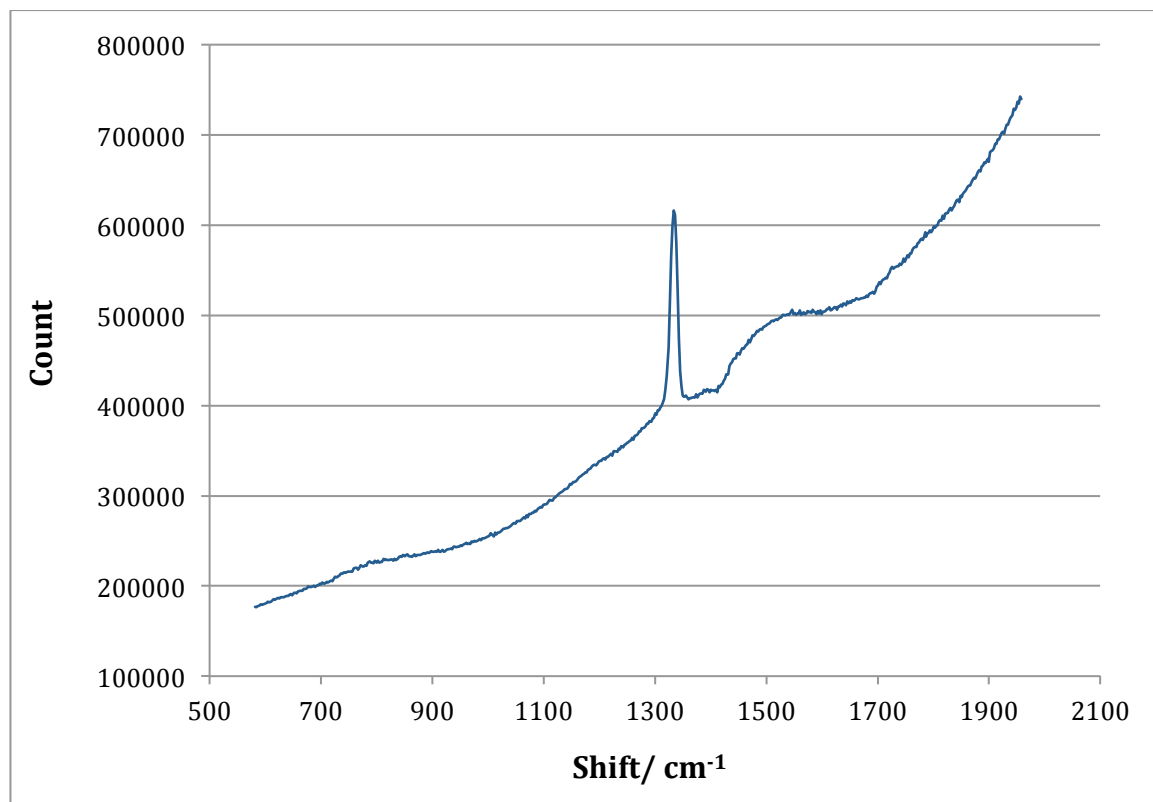


Figure 29. The Raman spectrum obtained with the use of a 514 nm green laser. The sharp peak situated at a shift of 1332 cm⁻¹ corresponds to the characteristic diamond vibration while the smaller, broader peak just to the right at 1580 cm⁻¹ confirms that graphite was also deposited alongside diamond.

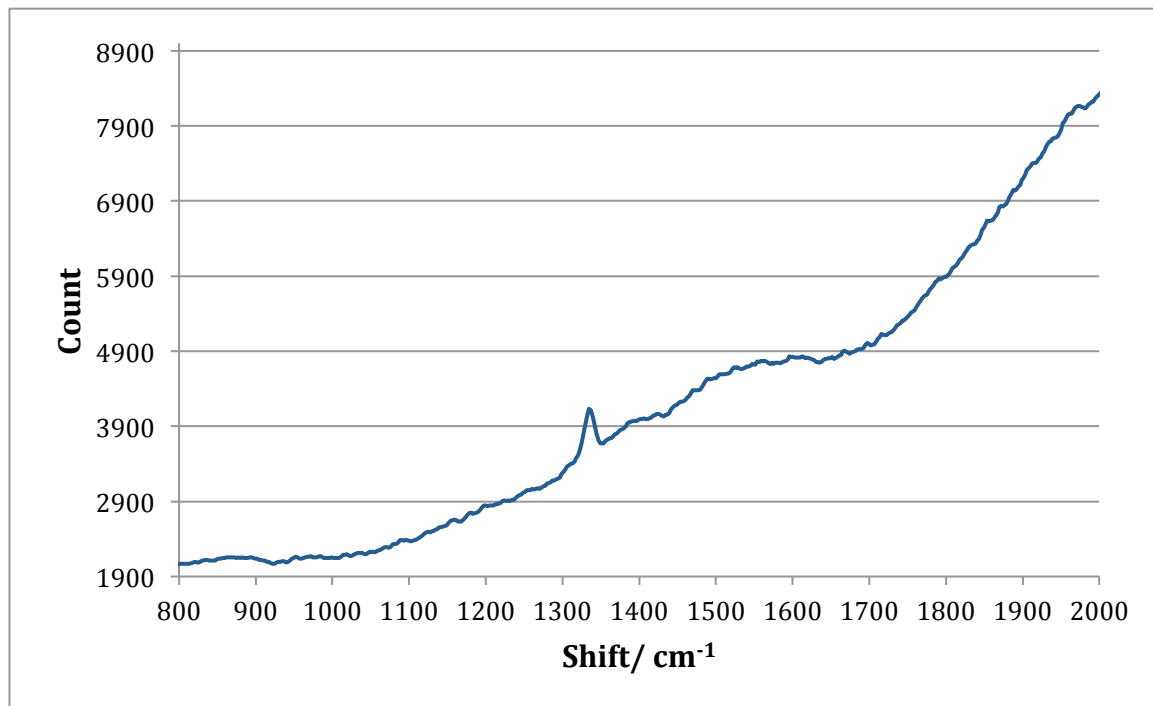


Figure 30. The Raman spectrum obtained from the same sample used in fig. 29 under similar conditions (the intensity of the laser was changed and a full scan undertaken). The peak at 1332 cm^{-1} for diamond is clearly visible, though diminished in size when compared to previous spectra. To the right, the G-band or graphite signal is visible at 1580 cm^{-1} . Of note is that the intensity of the signal for diamond (or graphite) is not proportional to the amount present on the sample; rather the difference is more likely to be due to other reflections from the shiny metal substrate reflecting a large amount of light into the detector, diminishing the signals detected for diamond and graphite.

3.2.5.2 SEM imaging

SEM images show a very nearly, but not quite continuous, diamond film was formed during this deposition. This is progress compared to the previous deposition, yet until a complete coating of diamond is observed across the sample; it is not known whether the compressive stresses exerted on the film upon cooling have been reduced sufficiently to maintain the adhesion of diamond to metal.

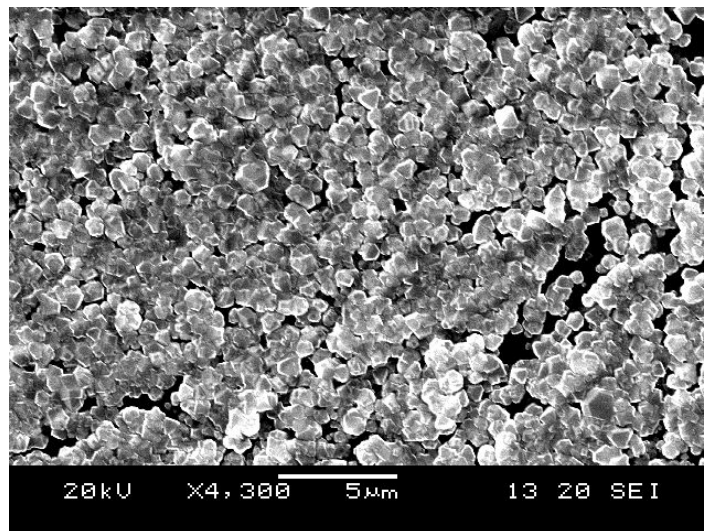


Figure 31. SEM image taken of a random area of the sample at 4,300× magnification. The coating was very close to continuous across the whole of the substrate at 90% or higher. The consistency of the film across the substrate means that this image is representative of the majority of the coverage over the whole sample (further images located in the appendix).

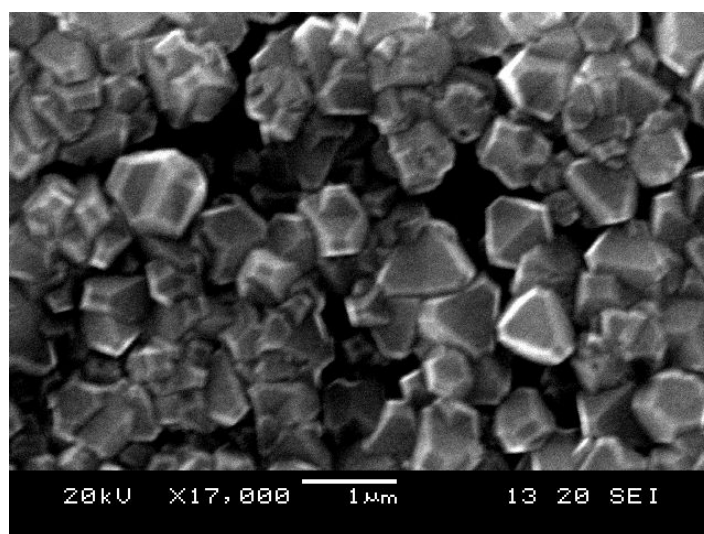


Figure 32. This image taken at a greater magnification shows an average grain size of <math><1 \mu\text{m}</math>, which is likely due to the very slow deposition and growth rate at the

temperature used. The single-grain coating also means that grain size is equivalent to the thickness of the diamond layer.

The growth and adhesion observed in this experimental run was undoubtedly the most promising so far, yet despite this, the small gaps between some grains would allow for extra expansion and compression before stressing forces caused a breakup of the film. Consequently, a conclusion on the efficacy of this growth technique cannot be fully made at this point.

3.2.5.3 SIMS

A comparison was made between the composition of this sample, untreated zirconium and the 1st deposition via SIMS analysis conducted on the sample obtained from this reaction:

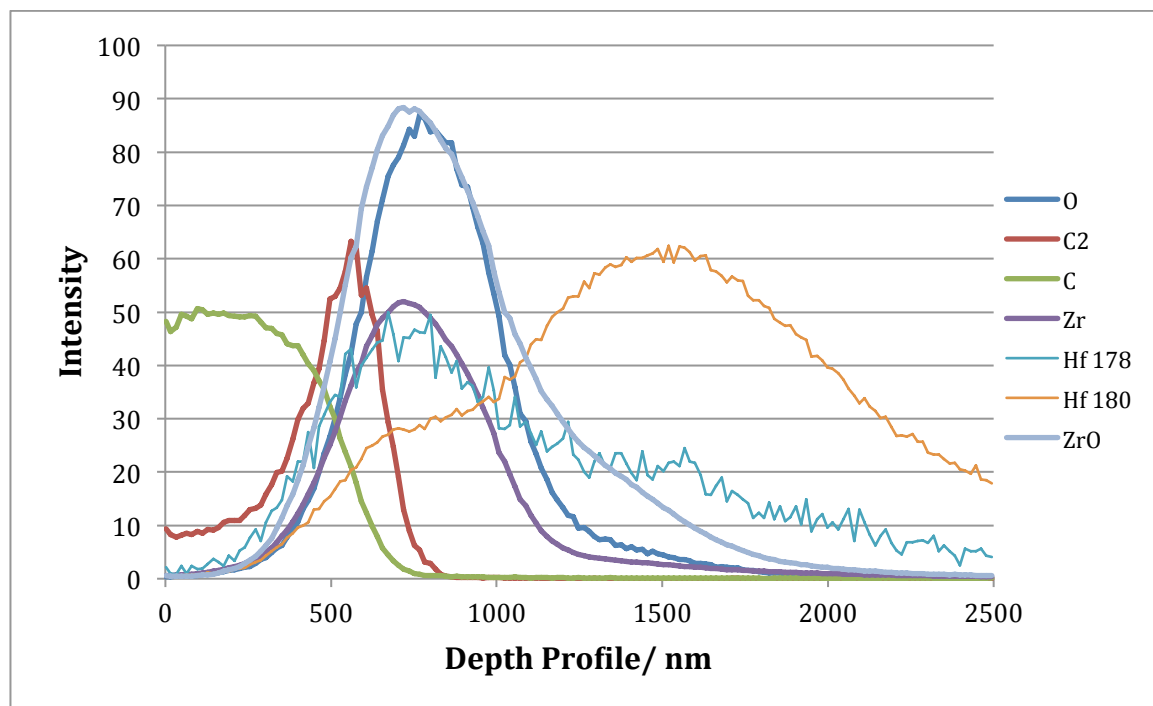


Figure 33. Result of SIMS analysis conducted on sample 7, scan conducted for positive ions. The depth profile compiled from the known etch rate for diamond (0.5 nm/s) suggested the diamond layer had a thickness of ~200 nm and a zirconium-carbon interface of 100-150 nm. In contrast to the previous scan taken of sample 1, there is a very pronounced presence of oxygen and ZrO across several hundred nm, and appears to penetrate the entire depth of the zirconium metal. A certain amount of this can be attributed to the scanning process, but nonetheless it must be taken into consideration that the oxide layer on the zirconium surface was not burnt off *in situ* as first assumed.

The presence of ZrO and oxygen in this scan suggests the original theory that the passivation layer on the metal may hinder carbide formation and thus adsorption of diamond has more credence than was recently presumed.

3.3 Pre-carburisation

Another route of exploration investigated was the pre-carburisation of the zirconium substrate. In industry, extreme conditions are necessary for the formation of ZrC; the most replicable of industrial methods in the laboratory was the heating of the metal by an oxyacetylene torch.

Unfortunately, the degree of control and knowledge over the exact composition and temperature of the torch used was limited; therefore several attempts were made to achieve the (apparent) desired result.

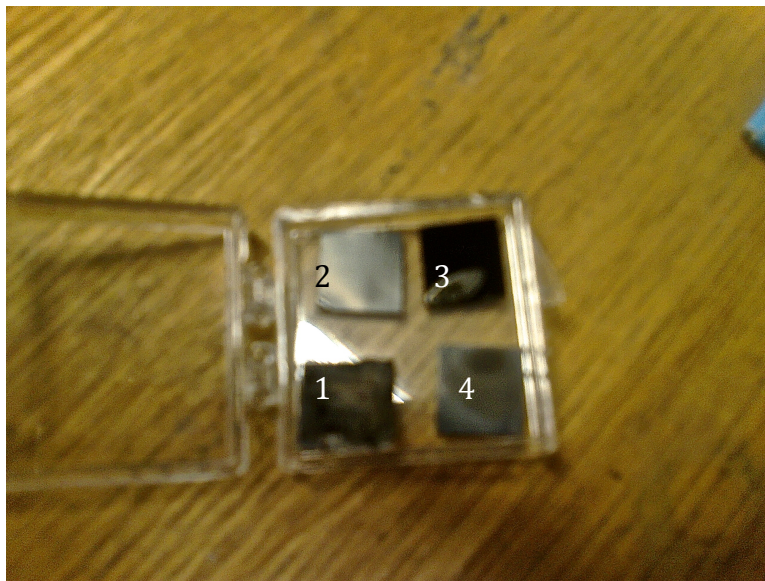


Figure 34. A photograph taken of the four samples which remained intact after firing with the oxyacetylene torch; though of a poor resolution, some detail can be discerned. The bottom left sample is visibly darker in colour and has a matte or rough texture, in contrast to the others that still appear metallic. The edges became uneven and the whole sample was very brittle, implying that the temperature was too high or that the time spent beneath the flame was too long.

The top two samples appeared very similar; the top right still has the black, sooty coating present after the process whilst the top left has had this coating wiped off. Aside from this coating, the only perceptible change was a slight dulling of the colour and shine of the metal which indicated that some kind of change had taken place upon the surface of the metal; though whether or not this showed carbide formation remained undetermined.

The sample pictured on the bottom right displays several different coloured 'rings' that would suggest a layered structure of some sort, which provided a strong indication that a change in or on the surface of the zirconium had occurred. The samples selected for reaction 6 (samples named 6a and 6b) were 2 and 4, as 1 was deemed unusable, as the metal had been changed too much and 3 appeared to be nearly identical to 2.

3.3.1 Raman spectroscopy

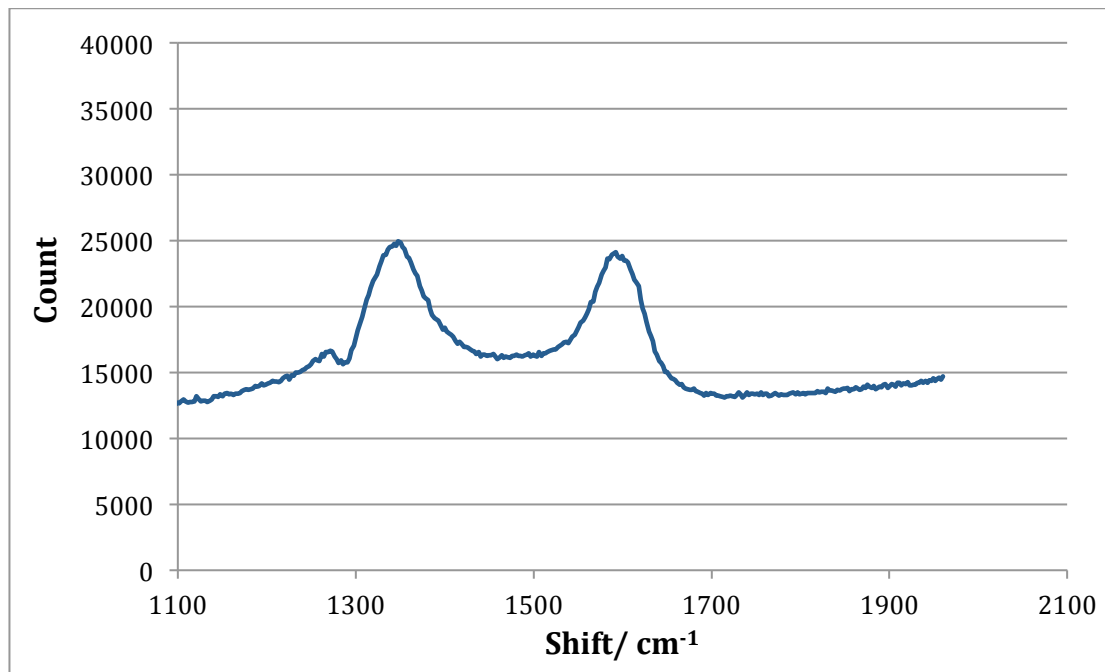


Figure 35. Raman spectrum obtained from sample 3 (as described in figure 34)

Peaks are observed for both disordered carbon and graphite at 1350 and 1580 cm^{-1} respectively, which was expected after exposure to acetylene in the welding torch.

3.3.2 SEMs

After a deposition run of 6 hours at 22A (approximately 800°C), a diamond film was noticeable on substrate 6a, though had not adhered strongly. Both samples were imaged by scanning electron microscopy, however under the vacuum in the microscope chamber the diamond that had failed to adhere fully to sample 6a exfoliated and was lost.

Diamond had adhered properly to sample 6b, but upon mounting to the substrate holder cracks appeared throughout the entire sample. This suggested that a change has taken place throughout the metal, most likely during the carburisation process. Metal is not usually brittle, however the ceramic zirconium carbide is; therefore it is quite possible that carburisation of the metal was too successful and penetrated through most of the depth of the sample.

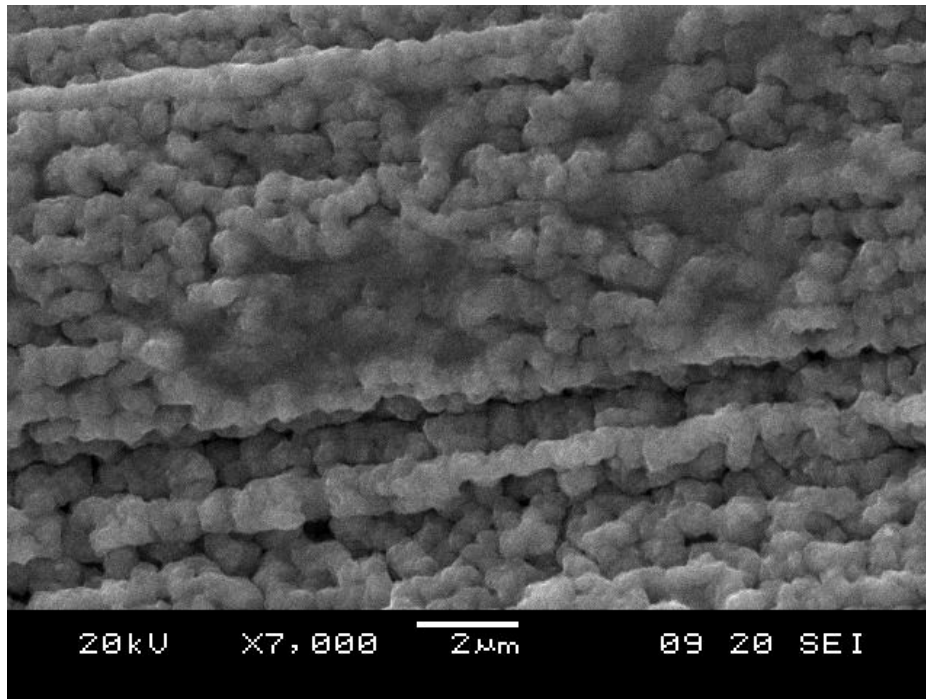


Figure 36. SEM image taken of sample 6b demonstrating a continuous and adhered diamond coating on the substrate. The average grain size is approximately 0.3-0.5 µm; the depth of the coating cannot be ascertained from this image.

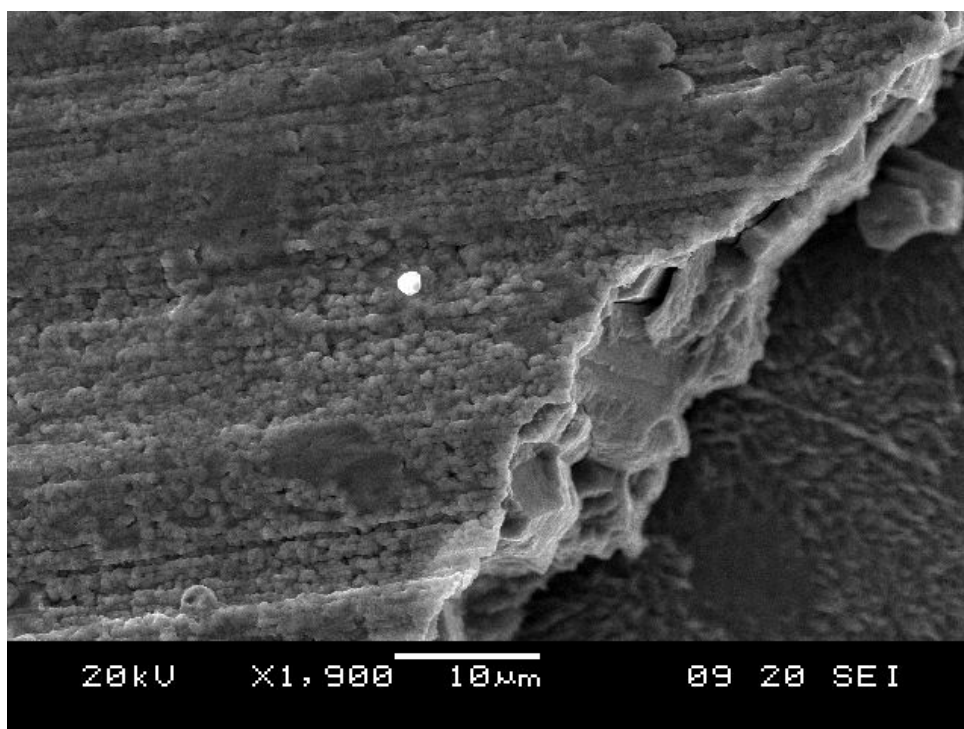


Figure 37. SEM image of one of the cracks present in sample 6b after mounting upon the substrate holder

The crack is sharp and jagged indicating that the sample shattered: a characteristic of brittle materials that would not usually include metals. This further implies that the composition of the sample was altered throughout its depth.

As the film completely covers and adheres to the sample, it can be inferred that diamond is able to bear a certain amount of stress upon cooling of the sample. If zirconium carbide was indeed formed, then diamond is capable of withstanding the difference in thermal expansion coefficients between ZrC and diamond. This was an informative result that demonstrated diamond does have the capability to resist the compressive stresses exerted upon it during the cooling and shrinking of the substrate after deposition. This suggests that the repeated failure of a continuous diamond film to remain adhered to the substrate was due in part to the thermal mismatch, but mostly because the formation of a strong carbide layer was hard to achieve in the reactor.

This explanation is quite possible, and was not completely unanticipated given the extreme methods necessary for ZrC synthesis in industry. The oxyacetylene welding torch was able to more closely replicate the conditions necessary for formation of zirconium carbide than either reactor used in this study could. A possible way to rectify this could be the use of an arc-jet reactor, which activates the gas precursors via the use of an oxyacetylene flame. This would provide more information and greater control over the temperature and composition of the flame, potentially allowing for the carburisation of the substrate surface, but avoiding the penetration of carbon throughout the whole sample.

4. Conclusion

The investigations carried out during the construction of this thesis have shown that it is possible to grow polycrystalline diamond by chemical vapour deposition on substrates made from a sheet of zirconium metal. However, the effectiveness of this, and the extent to which a diamond film will cover and adhere to a substrate has proven to vary according to temperature, deposition time and method of substrate preparation.

It was found that, as a general rule diamond grains adhered to the substrate better at lower temperatures; the lower the voltage supplied to the filament, the less likely the diamond film formed was to exfoliate. This was initially attributed to a large difference in the thermal expansion coefficients diamond zirconium, and the presence of a strong, unreactive layer of ZrO_2 on the surface of the metal substrate. Evidence for a thermal mismatch causing delamination was presented by the fact that whenever an incomplete coating of diamond was formed across the substrate it would remain attached; it was only when a continuous film was made across the sample that delamination occurred. Micrographs obtained from the use of an optical and scanning electron microscope further supported this conclusion. The oxide layer became the subject of some debate throughout the course of the project, as early SIMS analyses suggested that this passivation layer had been burnt off or displaced during depositions. However, later analyses showed a very distinct presence of oxygen and ZrO , suggesting that this was not the case.

Some greater success with respect to diamond adhesion was achieved by pre-carburising the zirconium substrate prior to deposition. This lends weight to the hypothesis reached after the first few initial experiments: that a strong enough carbide layer or interface between metal and diamond was not being formed during the deposition process. Given the conditions necessary to produce ZrC industrially, this was not unexpected and the use of an oxyacetylene welding torch appeared to provide the heat necessary for carburisation. Analysis by Raman spectroscopy showed the presence of D and G-bands for carbon, though no additional information about the exact composition was obtained at this point and all conclusions are thus speculative. After a deposition at 22A for 6 hours on two pre-carburised samples, diamond grew on and adhered to one sample, though delaminated from the other. Unfortunately, the latter sample shattered upon handling, suggesting whatever change had occurred due to the preparation process had disseminated through the full depth of the substrate. This shows that the preparation technique, though effective and useful, was also somewhat unreliable; of the seven samples heated with the torch, only three were deemed usable, and of these samples successful growth was only observed upon one.

Overall, the work presented in this investigation has shown that under certain conditions it is possible to grow diamond on zirconium with some success, nevertheless further work would be necessary in order to determine whether or not it would be possible to make the transition of this process from the laboratory to industry. Despite the positive results obtained from low temperature depositions, the slow growth rate prevented the formation of a complete diamond coating during the course of the experiments conducted. Therefore, a solid conclusion cannot be made about the outcome of these reactions. The adhesion of diamond to zirconium appeared

to improve as the temperature of reaction was lowered, so it is quite possible that a deposition at 18 A or lower could be entirely successful. However, since almost every experiment that resulted in a continuous diamond film resulted in exfoliation from the substrate, this conclusion is merely speculative. The process of pre-carburisation prior to CVD does appear to have more prospective use, but needs refining before its utilisation on a larger scale. The lack of information about the exact composition and temperature of the oxyacetylene torch have proved problematic, as it took several attempts to achieve the desired result. Once this was attained, there were still problems with the sample; the lack of precision during the pre-processing meant that the only sample that appeared to have been carburised shattered, suggesting that carburisation had not occurred just on the surface, but throughout the metal which would render it useless in an industrial capacity. However, despite this there have been some encouraging advances made that provide a solid foundation for further investigation, by no means ruling this out as a method of improving the safety of nuclear reactors.

5. Further Work

Promising results were obtained from the investigations conducted during this study, which provided several suggestions of further work that could be carried out in order to advance the possibility of this technique being used in an industrial capacity.

Firstly, it would be useful to replace sample 7 in the reactor for a further 6 hours or so, in order to complete the diamond coating upon it. This would allow a determination of whether low temperature deposition really works, and if so the temperature required to do so. This would be a simple advancement, but was unfortunately unachievable within the time constraints of this particular investigation. Additionally, and especially if further deposition at 18A is unsuccessful, it could be possible that growth would be successful at even lower temperatures (for example using a current of 16 or 17A). Temperatures this low may or may not result in diamond growth, or could deposit a high proportion of graphitic carbon in addition to diamond, and would also be subject to an extremely slow growth rate, however it would be an interesting route to try.

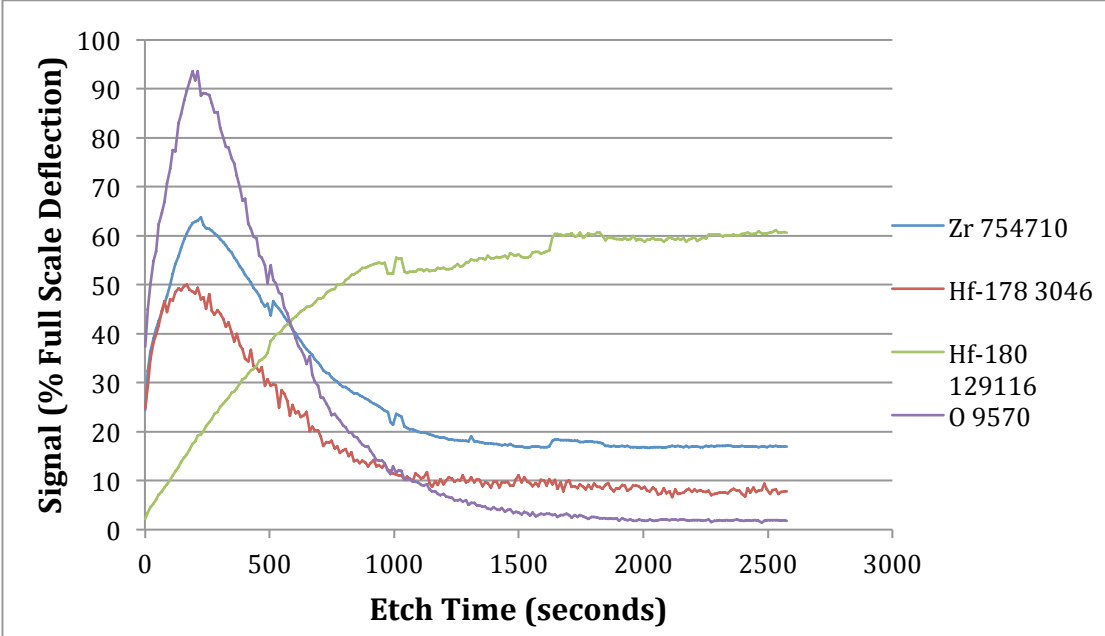
A different possible method to try and combat the difference in thermal expansion coefficients could be to attempt a deposition upon zirconium wires. The cylindrical shape of diamond grown upon the surface of the wire would mean that there should be no edges for the film to delaminate from, and it would therefore remain in place. An additional option when carrying out a deposition of this nature could be to cool down the experiment slowly, which may prevent the shattering observed on some samples in this investigation, and also allow the main deposition to be carried out at a higher temperature. The use of zirconium wire in place of sheets may also prove advantageous when trying to predict the result of a deposition carried out on the cylindrical fuel rod cladding. In the absence of the actual cladding used in reactors, zirconium wire could provide a useful small-scale model.

Further investigation into pre-carburisation could provide a means to deposit diamond onto zirconium at temperatures of 800-900°C, if a reliable method of achieving carburisation could be developed. Although one case in this investigation appeared to be successful, in-depth information about the exact composition was not obtained, and this was only one sample out of a total of seven that were fired with the oxyacetylene torch.

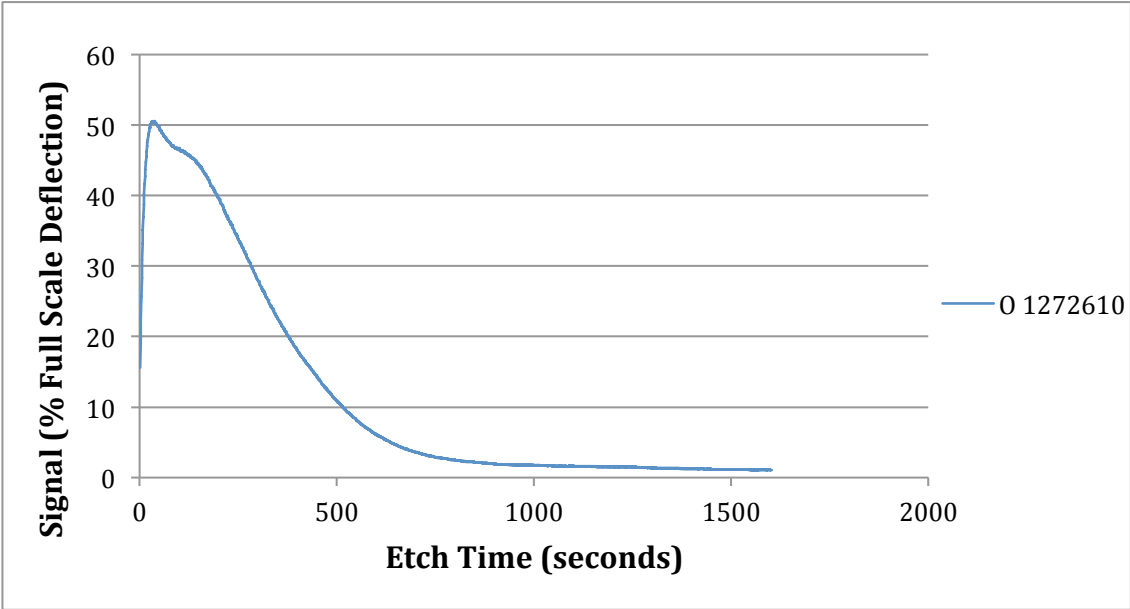
6. Appendix

6.1 SIMS Results

6.1.1 Untreated zirconium

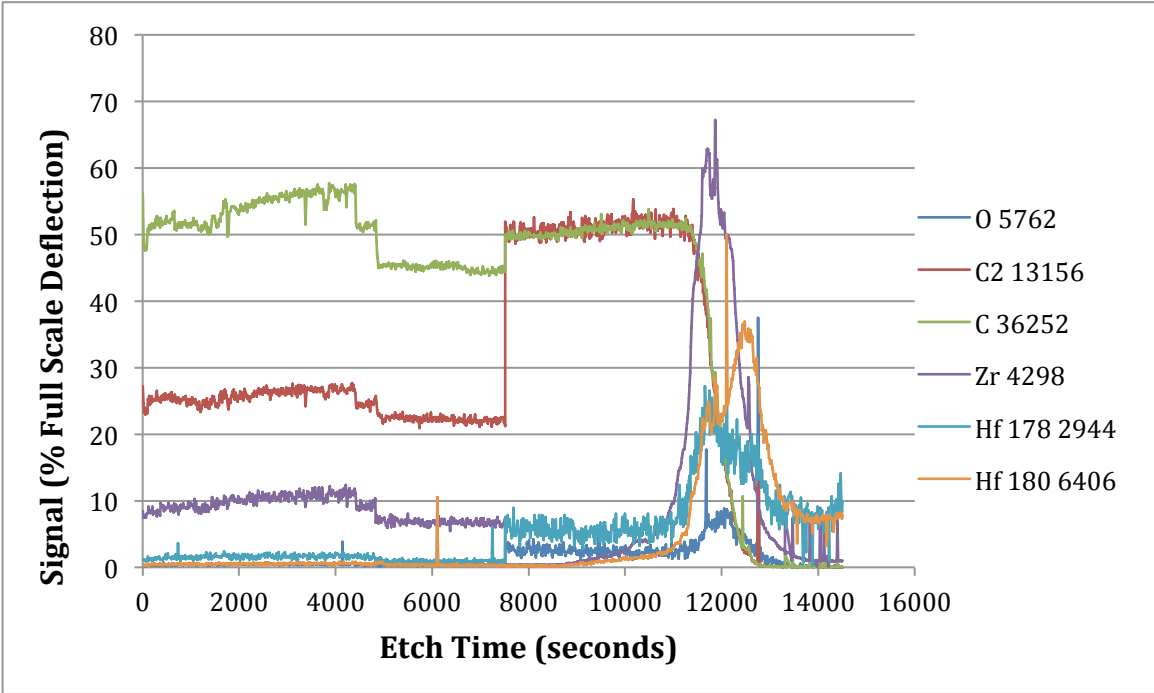


Zr0 3nA positive x2000 magnification, electronic gating on (legend shows Full Scale Deflection for each species)

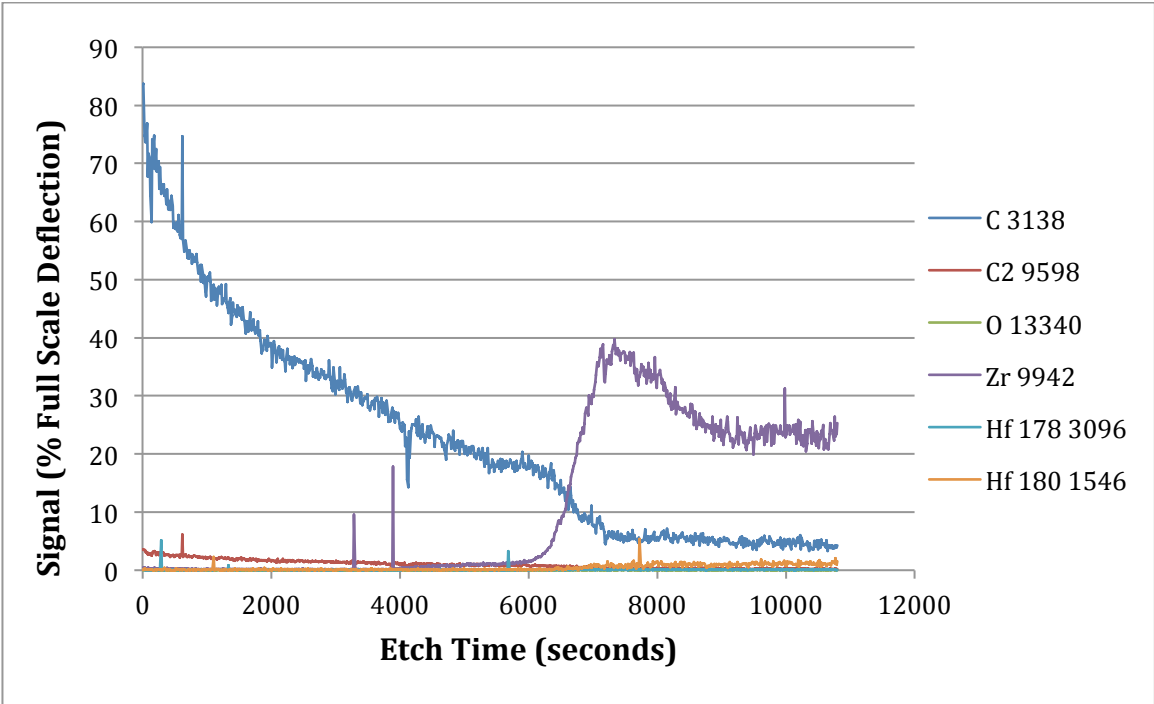


Zr0 3nA negative x2000 magnification, electronic gating on.(legend shows Full Scale Deflection for each species)

6.1.2 Sample 1

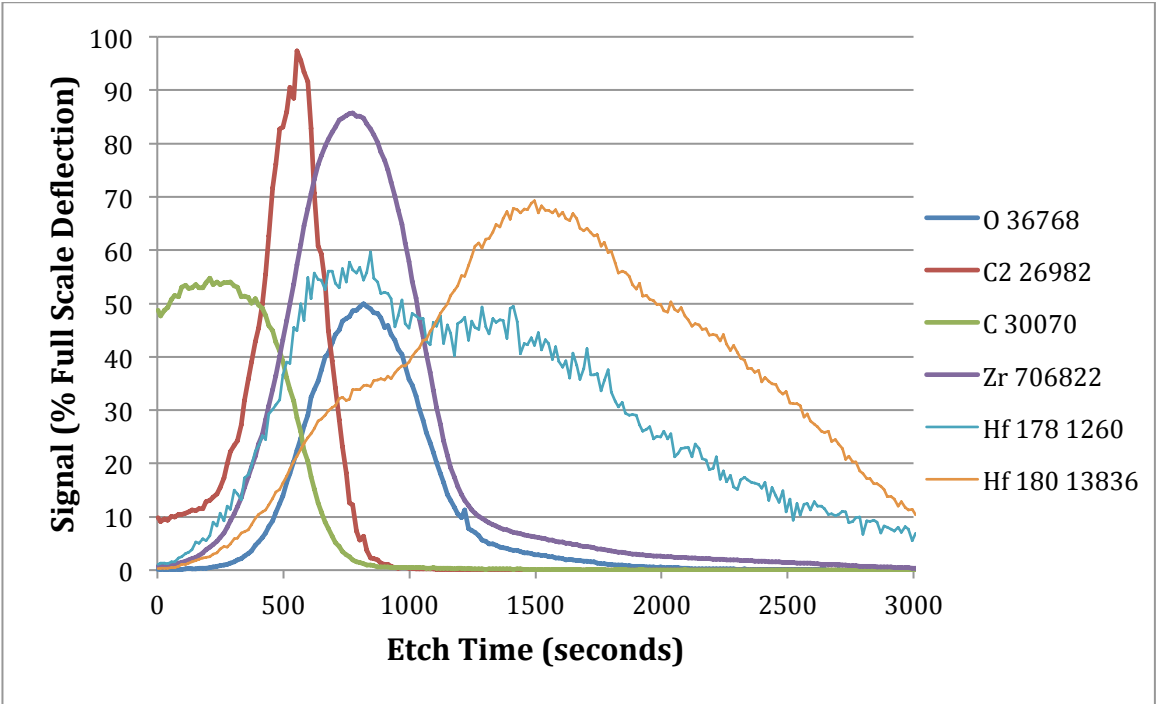


Zr1 3nA positive x5000 magnification, electronic gating on, stopped and started halfway through.

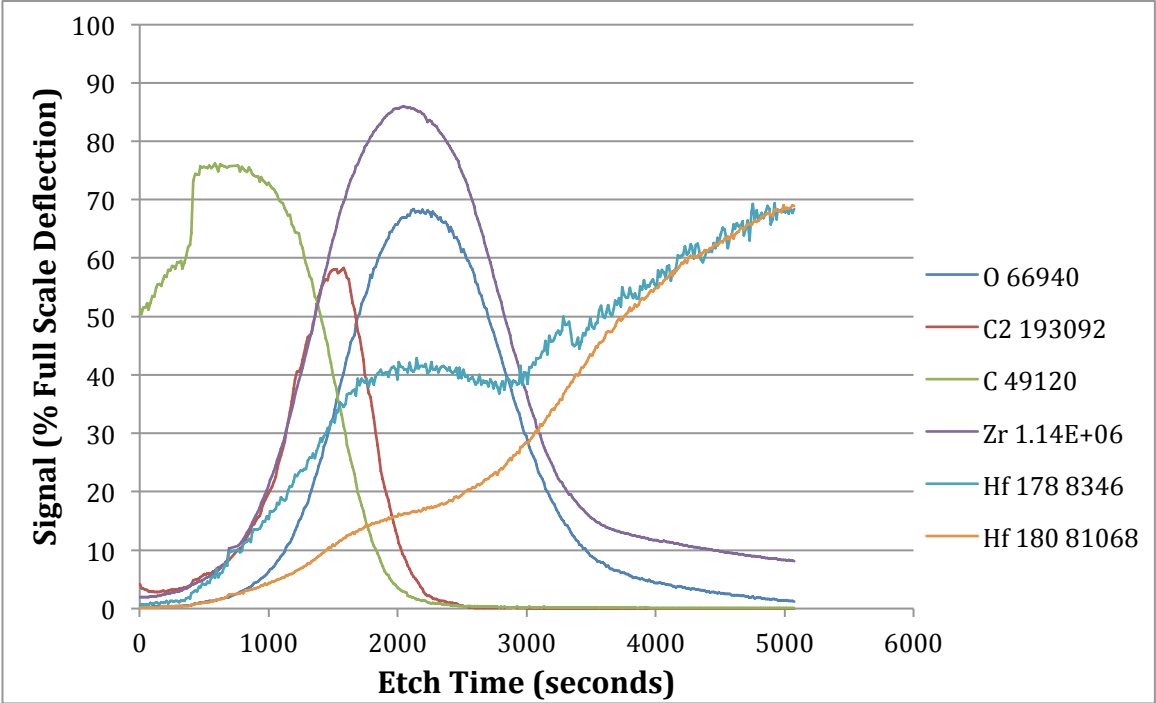


Zr1 3nA positive x5000 magnification, electronic gating on (legend shows Full Scale Deflection for each species)

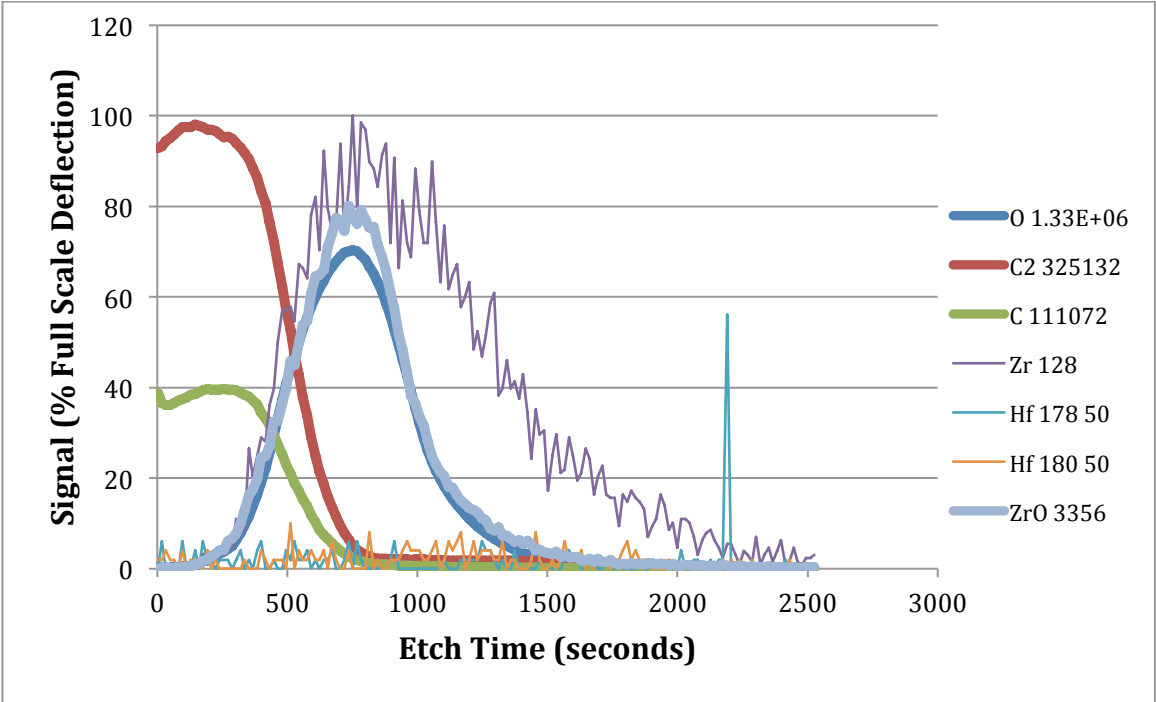
6.1.3 Sample 7



Zr5 3nA positive x5000 magnification, electronic gating on (legend shows Full Scale Deflection for each species)



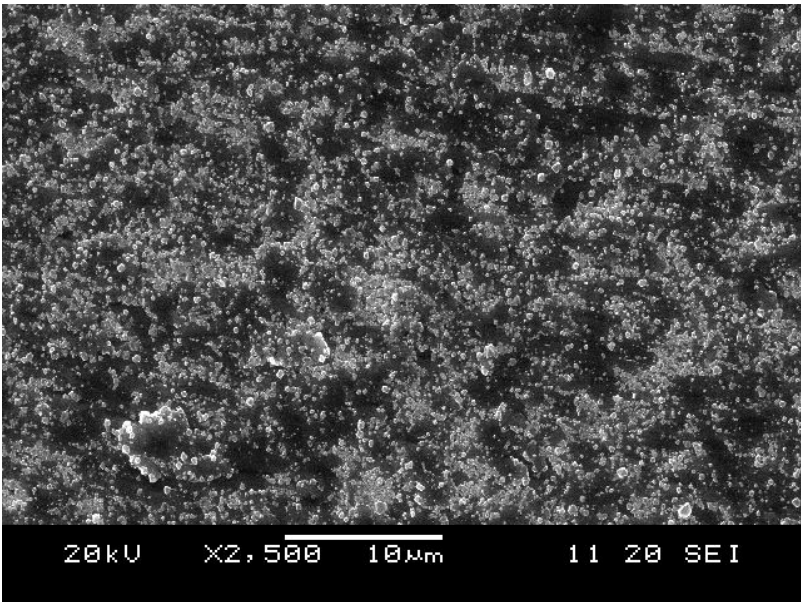
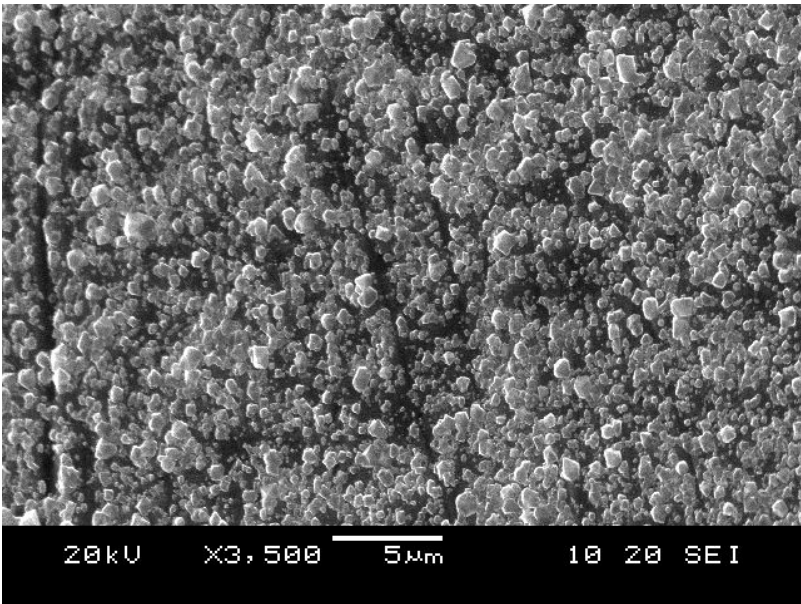
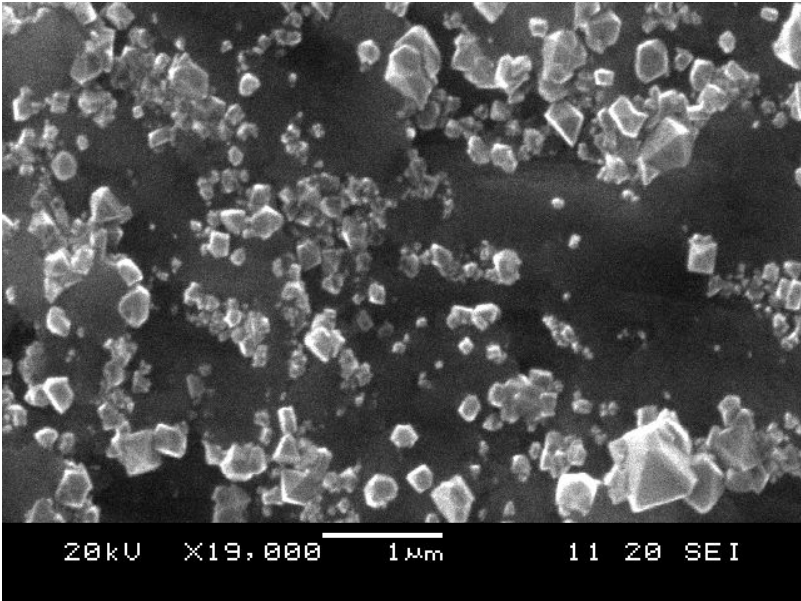
Zr5 3nA positive x3000 magnification, electronic gating on (legend shows Full Scale Deflection for each species)



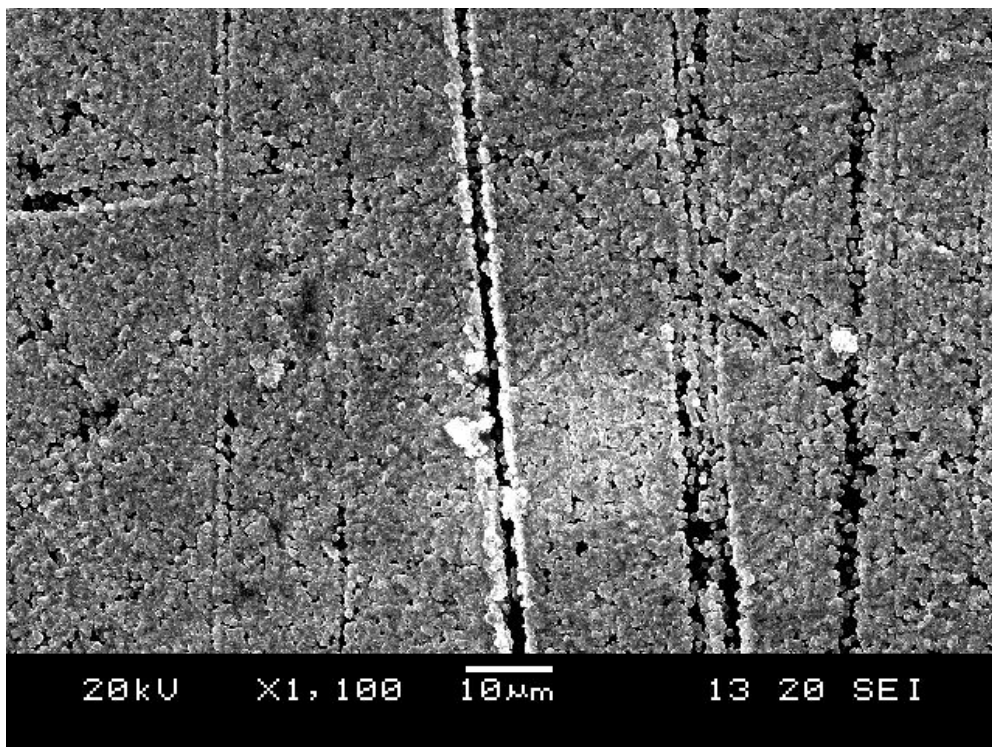
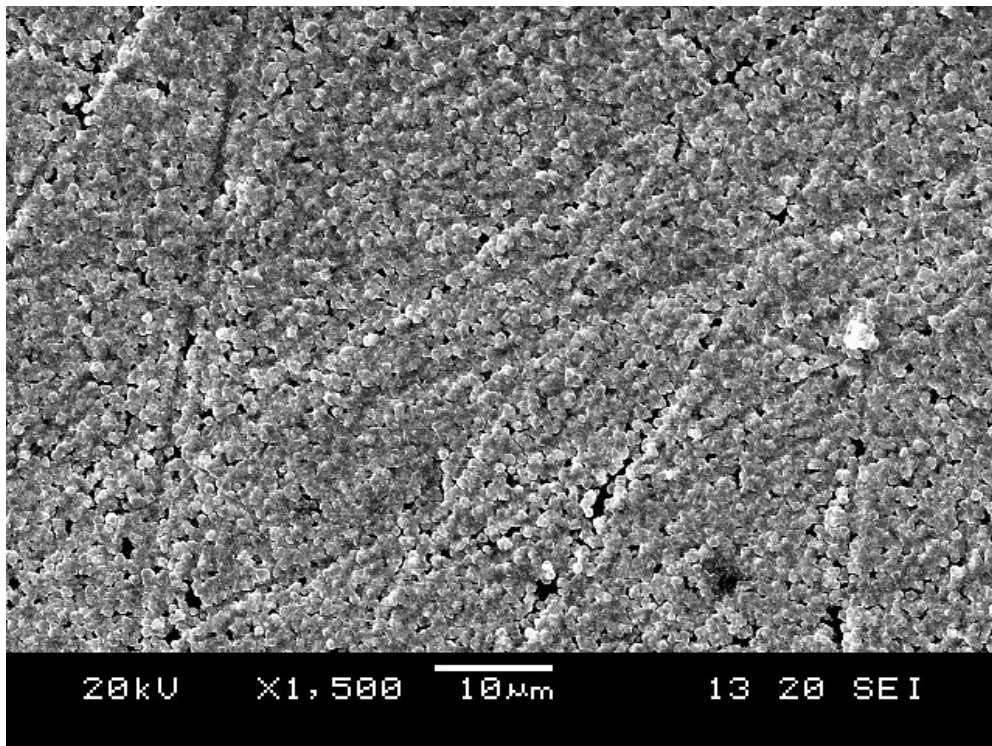
Zr5 3nA negative x5000 magnification, electronic gating on (legend shows Full Scale Deflection for each species)

6.2 SEMs

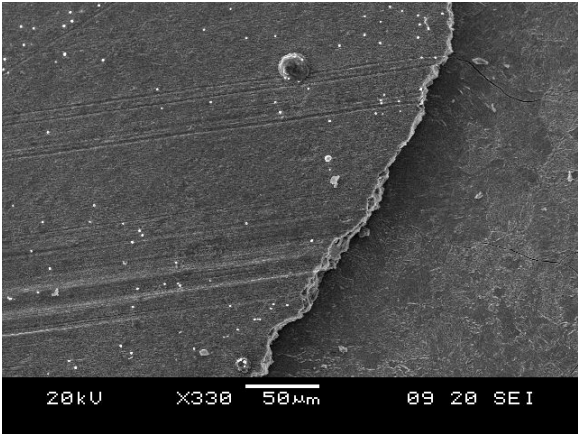
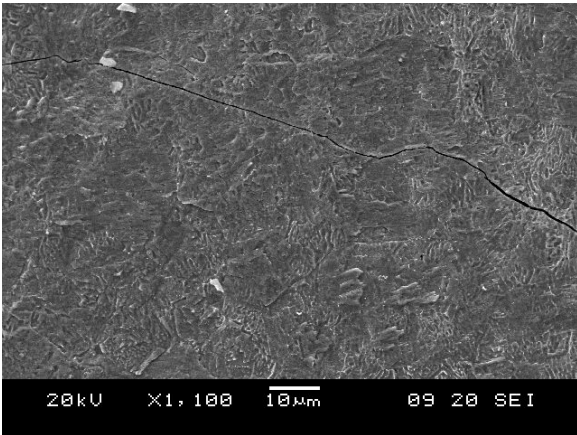
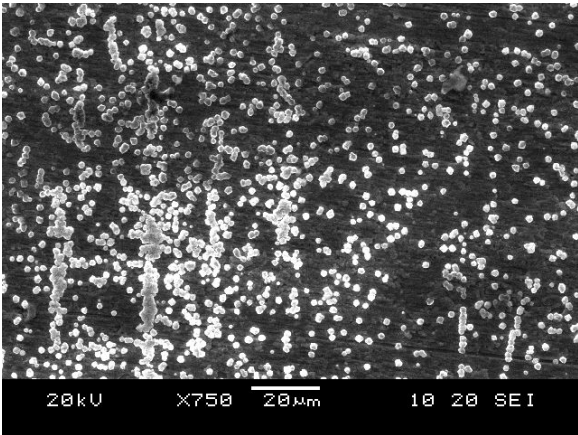
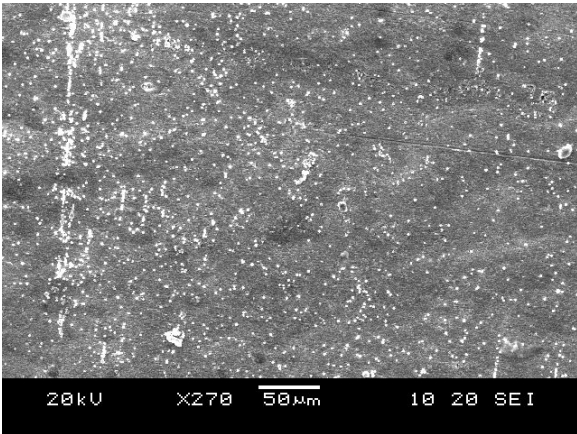
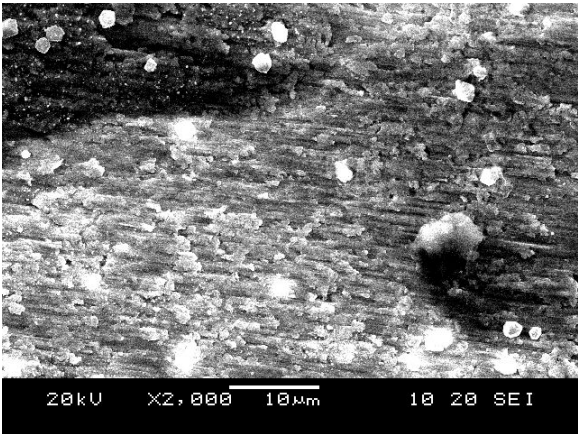
6.2.1 Deposition 4



6.1.2 Deposition 7



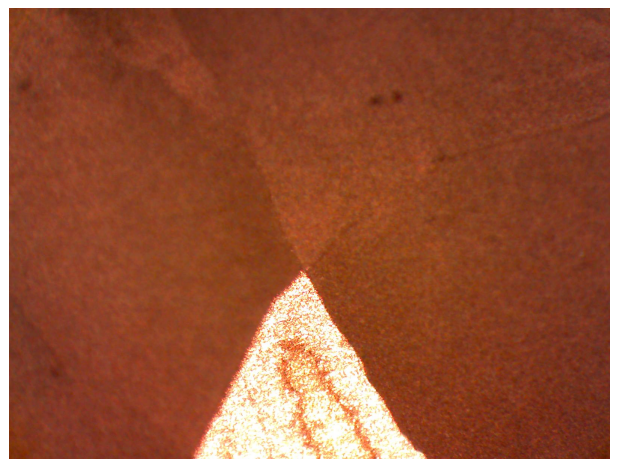
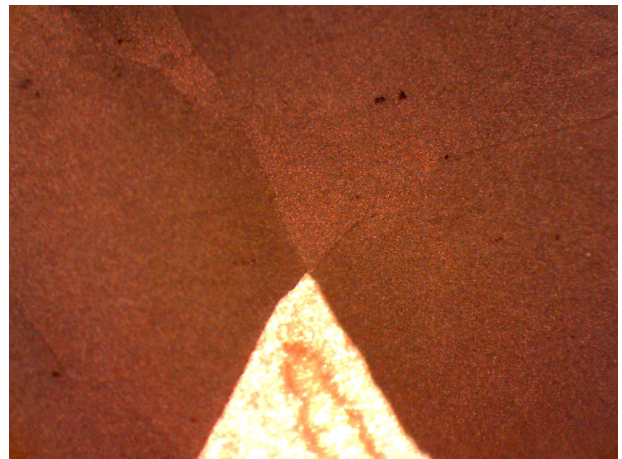
6.1.3 Deposition 6



6.3 Optical Microscope Images

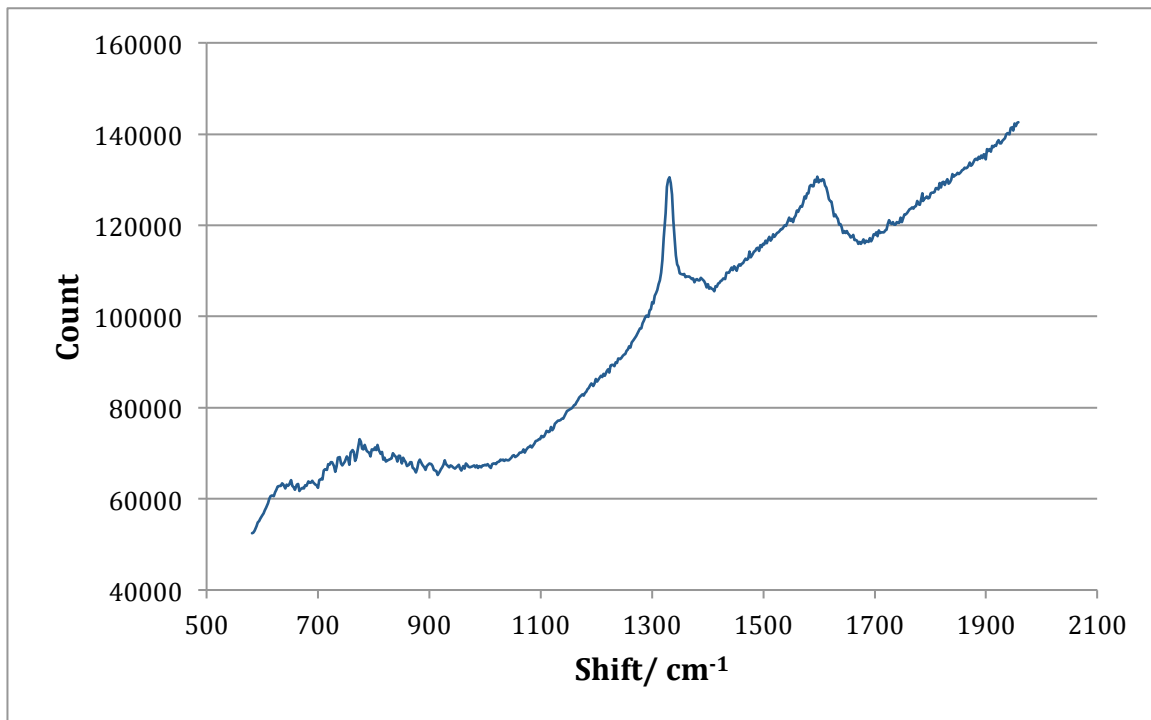
6.3.1 Deposition 4

Images taken at 10× magnification



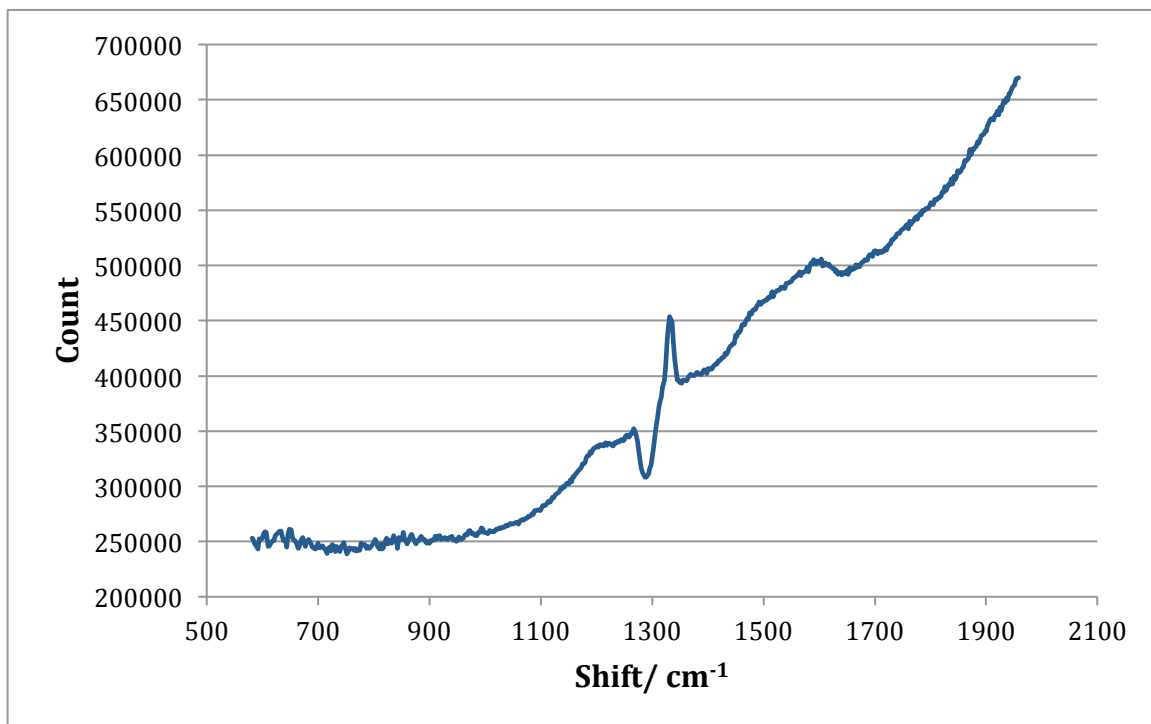
6.4 Raman Spectra

6.4.1 Raman spectrum of sample 5

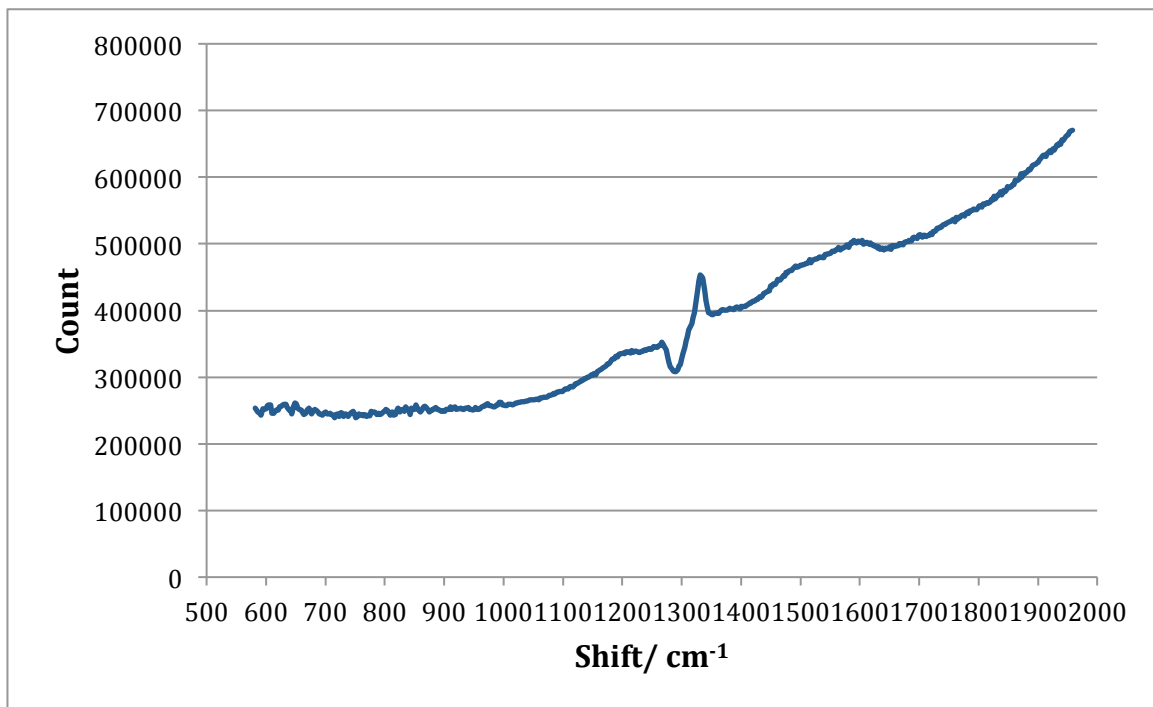


Raman spectrum of sample 7, curve unsmoothed or altered

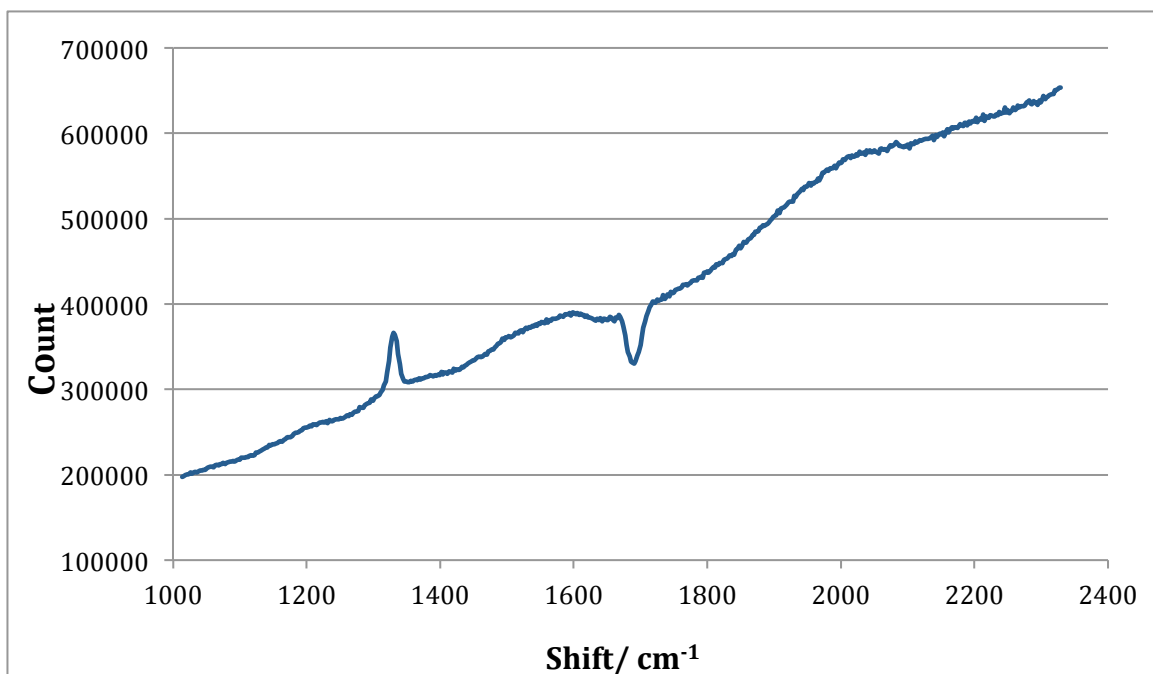
6.4.2 Raman spectra of sample 7



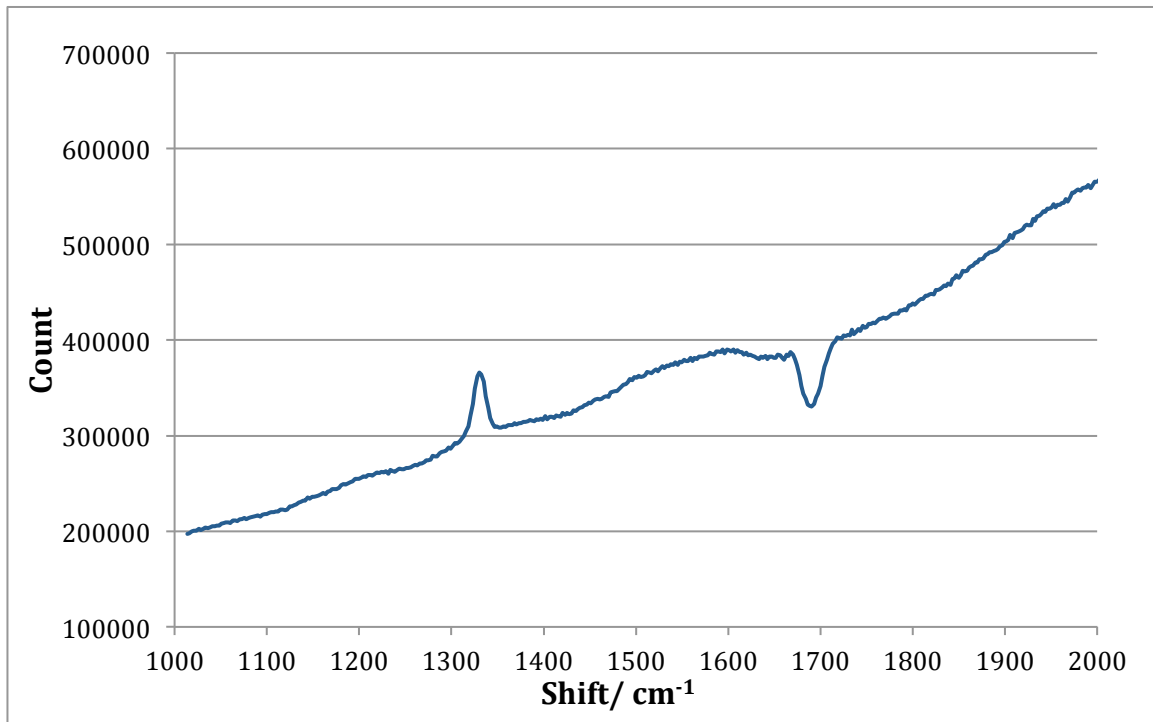
Raman Spectrum of diamond grown on Zr at low temperature for 18 hours (1)



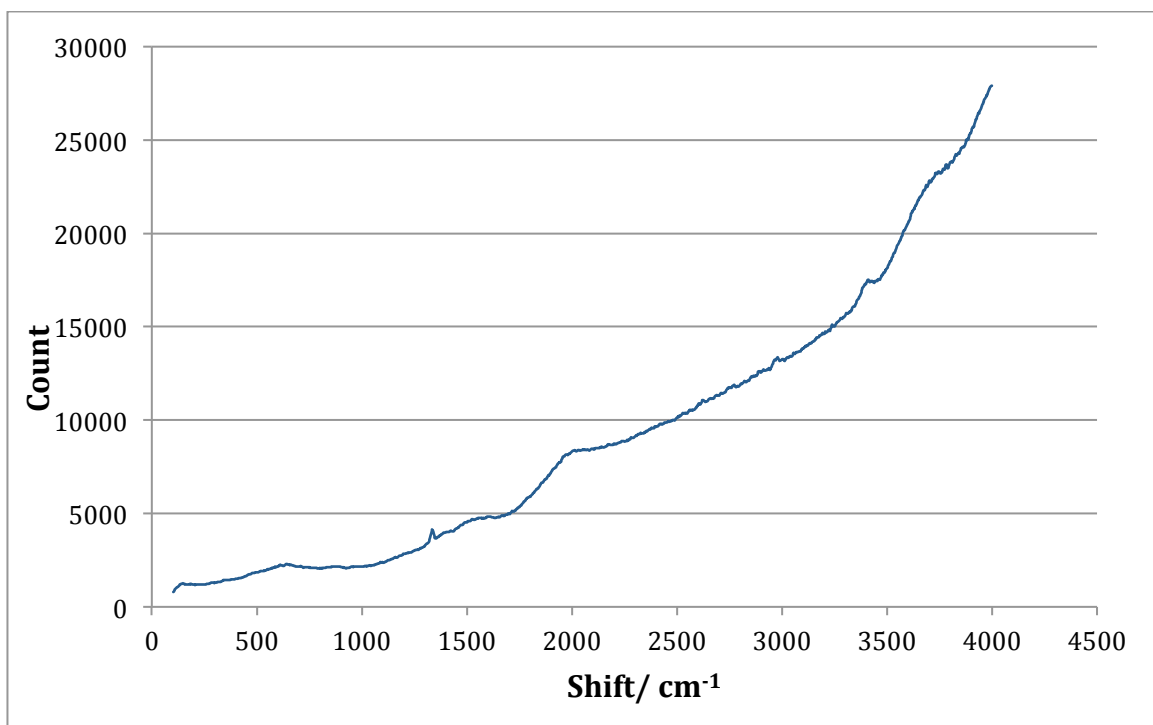
Raman spectrum of diamond grown on Zr at low temperature for 18 hours (1) - zoomed in



Raman spectrum of diamond grown on Zr at low temperature for 18 hours (2)

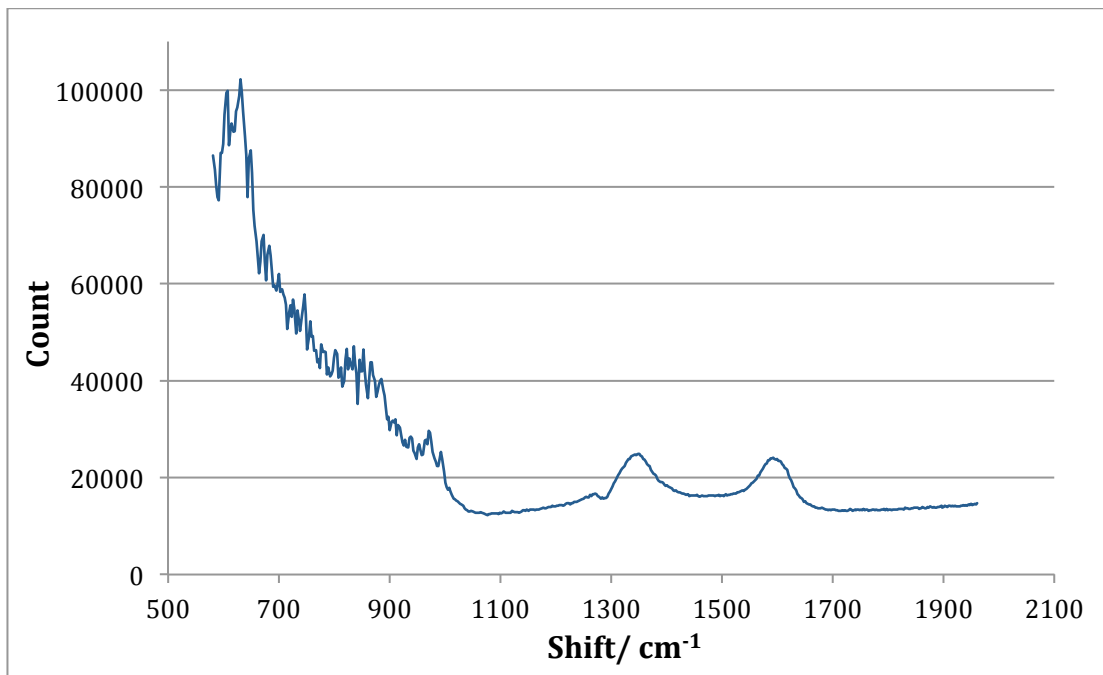


Raman spectrum of diamond grown on Zr at low temperature for 18 hours (2) - zoomed in



Raman shift of diamond grown on Zr at low temperature for 18 hours (scanned across all wavelengths and smoothed)

6.4.3 Raman spectrum of sample 6



Raman Spectrum of zirconium after possible carburisation - the peaks visible to the left of 1100 cm^{-1} are due to reflection of laser light off the metal back into the detector. This unwanted was due to the Raman being poorly aligned at this time, so all peaks below 1100 cm^{-1} should be ignored.

Bibliography

- [1] R. M. Hazen, *The Diamond Makers*. Cambridge: Cambridge University Press, 1999.
- [2] K. E. Spear & J. P. Dismukes, *Synthetic Diamond: Emerging CVD Science and Technology*. NY: Wiley, 1994.
- [3] J. P. Dismukes and K. V. Ravi, *Diamond Materials*. New Jersey: The Electrochemical Society, 1993.
- [4] J. C. Angus & C. C. Hayman, "Low Pressure, Metastable Growth of Diamond and "Diamond-like" Phases," *Science*, vol. 241, p. 914, August 1988.
- [5] H. D. Holland & K. K. Turekian, *The Mantle and Core*. Oxford: Elsevier, 2005.
- [6] M. L. Delitsky & K. H. Baines, "Diamond and Other Forms of Elemental Carbon in Saturn's Deep Atmosphere," in *45th Meeting of the American Astronomical Society Division for Planetary Sciences*, 2013.
- [8] D. Kopeliovich. (2013, June) SubSTech Substances and Technologies. [Online]. <http://www.substech.com/dokuwiki/doku.php?id=graphite>
- [7] Z. Lin & X. Jiang S. T. Lee, "CVD Diamond Films: Nucleation and Growth," *Materials Science and Engineering*, vol. 25, pp. 124-125, 1999.
- [9] C. Wild and E. Worner, Ed., *CVD Diamond Booklet*. Freiburg: Fraunhofer IAF, 2008.
- [10] R. D. Boehm and A. V. Sumant R. J. Narayan, "Medical Applications of Diamond Particles," *Materials Today*, vol. 14, no. 4, pp. 154-163, 2011.
- [11] N. J. Archer, "Chemical Vapour Deposition," *Physics in Technology*, vol. 10, p. 1428, 1979.
- [12] W. A. Bassett, M. S. Weathers, R. J. Hemley, H. K. Mao and A. F. Goncharov F. P. Bundy, "The Pressure-Temperature Phase and Transformation Diagram for Carbon; Updated Through 1994," *Carbon*, vol. 34, no. 2, pp. 141-153, 1996.
- [13] D. V. Fedoseev, V. M. Lukyanovich, B. V. Spitzin, V. A. Ryabov and A. V. Lavrentyev B. V. Derjaguin, "Filamentary Diamond Crystals," *Journal of Crystal Growth*, vol. 2, p. 380, 1968.
- [14] N. C. Gardner & J. C. Angus D. J. Poferl, "Growth of Boron-Doped Diamond Seed Crystals by Vapour Deposition," *Journal of Applied Physics*, vol. 444, p. 1428, 1973.
- [15] N. M. Everitt, C. G. Trevor, M. N. R. Ashfold and K. N. Rosser P. W. May, "Diamond Deposition in a Hot Filament Reactor Using Different Hydrocarbon Precursor Gases," *Applied Surface Science*, vol. 68, p. 300, 1993.
- [16] P. W. May, C. A. Rego & N. M. Everitt M. N. R. Ashfold, *Chemical Society Reviews*, p. 22, 1994.
- [18] K. Kobashi, *Diamond Films*. Oxford: Elsevier, 2005.
- [17] W. A. Carrington, J. E. Butler and K. A. Snail L. M. Hanssen, "Diamond Synthesis Using an Oxyacetylene Torch," *Materials Letters*, vol. 7, no. 7, pp. 289-292, 1988.
- [19] K. Sasaki, M. Kawarada & N. Koshina K. Kurihara, "High rate synthesis of diamond by DC plasma jet chemical vapour deposition," *Applied Physics Letters*, vol. 52, pp. 437-438, 1988.
- [20] K. L. Choy, *Progress in Materials Science*, vol. 48, p. 71, 2003.

- [21] Y. Wang & M. Sunkara J. C. Angus, *Annual Review of Materials Science*, vol. 21, p. 229, 1991.
- [22] S. J. Harris and L. R. Martin, "Methyl versus acetylene as diamond growth species," *Journal of Materials Research*, vol. 5, no. 11, pp. 2313-2319, November 1990.
- [23] J. C. Angus and N. C. Gardner S. P. Chauhan, *Journal of Applied Physics*, vol. 47, p. 4746, 1976.
- [24] J. H. Schemel, Ed., *ASTM Manual on Zirconium and Hafnium*.: ASTM International, 1977, vol. 639.
- [25] J. Emsley, *Nature's Building Blocks; an A-Z Guide to the Elements*, 2nd ed. Oxford: Oxford University Press, 2011.
- [26] W. M. Hayes, *CRC Handbook of Chemistry and Physics*, 94th ed. Boca Raton: CRC Press, 2013.
- [28] J. H. de Boer A. E. van Arkel, "Darstellung von reinem Titanium-, Zirkonium-, Hafnium- und Thoriummetall," *Zeitschrift für anorganische und allgemeine Chemie*, vol. 148, no. 1, pp. 345-350, 1952.
- [27] R. Nielsen, *Zirconium and Zirconium Compounds: Ullmann's Encyclopaedia of Industry Chemistry*. NY: Wiley, 2000.
- [29] Greg Roza, *Understanding the Elements of the Periodic Table: Zirconium*, 1st ed. NY: The Rozen Publishing Group, Inc., 2009.
- [30] [Online]. <http://pse-mendelejew.de/zirconium/>
- [31] [Online]. <http://images-of-elements.com/zirconium.php>
- [32] A. F. Holleman & E. Wiberg, *Inorganic Chemistry*. San Diego: Academic Press, 2001.
- [33] W. J. Kroll, "The Production of Ductile Titanium," in *Transactions of the Electrochemical Society*, vol. 78, 1940, pp. 35-47.
- [34] F. Habashi, Ed., *Handbook of Extractive Metallurgy*. Weinheim: Wiley-VCH, 1997.
- [35] W. C. Conard, & L. Quill E. Larsen, "Concentration of Hafnium. Preparation of Hafnium-Free Zirconia," *Industrial & Engineering Chemistry, Analytical Edition*, vol. 15, no. 8, p. 512, 1943.
- [36] S. Amer, "Solvent extraction applications in hydrometallurgy — 4: titanium, zirconium and hafnium," *Revista de Metalurgia (Madrid)*, vol. 17, no. 6, pp. 377-395, 1981.
- [38] M. Ghanadi & E. Zolfonoun M. Taghizadeh, "Separation of zirconium and hafnium by solvent extraction using mixture of TBP and Cyanex 923," *Journal of Nuclear Materials*, vol. 412, no. 3, pp. 334-337, 2011.
- [37] A.E.P. Brown & T.V. Healy, "Separation of zirconium from hafnium in nitric acid solutions by solvent extraction using dibutyl butyl-phosphonate," *Hydrometallurgy*, vol. 3, no. 3, pp. 265-274, 1978.
- [39] V. Ya. Kudyakov, M.V. Smirnov & N.I. Moskalenko A.B. Salyulev, "Separation of hafnium and zirconium in solutions of their tetrachlorides in molten alkali-metal chlorides," *Journal of Applied Chemistry of The USSR*, vol. 57, no. 8, pp. 1710-1713, 1985.
- [40] P. Thouvenin & P. Brun L. Moulin, "New Process for Zirconium and Hafnium Separation," *ASTM Special Technical Publication*, pp. 37-44, 1984.

- [41] J. M. Begovich & W. G. Sisson, "Continuous Ion-Exchange Separation of Zirconium and Hafnium Using an Annular Chromatograph," *Hydrometallurgy*, vol. 10, pp. 11-20, 1983.
- [42] H. L. Gilbert and M. M. Barr, "Preliminary Investigation of Hafnium Metal by the Kroll Process," *Journal of the Electrochemical Society*, vol. 102, no. 5, p. 243, 1955.
- [43] G. D. Considine, Ed., *Zirconium: Van Nostrand's Encyclopaedia of Chemistry*. NY: Wiley, 2005.
- [44] B. Cox, "Some thought on the mechanisms of in-reactor corrosion of zirconium alloys," *Journal of Nuclear Materials*, vol. 336, no. 2-3, pp. 331-368, 2005.
- [45] Y. C. Kang & R. D. Ramsier, "Kinetic effects of subsurface species on Zr(0001) surface chemistry," *Surface Science*, vol. 519, pp. 229-236, 2002.
- [46] B. Craft, J. Cantrell & E. Venturini R. Bowman, *Physical Review B*, vol. 31, p. 5604, 1985.
- [48] E. Friederich & L. Sittig, *Zeitschrift für anorganische und allgemeine Chemie*, vol. 144, p. 169, 1925.
- [47] W. B. Blumenthal, *The Chemical Behaviour of Zirconium*. USA: D. Van Nostrand Company, Inc., 1958.
- [49] A. Earnshaw & N. Greenwood, *Chemistry of the Elements*, 2nd ed. Oxford: Elsevier Butterworth-Heinmann, 1997.
- [50] F. G. Reshetnikov & E. N. Oblomeev, "Mechanism of formation of zirconium sponge in zirconium production by the magnesothermic process," *The Soviet Journal of Atomic Energy*, vol. 2, no. 5, pp. 561-564, 1957.
- [51] L. Carter & E. R. Peterson R. C. Banks, "Heat of combustion of zirconium. A general chemistry experiment," *Journal of Chemical Education*, vol. 52, no. 4, p. 235, 1975.
- [52] I. Denry & J. R. Kelly, "State of the art zirconia for dental applications," *Dental Materials*, vol. 24, pp. 299-307, 2008.
- [53] N. Vast, P. Baranek, M.-C. Cheynet and L. Reining L. K. Dash, *Phys. Rev. B: Condens. Matter Mater. Phys.*, vol. 70, pp. 245116-245132, 2004.
- [54] H. Fukui, T. Kunisada, T. Fujisawa, K. Funakoshi, W. Utsumi, T. Irifune, K. Kuroda and T. Kikegawa O. Ohtaka, *Phys. Rev. B: Condens. Matter*, vol. 63, pp. 174108-174115, 2001.
- [55] S. Desgreniers * K. Lagarec, *Phys. Rev. B: Condens. Matter*, vol. 59, pp. 8467-8472, 1999.
- [56] [Online]. http://old.irocks.com/db_pics/pics/md12a.jpg
- [58] R. Stevens, *Zirconia and Zirconia Ceramics*. Manchester: Magnesium Elektron Limited, 1986.
- [57] (2013, Dec.) [Online]. <http://cubiczirconiablog.files.wordpress.com/2012/07/cubic-zirconia.jpg>
- [59] P. Read, *Gemmology*, 2nd ed. Oxford: Butterworth-Heinemann, 1999.
- [60] C. Di Valentin & G. Pacchioni F. Gallino, "Band gap engineering of bulk ZrO₂ by Ti doping," *Phys. Chem. Chem. Phys.*, vol. 13, pp. 17667-17675, 2011.
- [61] R. Nieh, B. H. Lee, L. Kang, Y. Jeon, and J. C. Lee W-J. Qi, "Electrical and reliability characteristics of ZrO₂ deposited directly on Si for gate dielectric application,"

- Applied Physics Letters*, vol. 77, pp. 3269-3270, 2000.
- [62] V. S. Stubican * R. C. Bradt C. C. Sorrel, "Mechanical Properties of ZrC-ZrB₂ and ZrC-TiB₂ Directionally Solidified Eutectics," *Journal of the American Ceramic Society*, vol. 69, pp. 317-321, 1986.
- [63] D. P. Butt, J. W. Richardson & J. Li A. C. Lawson, "Thermal expansion and atomic vibration of zirconium carbide to 1600 K," *Philosophical Magazine*, vol. 87, no. 17, pp. 2507-2519, 2007.
- [64] T. Yamaguchi, "Application of ZrO₂ as a catalyst and a catalyst support," *Catalysis Today*, vol. 20, no. 2, pp. 199-217, 1994.
- [65] T. F. Baumann, B. C. Bayer, R. Blume, M. A. Worsley, W. J. MoberlyChan, E. L. Shaw, R. Schlogl, A. J. Hart, S. Hofmann, & B. L. Wardle S. A. Steiner, "Nanoscale Zirconia as a Nonmetallic Catalyst for Graphitization of Carbon and Growth of Single and Multiwall Carbon Nanotubes," *Journal of the American Chemical Society*, vol. 131, pp. 12144-12154, 2009.
- [66] S. C. Singhal & K. Kendall, *High Temperature Solid Oxide Fuel Cells: Fundamentals, Design and Applications*. Oxford: Elsevier, 2003.
- [68] Dental Uses of Zirconia Ceramics. [Online]. <http://www.ceramtec.com/dental-ceramics/>
- [67] W. J. Fleming, "Physical Principles Governing Nonideal Behavior of the Zirconia Oxygen Sensor," *Journal of the Electrochemical Society*, vol. 124, no. 1, pp. 21-28, 1977.
- [69] W. Gruner & S. Stolle L-M. Berger, "On the mechanism of carbothermal reduction processes of TiO₂ and ZrO₂," *International Journal of Refractory Metals and Hard Materials*, vol. 17, no. 1-3, pp. 235-243, 1999.
- [80] C. H. Jung, D. J. Kim & J. Y. Park J. H. Park, "Effect of H₂ dilution gas on the growth of ZrC during low pressure chemical vapor deposition in the ZrCl₄-CH₄-Ar system," *Surface and Coatings Technology*, vol. 203, pp. 87-90, 2008.
- [81] J. Aihara, A. Yasuda, H. Ishibashi, T. Takayama & K. Sawa S. Ueta, "Fabrication of uniform ZrC coating layer for the coated fuel particle of the very high temperature reactor," *Journal of Nuclear Materials*, vol. 376, pp. 146-151, 2008.
- [82] K. Ikawa & K. Iwamoto K. Fukuda, "Fission product diffusion in ZrC coated fuel particles," *Journal of Nuclear Materials*, vol. 87, pp. 367-374, 1979.
- [83] J. C. Janvier, J. L. Kaae & J. P. Morlevat G. H. Reynolds, "Irradiation behaviour of experimental fuel particles containing chemically vapour deposited zirconium carbide coatings," *Journal of Nuclear Materials*, vol. 62, pp. 9-16, 1976.
- [84] X. Xiang, H. Bai-yun, L. Guo-dong, Z. Hong-bo, C. Zhao-ke & Z. Xiang-Lin S. Wei, "ZrC ablation protective coating for carbon/carbon composites," *Carbon*, vol. 47, pp. 3368-3371, 2009.
- [85] V. M. Gropyanov & V. G. Sobolev, "Sintering and properties of solid solutions of carbides," *Poroshkovaya*, vol. 4, no. 52, p. 30-33, 1967, Translated into english.
- [86] Q. Liu, J. Liu, L. Zhang & L. Cheng Y. Wang, "Deposition mechanism for chemical vapour deposition of zirconium carbide coatings," *Journal of the American Ceramic Society*, vol. 91, no. 4, pp. 1249-1252, 2008.
- [88] G. V. Chertihin & L. Andrews, "Reactions of laser-ablated Zr and Hf atoms with hydrogen. Matrix infrared spectra of the MH, MH₂, MH₃ and MH₄ molecules,"

- Journal of Physical Chemistry*, vol. 99, pp. 15004-15010, 1995.
- [87] V. G. Varanasi, O. Kryliouk, T. J. Anderson, L. McElwee-White & R. J. Perez Y. Sun Won, "Equilibrium analysis of zirconium carbide CVD growth," *Journal of Crystal Growth*, vol. 307, pp. 302-308, 2007.
- [89] B. Elvers, Ed., *Ullmann's Fine Chemicals*. Weinheim: Wiley-VCH, 2014, Handbook containing articles from the 7th ed. of Ullmann's Encyclopaedia of Industrial Chemistry.
- [70] P. Duwez & F. Odell, "Phase relationships in the binary systems of nitrides and carbides of zirconium, columbium, titanium and vanadium," *Journal of the Electrochemical Society*, vol. 97, no. 10, pp. 299-304, 1950.
- [71] K. Edmund & E. Charles B. F. Baker, *Journal of Chemical and Engineering Data*, vol. 14, pp. 244-246, 1969.
- [72] S. R. Hall. (2013) Dynamic Laboratory Manual. [Online].
https://dml.chm.bris.ac.uk/dml2013-14/pluginfile.php/6687/mod_resource/content/1/SRH_Intermediate_Materials_Handout.pdf
- [73] Kaier Nano. (2014) Hefei Kaier Nanometer Energy & Technology Co. Ltd. [Online]. <http://www.nano-powders.com/nano-zirconium-carbide.html>
- [74] L. Kollo, I. Hussainova & A. Zikin D-L. Yung, "Reactive sintering of ZrC-TiC composites," *Key Engineering Materials*, vol. 527, pp. 20-25, 2013.
- [75] G. E. Hilmas, W. G. Fahrenholtz, I. G. Talmy & S. G. DiPietro S. E. Landwehy, "Microstructure and mechanical characterization of ZrC-Mo cermets produced by hot isostatic pressing," *Materials Science and Engineering A*, vol. 497, pp. 79-86, 2008.
- [76] R. Ebrahimi & E. Amini-Kahrizsangi, "Zirconia carbothermal reduction: Non-isothermal kinetics," *International Journal of Refractory Metals and Hard Materials*, vol. 27, no. 3, pp. 637-641, 2009.
- [78] Y. Fukuda & M. Kajiwara I. Hasegawa, "Inorganic-organic hybrid route to synthesis of ZrC and Si-Zr-C fibres," *Ceramics International*, vol. 25, no. 6, pp. 523-527, 1999.
- [77] C-A. Wang, Z. Yang & A. Jain M. D. Sacks, "Carbothermal reduction synthesis of nanocrystalline zirconium carbide and hafnium carbide powders using solution-derived precursors," *Journal of Materials Science*, vol. 39, pp. 6057-6066, 2004.
- [79] D. Chen, Y. Liu, K. Tang & Y. Qian G. Shen, "Synthesis of ZrC hollow nanospheres at low temperature," *Journal of Crystal Growth*, vol. 262, no. 1-4, pp. 277-280, 2004.
- [90] C. J. Lu & Q. Li, *Journal of Alloy Compounds*, vol. 509, pp. 1211-1216, 2010.
- [91] V. N. Fokin, *Russian Journal of General Chemistry*, vol. 74, pp. 489-494, 2004.
- [92] B. Craft, J. Cantrell & E. Venturini R. Bowman, *Physical Review B*, vol. 31, p. 5604, 1985.
- [93] M. P. Puls, *The Effect of Hydrogen and Hydrides on the Integrity of Zirconium Alloy Components*. London: Springer, 2012.
- [94] J. D. Atwood & J. J. Zuckerman, *Inorganic Reactions and Methods: Formation of Ceramics*. NY: Wiley, 1999.
- [95] Mitsubishi Nuclear Fuel Co. (2013) World Nuclear Association. [Online].

- <http://www.world-nuclear.org/info/Nuclear-Fuel-Cycle/Conversion-Enrichment-and-Fabrication/Fuel-Fabrication/>
- [96] K. Dorius. (2011, March) Energy from Thorium. [Online].
<http://energyfromthorium.com/2011/03/19/fuel-rod-lifecycle/>
- [98] P. D. Wilson, *The Nuclear Fuel Cycle*. Oxford: OUP, 1996.
- [97] P. D. Wilson. (2013, November) World Nuclear Association. [Online].
<http://www.world-nuclear.org/info/Nuclear-Fuel-Cycle/Power-Reactors/Nuclear-Power-Reactors/>
- [99] ATI Wah Chang. (2013) Allegheny Technologies. [Online].
www.alleghenytechnologies.com/wahchang
- [100] H-G. Kim & Y-H. Jeong Y-S. Lim, "Experimental Evaluation of the Rolling Reduction and Heat-Treatment Effects on the Texture and Creep Behavior of a Zircaloy-4 Sheet," *Materials Transactions*, vol. 49, pp. 1922-1925, 2008.
- [101] Y. Cho & Y-G. Kim K. Park, "The effects of adsorbates on Zircaloy oxidation in air and steam," *Journal of Nuclear Materials*, vol. 270, pp. 154-164, 1999.
- [102] J. F. Watters & R. W. Gilbert G. J. C. Carpenter, "Dislocations generated by zirconium hydride precipitates in zirconium and some of its alloys," *Journal of Nuclear Materials*, vol. 48, pp. 267-276, 1973.
- [103] R. A. Wolfe & R. M. Lieberman W. Yeniscavich, "Hydrogen absorption by nickel enriched Zircaloy-2," *Journal of Nuclear Materials*, vol. 3, pp. 271-280, 1959.
- [104] G. W. Lorimer & N. Ridley J. S. Bradbrook, "The precipitation of zirconium hydride in zirconium and Zircaloy-2," *Journal of Nuclear Materials*, vol. 42, pp. 142-160, 1972.
- [105] Y. S. Chu & A. T. Motta R. S. Daum, "Identification and quantification of hydride phases in Zircaloy-4 cladding using synchrotron X-ray diffraction," *Journal of Nuclear Materials*, vol. 392, pp. 453-463, 2009.
- [106] C. L. Whitmarsh, "Review of Zircaloy-2 and Zircaloy-4 preproperties relevant to N. S. Savannah reactor design," Reactor Division, Oak Ridge National Laboratory, Oak Ridge, Literature review 1962.
- [108] R. J. M. Konings & A. T. Motta T. R. Allen, "Corrosion of Zirconium Alloys," in *Comprehensive Nuclear Materials*, R. J. M. Konings, Ed. Amsterdam: Elsevier Ltd., 2012, pp. 49-68.
- [107] G. P. Sabol & G. D. Moan, Ed., *Zirconium in the Nuclear Industry*. West Conshocken: American Society for Testing and Materials, 2000.
- [109] B. Lustman & F. Kerze, *The Metallurgy of Zirconium*. Michigan: McGraw-Hill Book Company, 1955.
- [110] B. -J. Koo, J. -O. Honh, I. -S. Hwang & Y. -H. Jeong H. -I. Yoo, "A working hypothesis on oxidation kinetics of Zircaloy," *Journal of Nuclear Materials*, vol. 299, pp. 235-241, 2001.
- [111] D. F. Cowgill & B. H. Nilson R. A. Causey, "Review of the oxidation rate of zirconium alloys," Engineered Materials Department and Nanoscale Science and Technology Department, Sandia National Laboratories, Livermore, Review 2005.
- [112] D. Hudson, J. Wei, S. Lozano-Perez, G. D. W. Smith, J. M. Sykes, S. S. Yardley, K. L. Moore, S. Lyon, R. Cottis, M. Preiss & C. R. M. Grovenor N. Ni, "How the

crystallography and nanoscale chemistry of the metal/oxide interface develops during the aqueous oxidation of zirconium cladding alloys," *Acta Materialia*, vol. 60, no. 20, pp. 7132-7149, 2012.

- [113] T. Smith, "Kinetics and mechanism of hydrogen permeation of oxide films on zirconium," *Journal of Nuclear Materials*, vol. 18, no. 3, pp. 323-336, 1966.
- [114] C. E. Ells, "Hydride precipitates in zirconium alloys," *Journal of Nuclear Materials*, vol. 28, pp. 129-151, 1968.
- [115] C. Roy, "An experiment to clarify the effect of dissolved oxygen on the terminal solubility of hydrogen in zirconium," *Journal of Nuclear Materials*, vol. 13, no. 2, pp. 275-277, 1964.
- [116] T. Tanaka & M. Miyake S. Yamanaka, "Effect of oxygen on hydrogen solubility in zirconium," *Journal of Nuclear Materials*, vol. 167, pp. 231-237, 1989.
- [118] P. Efsing, "Delayed Hydride Cracking in Irradiated Zircaloy," Materials Science and Engineering, Royal Institute of Technology, Stockholm, Doctoral Thesis 1998.
- [117] B. Cox & Y.-M. Wong, "A hydrogen uptake micro-mechanism for Zr alloys," *Journal of Nuclear Materials*, vol. 270, no. 1-2, pp. 134-146, 1999.
- [119] E. C. Darby & J. S. Schofield A. McMinn, "The Terminal Solid Solubility of Hydrogen in Zirconium Alloys," in *Zirconium in the Nuclear Industry: 12th International Symposium*, G. P. Sabol & G. D. Moan, Ed. West Conshohocken: ASTM STP 1354, 2000.
- [120] G. J. C. Carpenter, "The dilatational misfit of zirconium hydrides precipitated in zirconium," *Journal of Nuclear Materials*, vol. 48, pp. 264-266, 1973.
- [121] Nuclear Power Development Section, "Delayed hydride cracking in zirconium alloys in pressure tube nuclear reactors," International Atomic Energy Agency, Vienna, Final part of a co-ordinated research project 2004.
- [122] J. Matson, "What happens during a nuclear meltdown," *Scientific American*, vol. 15, 2011.
- [123] B. Cox, "Pellet clad interaction failures of zirconium alloy fuel cladding - a review," *Journal of Nuclear Materials*, vol. 172, pp. 249-292, 1990.
- [124] World Nuclear Association. (2014) World Nuclear Association. [Online]. <http://www.world-nuclear.org/info/safety-and-security/safety-of-plants/fukushima-accident/>
- [125] S. Nebehay. (2013, February) Interlational Business Times. [Online]. <http://www.reuters.com/article/2013/02/28/us-japan-nuclear-cancer-idUSBRE91R0D420130228>
- [126] J. M. Acton & M. Hibbs. (2012) Carnegie Endowment for International Peace. [Online]. <http://carnegieendowment.org/2012/03/06/why-fukushima-was-preventable/a0i7>
- [128] Bristol University Diamond Group. (2011, June) University of Bristol: CVD Diamond Group. [Online]. <http://www.chm.bris.ac.uk/pt/diamond/image/electrospray-new.jpg>
- [127] Bristol University Diamond Group. (2011, June) University of Bristol: CVD Diamond Group. [Online]. <http://www.chm.bris.ac.uk/pt/diamond/image/electrospray2.jpg>

- [129] T. Uchiyama, K. Dokko, K. Yamada, T. Matsue & I. Uchida M. Nishizawa, "Electrochemical Studies of Spinel LiMn_2O_4 Films Prepared by Electrostatic Spray Deposition," *Bull. Chem. Soc. Jpn.*, vol. 71, no. 8, pp. 2011-2015, August 1998.
- [130] Bristol University Diamond Group. (2011, June) University of Bristol: CVD Diamond Group. [Online].
<http://www.chm.bris.ac.uk/pt/diamond/image/HFkit-new1.jpg>
- [131] Bristol University Diamond Group. (2011, June) University of Bristol: CVD Diamond Group. [Online].
<http://www.chm.bris.ac.uk/pt/diamond/image/HFCVDspring4.jpg>
- [132] P. W. May, E. Bartlett, M. N. R. Ashfold & K. N. Rosser S. M. Leeds, "Molecular beam mass spectrometry studies of the gas-phase chemistry occurring during microwave plasma assisted chemical vapour deposition of diamond," *Diamond and Related Materials*, vol. 8, no. 8-9, pp. 1377-1382, August 1999.
- [133] (2014, March) University of Bristol. [Online]. <https://research-equipment.bris.ac.uk/item/various-iac-magnetic-sector-sims-ion-milling-instrument/1843>
- [134] G. Yushin & Y. Gogotsi R. K. Dash, "Synthesis, structure and porosity analysis of microporous and mesoporous carbon derived from zirconium carbide ," *Microporous and Mesoporous Materials*, vol. 86, pp. 50-57, 2005.
- [135] J. Filik, "Fundamental Studies on the Deposition and Characterisation of Novel Diamond-Like Materials," University of Bristol, Bristol, PhD Thesis 2006.
- [136] J. B. Hannay, "On the Artificial Formation of Diamond," in *Proceedings of the Royal Society of London*, vol. 30, 1879, pp. 460-461.
- [138] J. W. French, On 'J. B. Hannay and the Artificial Production of Diamonds', 1944.
- [137] K. Lonsdale, "Further Comments on Attempts by H. Moissan, J. B. Hannay and Sir Charles Parsons to Make Diamonds in the Laboratory," *Nature*, vol. 196, p. 104, 1962.
- [139] W. G. Eversole, 3030187, 1962.
- [140] H. T. Hall, H. M. Strong & R. H. Wentorf Jr F. P. Bundy, "Man Made Diamonds," *Nature*, vol. 176, p. 51, 1955.
- [141] M. H. Nazare & A. J. Neves, *Properties, Growth and Applications of Diamond*. London: INSPEC, 2001.
- [142] R. W. Bormett, Z. Chi, N. Cho, X. G. Chen, V. Pajcini, S. A. Asher, L. Spinelli, P. Owen and M. Arrigoni J. S. W. Holtz, "Applications of a New 206.5 nm CW Laser Source: UV Raman Determination of Protein Secondary Structure and CVD Diamond Material Properties," *Applied Spectroscopy*, vol. 50, pp. 1459-1468, 1996.
- [143] J. N. Tiwari, G. Singh and K. L. Lin R. N. Tiwari, "Direct Synthesis of Vertically Interconnected 3-D Graphitic Nanosheets on Hemispherical Carbon Particles by Microwave Plasma CVD," *Plasmonics*, vol. 6, no. 1, pp. 67-73, 2011.
- [144] W. Vollenberg, L. J. Giling, W. J. P. van Enckervort, J. J. D. Schaminee & M. Seal G. Janssen, "Rapid Growth of Single-Crystal Diamond on Diamond Substrate," *Surface and Coating Technology*, vol. 47, no. 1-3, pp. 113-126, 1991.
- [145] P. W. Morrison Jr & J. T. Glass, *Properties and Growth of Diamond*. London:

- INSPEC, 1994.
- [146] S. J. Harris, "Mechanism for diamond growth from methyl radicals," *Applied Physics Letters*, vol. 56, p. 2298, 1990.
- [148] [Online]. <http://rruff.geo.arizona.edu/AMS/result.php?mineral=Baddeleyite>
- [147] S. J. Harris and A. M. Weiner, "Methyl radical and H atom concentrations during diamond growth," *Journal of Applied Physics*, vol. 67, p. 6520, 1990.
- [149] M. Krause, T. Höche, C. Patzig, Y. Hu, A. Gawronski, I. Tanaka & C. Rüssel H. Ikeno, *Journal of Physics: Condensed Matter*, vol. 25, p. 2, 2013.
- [150] C. E. Housecroft & A. G. Sharpe, *Inorganic Chemistry*, Third Edition ed. Edinburgh: Publisher, 2008.
- [151] H. K. Schmidt & E. Arpac R. Nass, "Synthesis and properties of transparent ZrO₂ containing SiO₂ polymethacrylate polymers," in *Sol-Gel Optics*, vol. 358, 1990.
- [152] E. Kim, J. Becker, & R. G. Gordon D. M. Hausmann, "Atomic Layer Deposition of Hafnium and Zirconium Oxides Using Metal Amide Precursors," vol. 14, no. 10, pp. 4350-4358, 2002.
- [153] D. Gozzi, T. Kimura, T. Noda & S. Otani A. Bellucci, "Zirconia growth on zirconium carbide single crystals by oxidation," *Surface & Coatings Technology*, vol. 197, pp. 294-302, 2005.
- [154] A. K. Kuriakose & J. L. Margrave, "The oxidation kinetics of zirconium diboride and zirconium carbide at high temperatures," *Journal of the Electrochemical Society*, vol. 111, no. 7, pp. 827-831, 1964.
- [155] M. Opeka et al., *Materials Science and Engineering: A*, vol. 528, pp. 1994-2001, 2011.
- [156] D. Moser & D. J. Bull, "Structure and stability of high pressure synthesised Mg-TM hydrides (TM-Ti, Zr, Hf, V, Nb and Ta) as possible new hydrogen rich hydrides for hydrogen storage," *Journal of Materials Chemistry*, vol. 19, no. 43, pp. 8150-8161, 2009.
- [158] Bristol University Diamond Group. (2011, June) University of Bristol: CVD Diamond Group. [Online]. <http://www.chm.bris.ac.uk/pt/diamond/image/electrospray-new.jpg>
- [157] Bristol University Diamond Group. (2011, June) University of Bristol: CVD Diamond Group. [Online]. <http://www.chm.bris.ac.uk/pt/diamond/image/electrospray2.jpg>
- [159] Bristol University Diamond Group. (2002, February) University of Bristol: CVD Diamond group. [Online]. <http://www.chm.bris.ac.uk/pt/diamond/image/sem.jpg>